AD-A058 302 SCIENCE APPLICATIONS INC MCLEAN VA F/G 18/3
EXPERIMENTAL STUDIES OF SOIL THERMAL IRRADIATION. VOLUME I. SOI--ETC(U)
APR 77 T M KNASEL DNA001-75-C-0209
UNCLASSIFIED SAI-78-540-WA-VOL-1 DNA-4484F-1 NL

1 OF 1
AD A058302

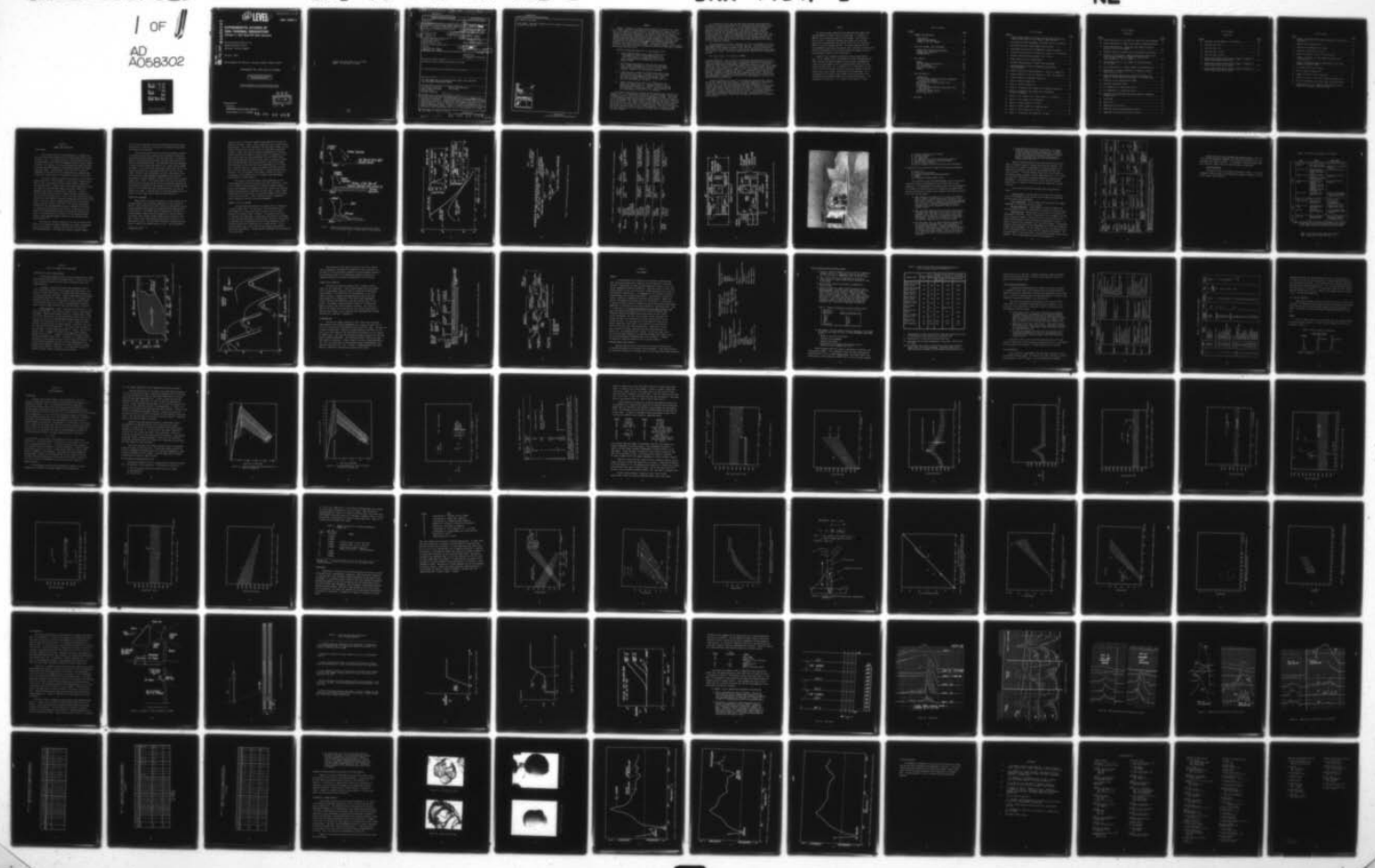

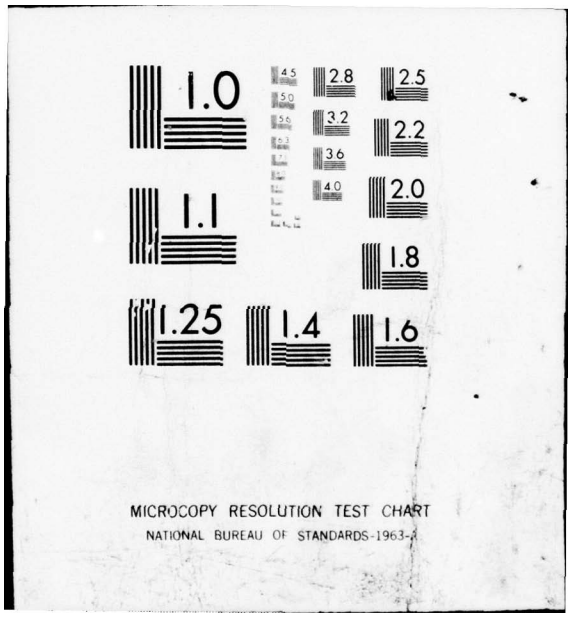
1.0
1.1
1.25
1.4
1.6
1.8
2.0
2.2
2.5
2.8
3.2
3.6
4.0
4.5
5.0
5.6
6.3
MICROCOPY RESOLUTION TEST CHART
NATIONAL BUREAU OF STANDARDS-1963-A

(12) LEVEL III

DNA 4484F-1

EXPERIMENTAL STUDIES OF SOIL THERMAL IRRADIATION

Volume I – Soil Blow-Off Data Analysis

Science Applications, Inc.
8400 Westpark Drive
McLean, Virginia 22101

15 April 1977

Final Report for Period 1 January 1976—1 March 1977

CONTRACT No. DNA 001-75-C-0209

THIS WORK SPONSORED BY THE DEFENSE NUCLEAR AGENCY
UNDER RDT&E RMSS CODE B344077464 Y99QAXSA00205 H2590D.

Prepared for
Director
DEFENSE NUCLEAR AGENCY
Washington, D. C. 20305

Destroy this report when it is no longer needed. Do not return to sender.

(18) DNA, SBIE | (19) 4484F-1, AD-E300 287

UNCLASSIFIED

SECURITY CLASSIFICATION OF THIS PAGE (When Data Entered)

REPORT DOCUMENTATION PAGE

READ INSTRUCTIONS BEFORE COMPLETING FORM

1. REPORT NUMBER: DNA 4484F-1	2. GOVT ACCESSION NO. (9)	3. RECIPIENT'S CATALOG NUMBER
4. TITLE (and Subtitle): EXPERIMENTAL STUDIES OF SOIL THERMAL IRRADIATION. Volume I Soil Blow-Off Data Analysis. (6)		5. TYPE OF REPORT & PERIOD COVERED: Final Report for [redacted] 1 Jan 76—1 Mar 77 (7)
		6. PERFORMING ORG. REPORT NUMBER: SAI-78-540-WA-VOL-1 (14)
7. AUTHOR(s): (10) T. M. Knasel (17) AD02		8. CONTRACT OR GRANT NUMBER(s): DNA 001-75-C-0209 (15)
9. PERFORMING ORGANIZATION NAME AND ADDRESS: Science Applications, Inc. 8400 Westpark Drive McLean, Virginia 22101		10. PROGRAM ELEMENT, PROJECT, TASK AREA & WORK UNIT NUMBERS: (16) NWED Subtask Y99QAXSA002-05
11. CONTROLLING OFFICE NAME AND ADDRESS: Director Defense Nuclear Agency Washington, D.C. 20305		(11) 12. REPORT DATE: 15 Apr [redacted]77 13. NUMBER OF PAGES: 96 (12) 970.
14. MONITORING AGENCY NAME & ADDRESS (if different from Controlling Office)		15. SECURITY CLASS (of this report): UNCLASSIFIED 15a. DECLASSIFICATION/DOWNGRADING SCHEDULE

16. DISTRIBUTION STATEMENT (of this Report)

Approved for public release; distribution unlimited.

17. DISTRIBUTION STATEMENT (of the abstract entered in Block 20, if different from Report)

18. SUPPLEMENTARY NOTES

This work sponsored by the Defense Nuclear Agency under RDT&E RMSS Code B344077464 Y99QAXSA00205 H2590D.

19. KEY WORDS (Continue on reverse side if necessary and identify by block number)

Soil Thermal Irradiation
Thermal Layer Development
Precursor Effect
Non-Ideal Blast Wave
Nuclear Burst Simulation
Solar Furnace

is based on a series of over 300 irradiation tests of basic soil types.

20. ABSTRACT (Continue on reverse side if necessary and identify by block number)

The total report describes three experimental activities in thermal layer experimental development. Volume I analyzes soil irradiation tests performed under previous contracts. Thorough cross comparison of over twenty soil types revealed that these could be apportioned into seven key categories of soil response behavior. Volume II reports on an innovative thermochemical pulse generator development program. Volume III contains descriptions of design and experimental work directed toward the use of a flux redirector for a large

DD FORM 1 JAN 73 1473 EDITION OF 1 NOV 65 IS OBSOLETE

UNCLASSIFIED

SECURITY CLASSIFICATION OF THIS PAGE (When Data Entered)

H08 404

78 06 16 033

20. ABSTRACT (Continued)

solar furnace. Successful completion of this design allows testing of soils at above 300 cal/cm^2 sec.

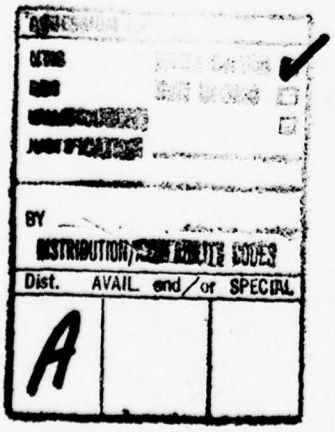

SUMMARY

Volume I is based on a series of over 300 tests of seven basic soil types. It provides an empirical understanding of the phenomenon of thermal blow-off. Due to the coupling of blown off dust to non-ideal blast wave effects and cloud loading in nuclear burst situations it is imperative that the soil thermal response be quantified. Unfortunately the lack of scaling of the theoretical parameters and the great variety of soil types worldwide of strategic or tactical interest have complicated the problem. Science Applications, Inc. (SAI) under the sponsorship of the Defense Nuclear Agency has conducted an experimental program of soil blow-off analysis utilizing a nearly exact thermal pulse simulation from a series of solar furnaces. The largest of these, a 25 KW furnace at the U.S. Army White Sands Missile Range, was used for over 300 hours of testing over the past two-year period.

Findings indicate that blow off is of four distinct types:

- Smoke is nearly always produced above a threshold of 7 cal/cm^{2}sec flux and 4 to 6 cal/cm^2 fluence. Its initial rise velocity is between 0.25 and 0.5 m/sec and is characterized by a temperature rise of 25 to 50^{o}K/(cal/cm^2).

- Small particulate ejection is seen in soils containing clay. Fluence thresholds of 5 to 20 cal/cm^2 are common, rise velocities the order of 1-2 m/sec. If blow off is abundant, volumetric air heating may be observed.

- Large particles or flakes are yielded from materials that contain significant clay. Thresholds of 20 to 40 cal/cm^2 and from 20 to 50 cal/cm^{2}sec are experienced. These particles are abundant at the higher heating rates, and have rise velocities up to 10 m/sec.

- Steam is emitted from all moist soils. Above about 3-5% moisture by weight, there is a noticeable effect in the air temperature above heated soil. Several cal/cm^2 are required per % moisture to drive the water off. Upon completion, the soil participates in blow off as if it were dry.

The results of the SAI tests indicate that as a general rule all soils lose between 2 to 6 x 10^{-4} gm material blow off per cal/cm^2 of fluence. The optical thickness of the soil varies over an order of magnitude 20 to 200μ. This layer is diathermanously heated, and using the accepted density and specific heats for soils, one estimates that several percent of the weight of this layer is blown off due to irradiation. This thermal erosion is more effective the thinner the layer and smaller the soil grain size. It was observed that those soils of smaller grain size did in fact have the most abundant blow off. Pure clays will approach 100 percent thermal erosion, as was verified dramatically in the tests; other soils of larger grain size will saturate, and form "scars" of glassy material over their surface.

It is important to note that the tests were performed in two-dimensional configuration by necessity and thus do not simulate one important aspect of soil response to a nuclear thermal pulse. In a one-dimensional case the smoke and particulate matter above the soil obscure the incoming radiation (possibly completely) and take up that radiation in the form of volumetric heating. Because of this fact all parameters have been measured as close to the soil surface as possible in order to be characteristic of one-dimensional flow. The reader should be very cautious of extrapolation of the results in height to the one-dimensional case. Ground level flux obscurations were measured up to 50 percent. One may conclude by calculation that further obscuration would result in a one-dimensional geometry.

The work reported in Volume II represents an initial development of a large scale thermochemical source of flash optical radiation. The initial criteria for development included area of coverage ($>1 m^2$), peak flux (>100 cal/cm^2/sec) and total fluence (>20 cal/cm^2) as well as the practical considerations of cost, ease of fielding and safety. Preliminary theoretical work identified the thermochemical reaction

$$2Al + \frac{3}{2} O_2 \rightarrow Al_2O_3 + 7.4 \text{ Kcal/gm al } (3900^oK)$$

as being appropriate. Tests of reaction systems were performed (about 50 in all) eventually leading to the fielding of an explosively ignited device consisting of primacord wrapped with aluminum powder, suspended on the axis of a cylindrical oxygen bag. Test results indicated an average optical fluence of about 10^3 cal/gmal (for an efficiency of about 17%), a peak flux of over 200 cal/cm^2/sec, fluence over 20 cal/cm^2 and coverage areas in excess of 10 m^2. The largest units tested had a peak optical power of 1 gigawatt (10^9 watts). Significant shock energy was also measured. Numerous fielding problems were encountered and solved. The devices have been successfully fielded in adverse weather conditions and no misfires have been encountered. Parametric scaling laws for the thermochemical reactions have been determined from test data.

Volume III reports on a study of flux redirection techniques that could be used at the 1 MWth French solar furnace. The unique capability of this furnace to reach flux of over 200 cal/cm^2/sec motivated the investigation of the practicality of soil blow-off experimental techniques analogous to those utilized at the 25 KWth White Sands Missile Range solar furnace. The use of a modified "ideal light collector" design allows turning of the flux by 90^o and blow-off containment in a vertical tube above the soil surface. Experimental verification of the design confirmed theoretical analysis work. Design and construction details were investigated. Constraints and thermal environments for instrumentation are given.

PREFACE

This work has been supported by the Defense Nuclear Agency under Contract DNA001-75-C-0209. We wish to thank Capt. J. Stockton of DNA/SPSS for continued assistance in this program. The irradiation tests at the U.S. Army Missile Range, White Sands, N.M. were made possible by the cooperation and technical help of Mr. Leo Flores and others at the Solar Furnace facility. Dr. Thomas Rooney of the Air Force Geophysics Laboratory, Hanscom AFB, Mass. provided invaluable contributions in performing a series of tests on the soil samples as well as giving geological advice on the test program.

A number of SAI scientists contributed to the program reported here. Mr. R. Higgins and Dr. Carl Murphy of the SAI, Albuquerque, N.M. office provided the design engineering of the unique instrumentation required for the program, as well as countless hours during the test program at White Sands. Mr. A. Houghton, Dr. R. Liner and Mr. R. Ryan of the SAI office in McLean, Virginia provided considerable technical support both in the fielding and analysis of the experiments. Mr. P. Versteegen of SAI, McLean, Virginia made critical evaluation of the analyzed data and provided insight into the blow-off mechanisms. The program was directed by Dr. T. M. Knasel of SAI, McLean, Virginia.

Table of Contents

List of Figures

List of Figures

- continued -

List of Figures

- continued -

List of Tables

Section 1

SUMMARY AND CONCLUSIONS

STUDY DESIGN

The initiating factor of the development of a thermal layer by an air burst nuclear weapon over a non-ideal ground surface is the blow-off of soil. This report describes a study designed to provide an understanding of soil blow-off phenomenon caused by nuclear thermal radiation. Its purpose is to allow some predictive capability based on an empirical understanding of the underlying physical and chemical processes studies. The objectives of this task are to provide a compendium of the results of soil irradiation tests, summarize data on basic soil types and give an indication of scaling of these data.

This work is based on a series of 303 tests on 25 soil types at heating rates of up to 80 $cal/cm^2 sec$. Solar furnace irradiation was used in order to accurately reproduce nuclear thermal radiation in spectrum and timing[1]. However, due to experimental necessity the tests are inherently two dimensional whereas the nuclear effects are expected to be largely one dimensional in character. The tests reported relate to the initial soil blowoff and layer creation but not to the fully developed layer. Thus in the tests reported here such properties as flow fields will diverge strongly when far from the surface source. For this reason all appropriate quantities are measured as close to the soil surface as practical. This gives an approximate simulation of the one dimensional situation. Readers are cautioned in using the results beyond the near surface for application to the nuclear (1-D) problem without taking into account the different geometry. An extrapolation of this data to a fully developed thermal layer via hydro and thermodynamic methods has been performed under separate contract[2,3].

The study has included a measure of the flux and fluence thresholds for soil blow-off and their dependency on a number of parameters such as soil moisture, irradiation time, and flux (in the case of the fluence threshold). The study was designed to measure tempera-

tures in the air and under the soil surface during blow-off, amount and velocity of blow-off as a function of irradiation and moisture, and numerous soil properties.

The blow-off obscuration of the soil and attendent volumetric air heating were not fully simulated, but calculations taking into account the two dimensionality of the tests were made. A prediction based on these data can be made about the effect the blow-off would have in a one-dimensional case. The experimental work was undertaken in Spring, 1974 by Science Applications, Inc., under contract DNA001-74-C-0229. A year later a two-volume report, DNA 3723F-1 and -2, was issued covering 157 soil tests made during the first year of the study[1]. The first year was devoted to an initial qualitative study of blow-off and to instrumentation development; the second year concentrated on careful parametric studies of certain soils of special interest (e.g., NTS)*. This present report covers over 300 tests performed during the two-year period and aims at developing quantitative and predictive information on the general area of soil thermal response. Results of this project have been introduced directly into the SAI thermal layer model, a separate effort to understand theoretically the behavior of soils under nuclear thermal heating conditions.

THEORETICAL BACKGROUND

Weapon thermal radiation impinging on an ideal surface will be reflected without surface heating, degregation or near surface air heating. Most surfaces are non-ideal, and do heat appreciably causing surface degredation-dust generation (popcorning) and conductive near surface heating. The thermal layer of the heated near surface air is further heated by weapon radiation attenuation in the dust material. The thermal layer created by weapon thermal output coupled to a non-ideal surface causes ideal blast wave deformation in the form of a precursed blast wave. An experimental program was desgined and undertaken to simulate the thermal coupling to soil. The key parameters

---

* Nevada Test Site

used were the soil conditions leading to dust generation and the subsequent air heating. Figure 1 shows schematically how a precursor blast wave develops. The surface conditions, the shock wave strength, and the thermal radiation prior to shock arrival all contribute to precursor formation. Actual test data on a precursor development over various surface conditions are shown in Figure 2, which is a composite of test data on blast waves and calculated thermal flux and fluence levels. Note that the precursor forms at a ground range of around one fireball radii (180 scaled feet) and attenuates past to about 5 radii [about 900 scaled feet for this particular shot (Teapot-Met, 22.5 KT at 400 ft)]. Extensive analysis of precursor formation conditions over NTS soils (alluvial playa) has yielded an HOB vs. ground range map of the precursor. This is developed in more detail in Section 2, which is a description of the physical basis for thermal layer development. See Reference 1 for more details.

The results of the experimental program summarized in this report provide basic input to non-ideal blast wave calculations. These in turn relate to system interests in a number of defense projects, such as the knowledge of the reduced blast over pressure, and increased dynamic pressure and dust loading for non-ideal waves. Figure 3 shows schematically the interrelation of the various elements of the program in non-ideal blast waves. Table 1 provides a series of examples of system interests in non-ideal blast wave phenomenon.

SUMMARY OF THE TEST PROGRAM

The test program was designed to simulate the soil response to a nuclear thermal pulse. The test setup in the White Sands Missile Range (WSMR) solar furnace test house is shown in Figure 4, and a picture of the furnace itself in Figure 5. The nature of the tests is inherently two dimensional. Despite this, the analysis is performed in such a way that these effects are minimized. The tests were designed to determine the air temperature and dust loading experienced under simulated nuclear burst conditions prior to shock arrival. This so-called "thermal layer" is the source of both sweep-up dust and non-ideal blast wave behavior. The key physical parameters that were measured in each test were:

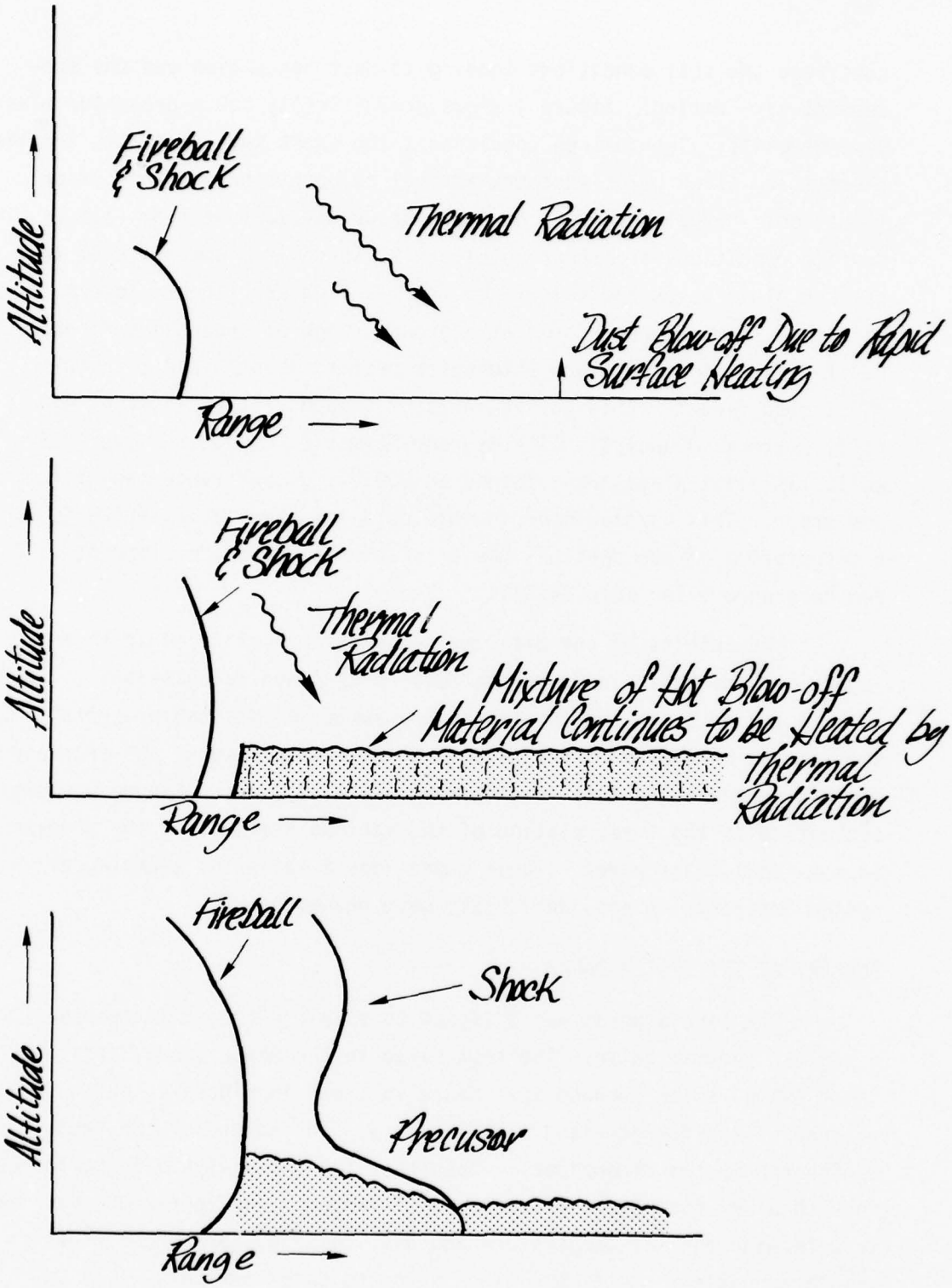

Figure 1. Schematic Representation of Fireball and Shock Wave Effects over a Real Surface, Shown in Three Stages as Shock Develops

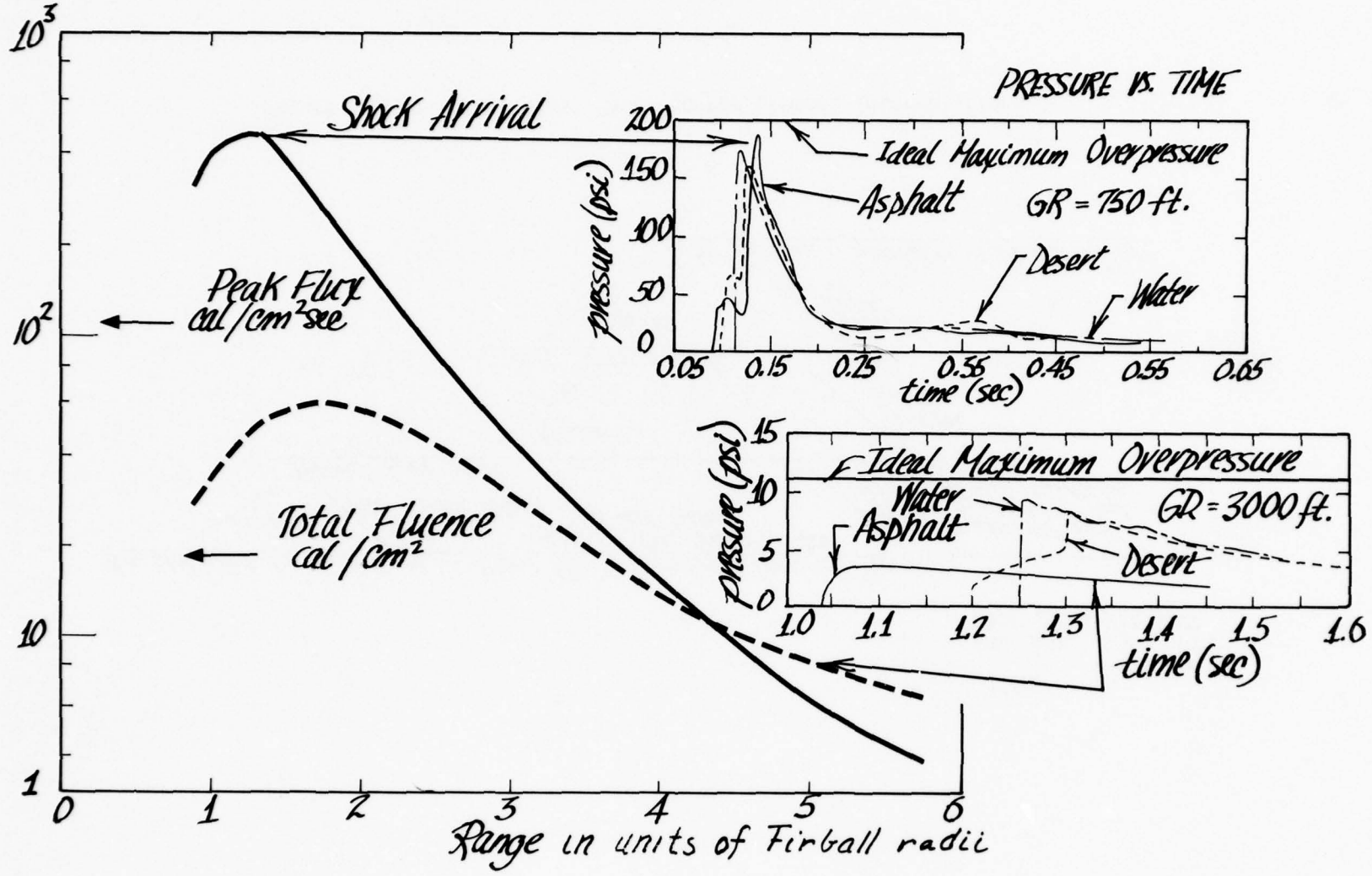

Figure 2. Blast Wave Precursor Development in Shot MET (22.5 KT at 400 ft)

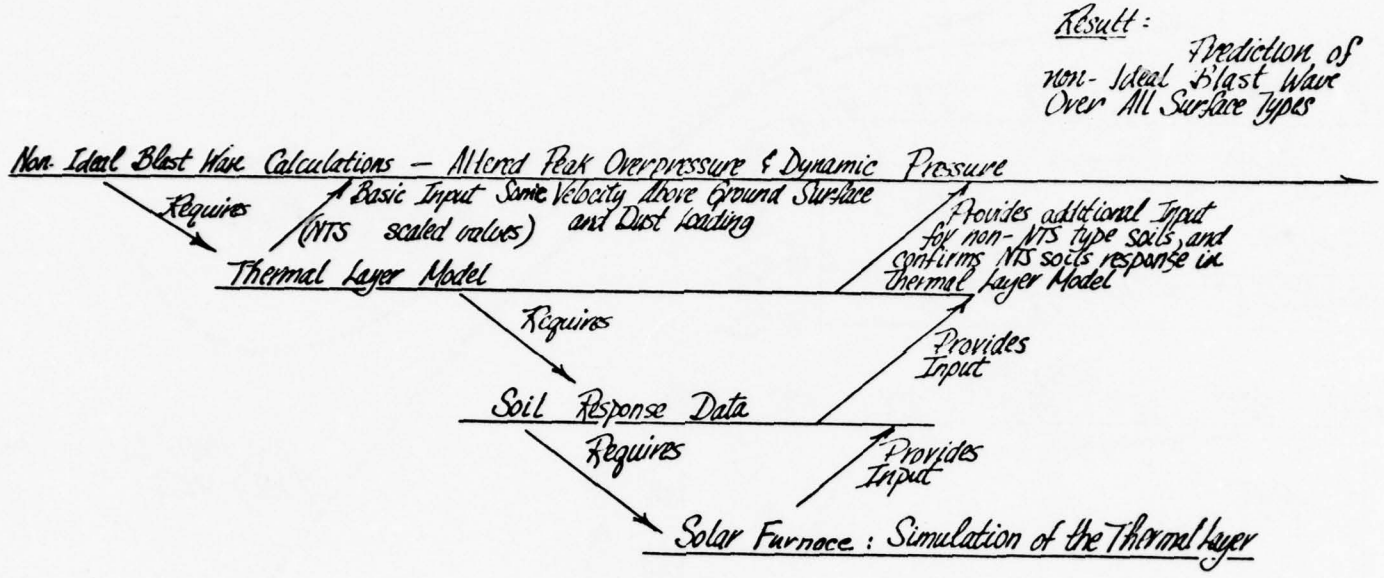

Figure 3. Non-Ideal Blast Wave Program Element Interrelations

Table 1. Examples of Program Related System Interests In Thermal Layer Developments

PROGRAM	SYSTEM INTEREST	GEOPHYSICAL SOIL DESCRIPTION	SOIL CONDITIONS	KEY PARAMETERS
NTS VERIFICATION	• INTERPOLATE PRECURSOR FORMATION CONDITIONS • EXPERIMENTAL VERIFICATION OF OVERPRESSURE AND DYNAMIC PRESSURE WAVEFORM	• ALLUVIAL FAN OR PLAYA • DESERT	• NO VEGETATION USUALLY VERY DRY -	• HEIGHT AND TEMPERATURE IN THERMAL LAYER FOR LOW YIELDS
MINUTEMAN	• STRUCTURAL HARDNESS VARIFICATION TO NON IDEAL BLAST WAVES	• MIXED GEOLOGICAL ORIGINS, MID LATITUDE STEPPE	• VEGETATION IS FREQUENTLY PRESENT • MOIST	• AS ABOVE, ALSO DUST LOADING CAUSING INCREASED DYNAMIC PRESSURE BUT FOR LARGE YIELDS.
TRIDENT	• DUST SWEEP UP IN STEM LEADING TO FRATRACIDE	• MIXED - GEOLOGICAL ORIGIN MOSTLY - HUMID PLANES, MID LATITUDE	• VERY FREQUENT SNOW COVER, VEGETATION	• DUST LOADING OF LAYER FOR TRIDENT HOB AND YIELD
MX	• SYSTEM HARDNESS VALIDATION ENVIRONMENT	• ALLUVIAL FAN OR PLAYA • DESERT	• PROBABLY NO VEGETATION. MOISTURE AND SNOW COVER MUST BE STUDIED PARAMETRICALLY	• AS ABOVE, BUT FOR THREAT YIELDS AND HOB's AT OR NEAR HARDNESS LIMITS FOR IDEAL BLAST WAVE CONDITIONS
THEATER NUCLEAR WEAPON	• Target and Collateral Damage by Air Blast	• MIXED - AS TRIDENT	• Variable	• AS ABOVE, LOW YIELD AIR BURST THERMAL LAYER

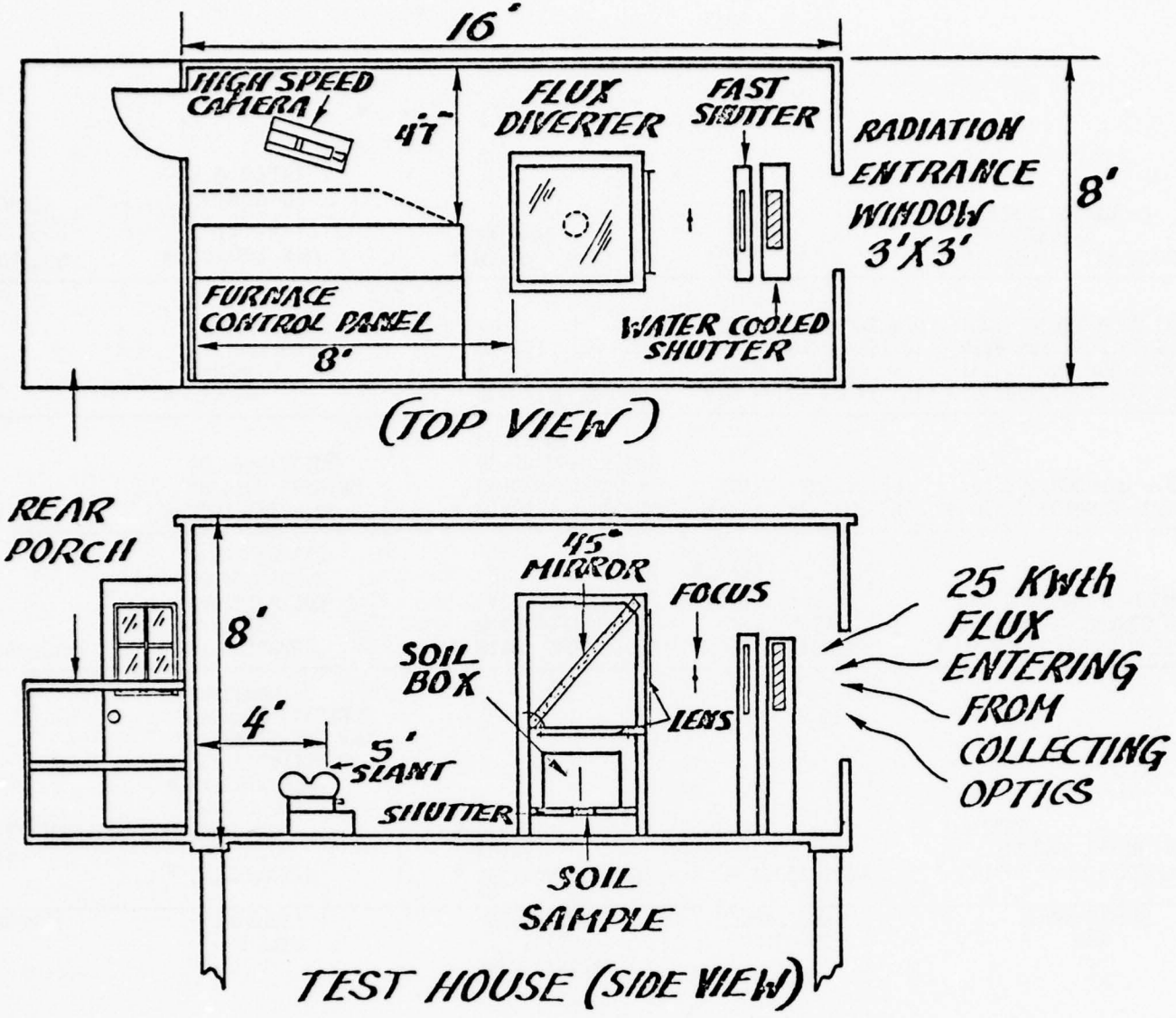

Figure 4. Experimental Set-Up Inside the WSMR Solar Furnace Test House

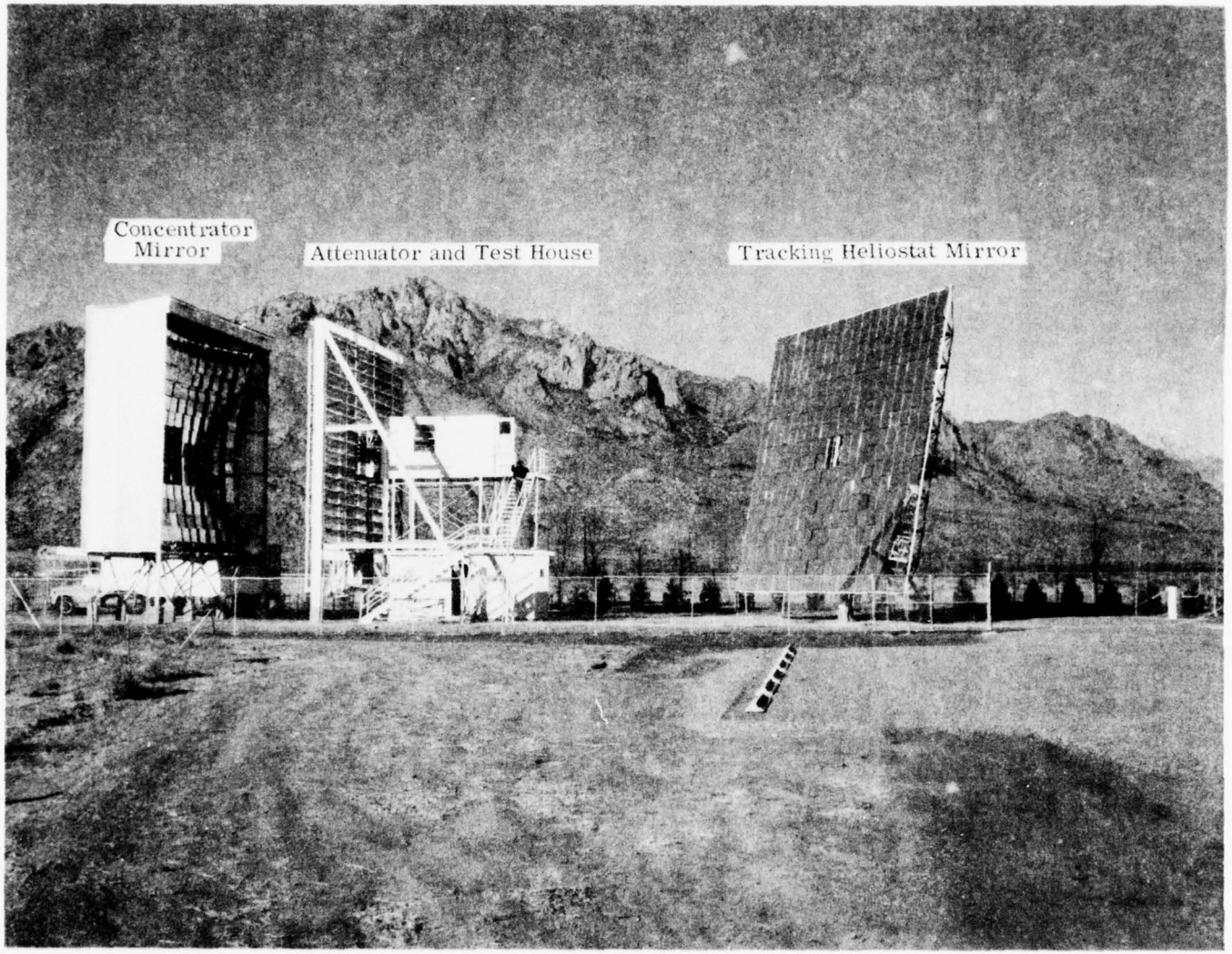

Figure 5. WSMR Solar Furnace (U.S. Army Photo)

- Incident radiation at soil surface
- Scattered radiation
- Soil temperature
- Air temperature at various heights above heated air
- Blow-off type, threshold in flux and fluence
- Initial blow-off velocity
- Mass of blow-off per unit area and per unit irradiation

In addition, for the various soil types the following were measured:

- Grain size
- Natural moisture content
- Presence or absence of vegetation/organics
- Albedo
- Differential thermal analysis scan.

Key correlations were anticipated between various initial soil conditions and blow-off phenomenon and the results bear out this expectation. The development of the thermal layer was highly dependent on the amount of radiation and the soil properties, and specifically, the driving mechanism of thermal layer formation (the blow-off material) was of four distinct types:

- Smoke emanating from nearly all soil types at a threshold level of about 5 cal/cm^2 fluence and 7 cal/cm^{2}sec flux. Smoke rises initially at 0.25 to 0.5 m/sec and is entrained in air that is rising in temperature at about 50^{o}K/(cal/cm^2) near the surface. The mass of the smoke particles is extremely small and its attenuation close to the soil surface is small.

- Small particles emitted by most but not all soil types at thresholds that range from 5 to 25 cal/cm^2 fluence, and 7 cal/cm^{2}sec flux. Particles rise at from 0.5 to 2 m/sec. Abundant particle ejection is accompanied by high obsuration values. The mass loss of particles is highly variable depending especially on soil moisture content.

- Fast particles, jets, or flakes explosively emitted from soils containing abundant clays. Their threshold is in the range 25 to 50 cal/cm^2. Although specialized to certain soil types and flux regions, this type of emission is abundant, and violent, when it occurs. Jet velocity up to 10 m/sec has been recorded. The particle sizes are quite large (over 100μ) on the average and are often in a flake form.

- Steam emitted from all moist soil samples. It is more noticeable above 5% moisture content in soil by weight. It has a profound effect on air temperature - holding it at 100°C until the soil moisture is driven off. Several cal/cm^2 are required per % moisture to dry the soil. Steam is transparent, but does contribute markedly to the mass loss of the soil.

Based on these distinctions and using available data and soil types, a composite summary of thermal layer data was compiled. The twenty-five soil samples are aggregated into seven key generic soil types and the geological and physical data obtained from each are shown in Table 2. This table contains essentially all the results of the present program, although in highly abbreviated form. It is useful to review this information for general orientation on thermal layer development. In the remaining sections of this report the studies made of each soil sample of the various physical quantities are shown in detail.

Certain general observations emerge after consideration of Table 2.

Fluence Scaling. The data show that in most cases fluence by itself is an adequate scaling variable for the complex processes that go into thermal layer development.

Flux Independency. Data on thermal layer properties are largely independent of flux within the range studied.

Moisture Dependency. Many parameters of blow-off depend upon moisture content of the soil, particularly in sands and in alluvial playas.

Thermal Erosion. Weight losses of the order of 5 10^{-4} g/cm^2 are experienced in the tests. Based on a mean grain size of between 5 and 200μ, this corresponds to between 1 percent (for 200μ) and 40 percent (for 5μ) thermal erosion (weight loss per thickness of monolayer per cal/cm^2). In general a monolayer will attenuate 1/e of the optical energy. A 3-monolayer thickness may be considered as the diathermanous soil layer that drives the thermal layer development. Thus for large grain size a very small fraction of the diathermanous layer is lost, even for significant irradiation. On the other hand, for fine clays (few μ size particles) thermal erosion can be complete. This was experimentally verified with Sample No. 8.

Table 2. Summary of Soil Blow-Off Data[1]

Physical Description and Data / Soil Types	Pure Clays	Pure Sands	Top Soils Eastern US	Minuteman Sites	Alluvial Playas Frenchman Flats	Yucca Flats	Tularosa Basin
Geophysical Soil Description:							
Formation Geography	Fluvial	Littorial	Fluvial Humid Mid Latitude	Glacial Mid Latitude Steppe with Vegetation and Organics	Alluvial Desert	Alluvial Desert	Alluvial Desert
Physical Properties[2]	High Albedo (~30%) Mean Grain Size About 10μ	Very High Albedo (~40%) Mean Grain Size about 100μ	Vegetation Cover Low Albedo Grain Size~50μ	Very Low Albedo Mean Grain Size in Range 50-100μ	High Albedo (~30%) Mean Grain Size 150μ	High Albedo (~30%)	High Albedo (~30%) Mean Grain Size 5μ
Blow-Off Fluence Thresholds:[3]							
Smoke (cal/cm^2)	4	6	4	5	7	Little or no Smoke Activity	7
Particulate (cal/cm^2)	4 Small Particles 10-30 Large Flakes (At High Flux Only)	5-20 Depending on Moisture	7- and Higher Depending on Soil Type	None Observed	6	16	10-20
Initial Velocity							
Smoke (m/sec)	0.5	0.5	0.5	0.3 to 0.6	0.2 to 0.5	None observed	0.4
Particles	Up to 10.0 for Large Particles	1 to 2	1.0	None Observed	0.5 to 1.5	1 to 3	1 to 2
Normalized Weight Loss x 10^4 gm/cal	6	4 (Function of Moisture)	N/A	3 to 6.5	3	5 Depends Strongly on Moisture	2 to 3
% Obscuration (At 2 sec for Q = 20 cal/cm^2 sec)	30 to 50	% for Dry Sands - Up to 50% for Very Wet	Low	N/A	40% For Dry Sample -- Decreases with Moisture	Very low	0% for Dry Samples Up to 50% for very Moist Samples
Q_2/% Moisture (cal/cm^2/%)	3	Depends Strongly on Moisture[4]	N/A	2	Small	2	N/A
Air Temperature ΔT/ΔQ at ¼"(°K/cal/cm^2)	15	3		40	50	50	
Remarks	Pure clays exhibit unique blow-off mechanisms--very fast particle and flake blow-off.	Particulate blow-off highly dependent on moisture.	Sparce particulate blow-off	Glassy layer formed on surface		Absence of smoke is a unique feature. Weight loss is for 5% moisture in natural state.	

1) Based on 273 tests of 25 separate soil samples over a flux range of 5 to 80 cal/cm^2 sec, table values are independent of flux unless noted.
2) Samples were investigated in both natural moisture states, dried, and for various degrees of added water, unless noted table values refer to all moisture states.
3) Thresholds are independent of flux over a range 7 to 80 cal/cm^2 sec within a factor of 2. The main flux dependent effects are observed from flux threshold of about 7 cal/cm2 sec to about 15 cal/cm^2 sec however. See Figures 10 and 11 for further data.
4) The low value of air heating is accompanied by very high temperatures in the sand substrate.

Blow-off Particle Size Correlated with Ejection Velocity. As is anticipated from aerodynamic arguments, the larger size ejected particles are associated with larger velocities. A $v^{\frac{1}{2}}$ dependency, implying constant ejection energy and laminar drag loss seems to agree with these data.

Program Milestones

An historical look at the program is provided in Table 3. This gives a summary of the key points of the program and important milestones in simulating thermal layer formation.

Table 3. Overview of Experimental Test Program

	DATE	PURPOSE	ACCOMPLISHMENTS
PHASE 1	May 23 to 25, 1974	Initial Site Inspection	Furnace Operation Understood
	June 1974	Soils Tests at McLean, Va. Small Solar Furnace	Heating Rates to 80 cal/cm^{2}sec Achieved
	July 8 to 12, 1974	Furnace Calibration Diverter Materials Test Initial Soil Response Tests	25 KWth Peak Power Measured
	August 5 to 10, 1974	High Speed Photography Tests Installation of Diverter Soil Response Tests	Initial Soil Response Data Obtained
	September 15 to 28, 1974	Installation of High Speed Soil Catch Shutters Peak Air and Soil Temperature Indications Obtained Obscuration Tests Made Final Soil Response Tests Made	Final Soil Response Data Obtained
	April 15, 1975	Final Report Issued DNA 3723F-1 and 2	Total of 127 Data Runs Made in Phase 1 in Approximately 20 Days Running at WSMR
PHASE 2	March 18 to 21, 1975	Tests of NTS Soils	42 Runs Conducted
	June 2 to 6, 1975	Test of Aspirated Thermocouples	47 Runs Conducted Air Temperature Measurements Validated
	August 11 to 22, 1975	Final Data Runs at up to 57 CAL/CM^2 SEC Peak Flux	57 Runs Conducted, with Air Temperature Data Obtained
	May 1976	Interim Report on Phase 2 Tests Issued	Total of 146 Data Runs Made in 20 Days Running at WSMR in Phase 2
PHASE 3	March 1976	Initial Go-Ahead for Planning of CNRS	Tests up to 200 CAL/CM^2 SEC Are Planned. Program to be Completed by mid 1977.

Summary: 273 soil tests at up to 57 cal/cm^{2}sec were performed, a total of 320 hours of solar furnace time was utilized at WSMR and over 30 tests at the small SAI solar furnace in McLean, Va. at up to 80 cal/cm^{2}sec were performed.

WSMR - White Sands Missile Range Solar Furnace
CNRS - French Solar Furnace, See Vol. III

Section 2

PHYSICS OF THERMAL LAYER DEVELOPMENT

WEAPON OUTPUT SCALING CONSIDERATIONS

Significant statements concerning nuclear weapon effects involve the scaling of these effects with weapon yield, W. Effects such as air blast and thermal radiation tend to scale by different laws as are summarized below.

Air Blast. Experience has shown that hydrodynamic scaling ($W^{1/3}$) usually holds except in the non-ideal blast wave region. Precursors (non-ideal blast waves) are created under certain conditions of yield, surface HOB, and range. Figure 6 shows generally the allowed and forbidden regions for precursor formation for a 1 KT weapon (see reference 2 section 2.3.2). The problem in scaling to other yields is that thermal effects do not scale as the hydrodynamic variables. Figure 6 has only been verified in the restricted range 1 to 60 KT[2,3].

Thermal Radiation. Figure 7 shows the flux and fluence for two yields and three HOBs. The scaling of thermal effects is more complex than blast. Thermal energy output scales as W. Thermal power scales as $W^{.59}$ while the area for the same hydrodynamic levels scales as $W^{.66}$. Flux per unit area at the same hydrodynamic scaled range will show an increase of 1.6 times from 1 MT to 1 KT. Figure 7 shows this effect at times long with respect to thermal maximum. Fluence per unit area will scale as $W^{1/3}$ on the other hand. This again is seen in Figure 7 at late times. At early times the situation is complex. Shock arrival scales as $W^{1/2}$ in regions of interest, while t_{max} (time to second maximum scales) as $W^{.44}$. In general an extra $W^{.06}$ correction factor should be included at early times. In practice it is probably easier to compute flux and fluence to shock arrival for cases of interest. The lack of thermal/hydrodynamic scaling is further exacerbated by non-scalable ground response. Added to this is the variability of ground surface and the effect of cloud cover. The latter could reflect the thermal radiation, greatly increasing surface effects.

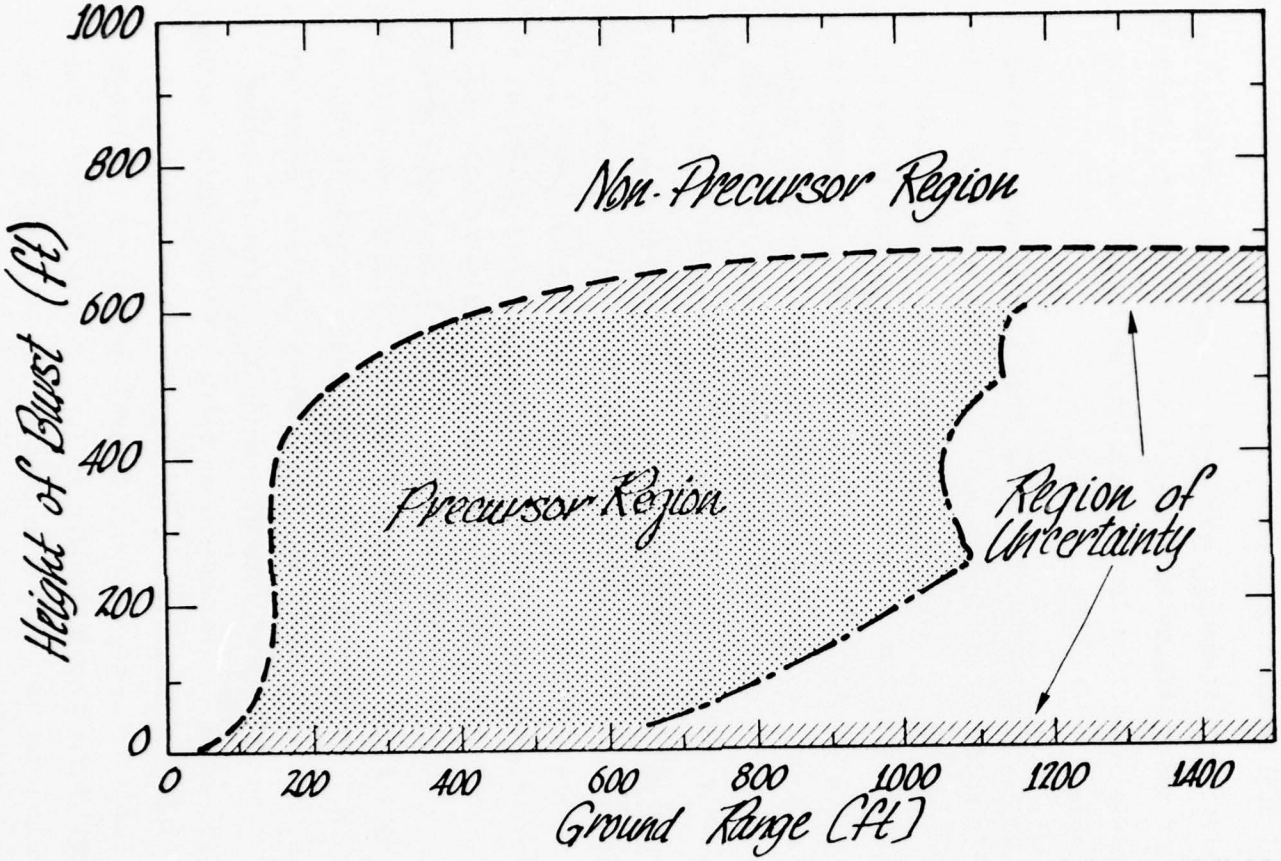

Expected Range of Validity 1 to 60 KT

Figure 6. Precursor and Non-Precursor Regions for 1 KT Case

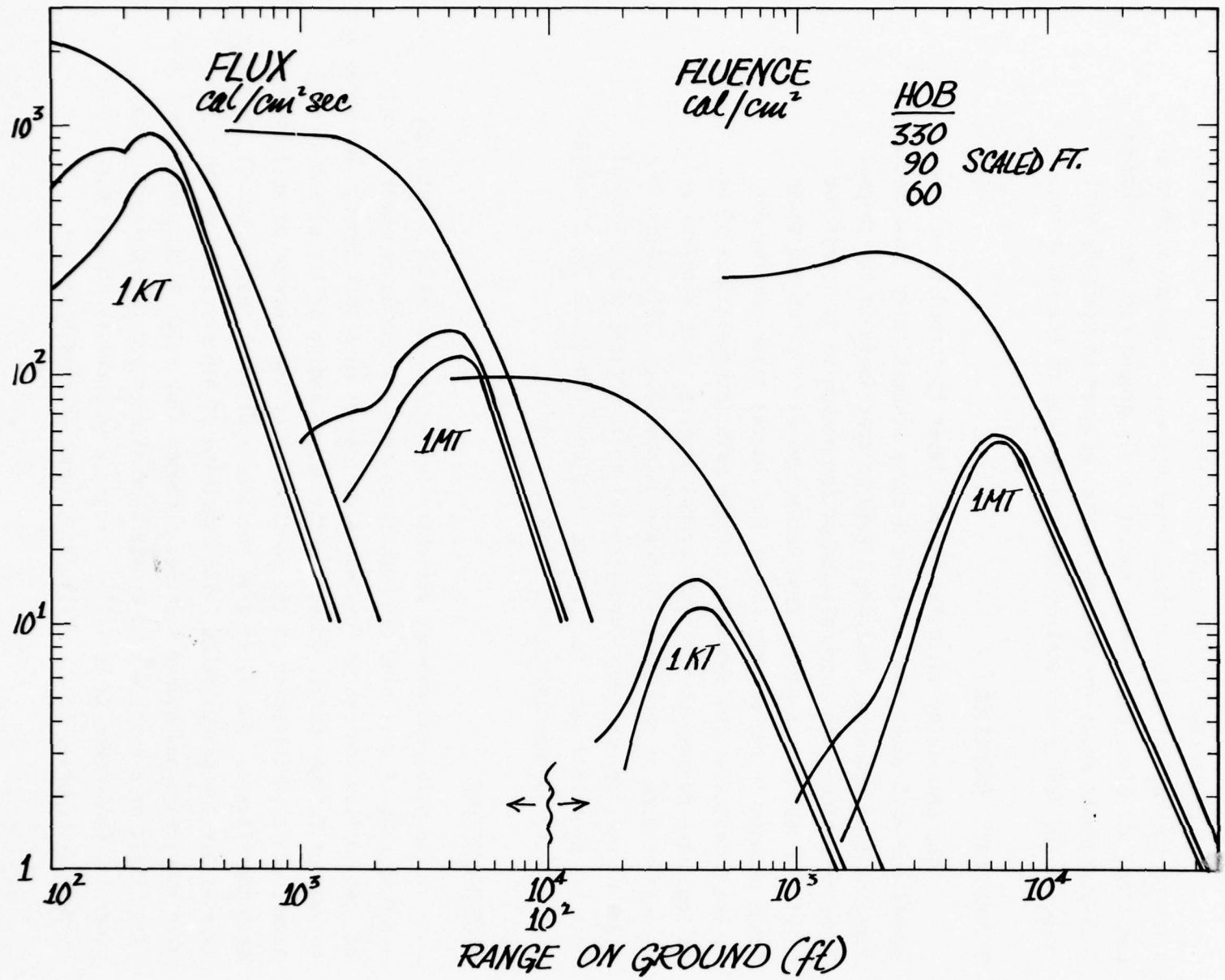

Figure 7. Weapon Thermal Flux and Fluence Output

The conclusion of the study of scaling is that only a combination of theoretical and empirical arguments will allow prediction of non-ideal air blast and thermal radiation via ground response (blow-off). Such statements argue for an experimental program to quantify soil response and deduce the scaling laws appropriate to the situation.

THERMAL LAYER FORMATION

The process by which the thermal layer is formed is neither simple nor well understood. Figure 8 shows schematically those mechanisms, in time sequence, that are likely to contribute to the thermal layer formation. The intrarelation of the mechanism is itself not simple in concept. Feedback type mechanisms exist which can cause large changes in the progression of the thermal layer development. Figure 9 indicates the complexity of the main interrelations of processes. The purpose of the experimental program is to simulate and measure as much of the initial process as possible. This leads to a model of the thermal layer formation for soil surfaces whose blow-off data has been recorded. Such a model has been developed under separate contract and is reported in reference 3.

RECOMMENDATIONS

The data, and summary presented in this volume allow a detailed understanding of soil blow-off phenomenon over a range up to about 30 cal/cm^2 sec in flux and over a reasonable variety of bare soil types. Two areas are in need of further work. These are the understanding of the effect of soil cover, and a verification of the consistency of the behavior of soil blow-off at higher fluxes. The first area requires additional testing but of the same type as already accomplished. The attaining of higher fluxes on the other hand requires a new source - either a higher flux solar furnace (described in Vol. III), or a novel way to create thermal energy, a thermochemical flash generator (described in Vol. II). Progress in understanding of both these sources is reported in the remaining volumes of this report.

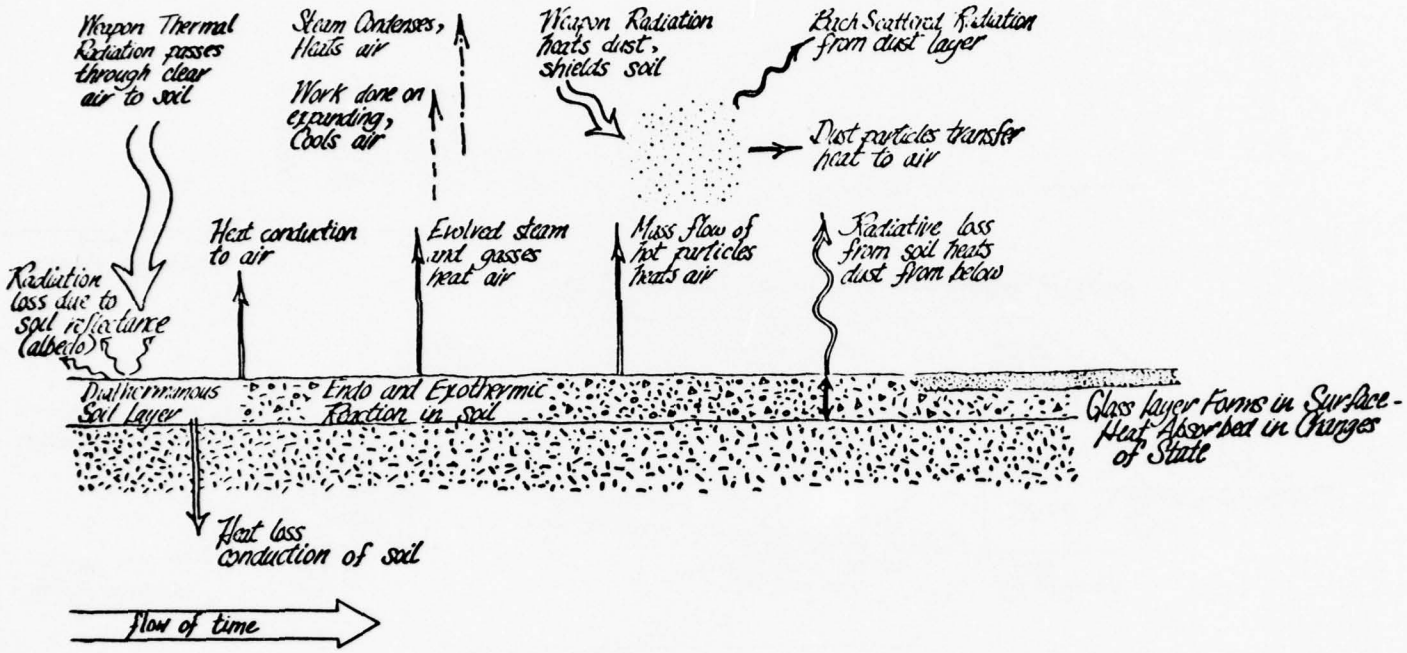

Figure 8. Schematic Representation of Thermal Layer Development

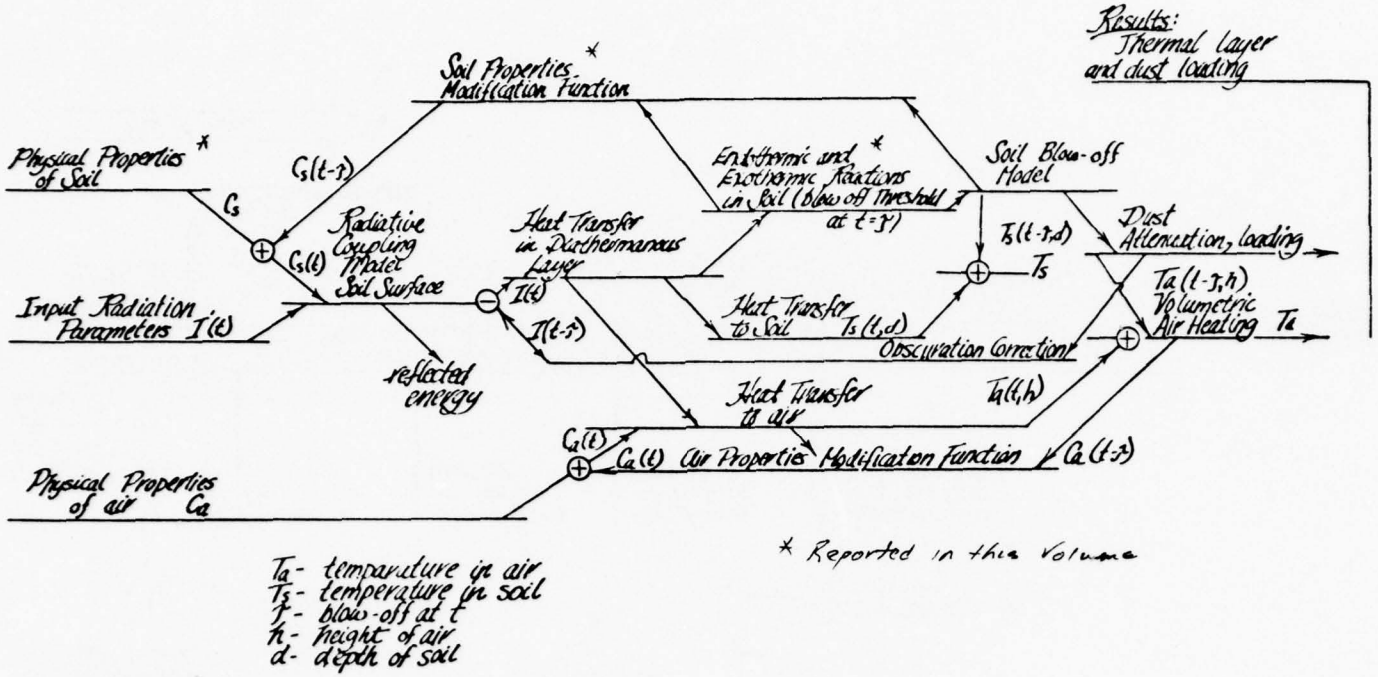

Figure 9. Interrelationship of Physical Phenomena Causing Thermal Layer Development

Section 3

SOIL GEOLOGY

GENERAL

In consideration of the effects of soil geologic conditions upon dust lofting and thermal layer formation, the soil type must first be determined. Engineering soil types are established on the basis of soil formation, geography and physical properties. Among the latter are grain sizes (coarse gravels to fine silts and clays), texture and plasticity, as well as other physical characteristics. The texture of a soil affects its ability to absorb water, and to absorb heat and air. The affinity of various soil types to retention or permeation of moisture varies greatly. Another important and generally overlooked aspect of soil moisture is the presence or absence of organic materials ranging from sparse (but possibly deep-rooted) vegetation in arid areas to thick grasses and bush in more humid areas. Thus, it is essentially the surface characteristics of the upper horizons of the soil that determine the properties of soil relevant to thermal layer formation; therefore attendent moisture and organic material need to be well documented. NTS soils are dry playas, former lake beds that covered the area in Pleisotocene Time, during the melting of the continental glaciers. As such they are far from typical of what may be termed "normal world soil types." The climate is arid and the soils are fine, with silts and clays predominating. Vegetation is minimal and as such has a minimal interaction with dust cloud formation and ejecta size. Wind generated dust is common. On the other hand, moist soils and associated vegetation, as found at Minuteman sites (Great Falls), are for more analogous to temperate-zone soils, worldwide. A summary of geophysical characterization of soils is given in Table 4.

MOISTURE CONTENT AND PLASTICITY

Moisture content and soil plasticity are the major characteristics in determining behavior in the nuclear burst environment. These characteristics are particularly important in inorganic soils, and in areas with minimal vegetation.

Table 4. Geophysical Classification of Soils

Soil Formation

- Atmospheric disintegration of rock
- Aqueous disintegration of rock
  - Chemical in-situ deposits in springs and lakes
  - Mechanical erosion, transportation and deposition
    - Fluvial - river
    - Alluvial - flood plain, fan or playa
    - Glacial
    - Estuarine
    - Lacustrine
    - Marine
    - Aeolian
    - Littorial - coastal
- Igneous formation - i.e., lava.

Physical Geography of Soil

- Location: Latitude
- Moisture: Humid or Desert
- Terrain: Mountain, Hills, Plateau, Plain
- Vegetation: Forest, Lakeland, Steppe, Grassland
- Cover: Tundra, Glacial, Snow Lake

Physical Properties of Soil

- Particle Size
  - Boulder
  - Cobble
  - Pebble
  - Granule
  - Sand
  - Silt
  - Clay
- Heat Conductivity
- Albedo
- Mechanical strength, shear, compression
- Plasticity
- Water Retention
- Organic Composition
- Mineral Composition

Factors Determining Soil Moisture Content

- Porosity - Ratio of volume of voids to total soil aggregate (common definition of "aggregate" refers to the entire soil mix, and not its components or most significant parts).
- Void - That portion of soil aggregate not occupied by mineral grains or organic matter; may be expressed as ratio or percentage.
- Water Content - Ratio of dry weight of aggregate to weight of water.
- Degree of Saturation - Water content expressed as ratio per unit volume. Identical coarse sands located above the water table are usually "humid" in temperate climates, "dry" in arid (e.g., NTS) climates. Finer sands, incorporating greater volumes of silt, are more likely to become moist, wet, or saturated (see Table 5 for terminology distinctions). Clays, on the other hand, are almost always saturated, except in surface soils that are subject to immediate local variations in temperature and moisture.

Table 5. Degree of Saturation of Sand in Various States

Condition Description	Degree of Saturation (%)
Dry	0
Humid	1-25
Damp	26-50
Moist	51-75
Wet	76-99
Saturated	100

- Unit Weight - The unit weight of the soil aggregate is the weight of the soil plus water per unit of volume and depends upon three factors:
  - Weight of the solid constituents
  - Porosity of the aggregate
  - Degree of saturation
  - Liquid limit - The maximum ratio of water to soil that still forms a cohesive soil mass.

Table 6 presents major soil types in the context of porosity, void ratio and unit weight. It is important to note that these represent the characteristics of soils in their natural state. The process used in preparing tests at sites ranging from the NTS to Ft. Polk, Louisiana seriously

Table 6. Porosity, Void Ratio, and Unit Weight of Typical Soils in Natural State (from Reference 4)

Description	Porosity (%)	Void Ratio	Water Content (sat % of dry wt)	Dry Unit Weight (grams/cm^3)	Saturated Unit Weight (grams/cm^3)
Uniformed-grained sand, loose*	46	.85	32	1.43	1.89
Uniformed-grained sand, dense*	34	.51	19	1.75	2.09
Mixed-grained sand, loose*	40	.67	25	1.59	1.99
Mixed-grained sand, dense*	30	.43	16	1.86	2.16
Mixed-grained glacial till**	20	.25	9	2.12	2.32
Soft glacial clay**	55	1.2	45	"dust"***	1.77
Stiff glacial clay**	37	.6	22	***	2.07
Soft, slightly-organic clay	66	1.9	70	****	1.58
Soft, very-organic clay	75	3.0	110	****	1.43
Soft Bentonite	84	5.52	194	****	1.27

* Characteristic of NTS sites (Pacific sites have coral-formed sands of considerably differing physical characteristics)

** Characteristic of Suffield and Grand Forks Area

*** Such clays do not retain homogeneity in dry state, identifiable as "clays"

**** A weathered clay, primarily of volcanic origin, most prevelent in U.S. West, but occurs worldwide. Exposures noted in the Grand Forks area, beneath and intermingled with the glacial till

disturbs the soils in the area. Therefore, both dust clouds and thermal layers do not necessarily react as similar surface materials would in a natural and undisturbed state.

Liquid Limits and Plasticity

An examination and postulation of behavior of various soil types as components of dust clouds must consider liquid limits and plasticity. These two factors are significant in establishing cohesiveness and the probability of the soil breaking down into individual grains or particles under externally-induced forces inherent in a nuclear burst.

One of the most important characteristics of a given soil type, in the context of its behavior under varying moisture contents, is its plasticity. Soil plasticity is expressed in terms of "Atterberg Limits." The Atterberg Limits are simply:

- Lower Plastic Limit - That state in which water is added to or absorbed by dry, non-cohesive soil that gradually becomes cohesive, starting with the formation of lumps and gradually getting to a point which permits rolling like dough in a single mass. The weight of water thus absorbed, as a factor of the weight of the dry soil, establishes the lower Atterberg limit.
- Upper Plastic Limit (or "liquid limit") - That state in which additional water is added until the soil approaches the state of a viscous liquid. The weight of water thus added establishes the upper Atterberg limit.
- The difference between the liquid limit and the plastic limit establishes the plasticity of the soil, and determines the "plasticity index" typically cited in an engineering description of a soil.

Non-plastic soils, such as most sands and some silts, will never achieve a lower plastic limit, and thus no cohesion will occur. Non-cohesive soils may appear to be cohesive if a heavy vegetation mat is present.

SIZE DISTRIBUTION

Test data from a large number of HE shots were reviewed in an SAI environmental defense study.[5] For cohesive soil types, the power law distribution given by $dn/da=a^{-3.5}$, where a is the average particle diameter,

Table 7. Summary of Solar Reflectance Data for Earth Features and Clouds (adapted from NASA CR 83954)[6]

Surface	Magnitude and Other Spectral Characteristics	Angular Distribution of Reflectance	Total Reflectance
Soils and Rocks	Increases to 1 μm Decreases above 2 μm.	Backscattering and forward scattering. Sand has large forward scattering. Loam has small forward scattering.	5 to 45 percent. Moisture decreases reflectance by 5 to 20 percent. Smooth surfaces have higher reflectance. Diurnal variation. Maximum reflectance for small Sun angles.
Vegetation	Small below 0.5 μm. A small maximum bump at 0.5 to 0.55 μm. Chlorophyll absorption at 0.68 μm. Sharp increase at 0.7 μm. Decrease above 2 μm. Depends on growing season.	Backscattering. Small forward scattering.	5 to 25 percent. Diurnal effects. Maximum reflectance for small angles. Marked annual variation.
Water Basins	Maximum at 0.5 to 0.7 μm. Depends on turbidity and waves.	Large back and forward scattering.	5 to 20 percent. Diurnal variation. Maximum for small Sun angles depends on turbidity and waves.
Snow and Ice	Decreases slightly with increasing wavelength. Large variability depends on purity, wetness, and physical condition.	Diffuse component plus mirror component. Mirror component increases with increasing angle of incidence.	Variable 25 to 80 percent. 84 percent in Antarctic. 74 percent in Ross Sea ice. 30 to 40 percent in White Sea ice.
Clouds	Constant from 0.2 μm to about 0.8 μm. Decreases with wavelength above 0.8 μm, showing water vapor absorption bands.	Pronounced forward scattering with small backscattering. Minimum for scattering angles of 80° to 120°. Fogbow* for scattering angle of 143°.	10 to 80 percent Varies with cloud type, cloud thickness, and type of underlying surface.

*A nebulous arc or circle of white or yellowish light sometimes seen in a fogbank.

Table 8. Soil Samples Used in Test Program

NUMBER	GENERAL TYPE	SPECIFIC LOCATION	AS RECEIVED MOISTURE (SEE TABLE 5)	ALBEDO %	PRESERVED ORIENTATION	SAI* TYPING	MEAN DIA (micron)
1	SAND	CONCRETE MIX	DRY		NO	SC	450
2	SAND	SPRINGFIELD, VA.	HUMID	30	NO	SM	200
3	LIME	CONCRETE MIX	DRY	62	NO	SECONDARY MATERIAL CL	270
4	TOP SOIL	MCLEAN, VA. (TMK)	(VEGETATION) DAMP	22	YES	ML	30
5	TOP SOIL	ANNANDALE, VA.	HUMID	25	YES	CL	90
6	TALC	DRUG FAIR	DRY	45	NO	(CL)	15
7	SAND	FABENS, TEXAS	HUMID		YES	SP	200
8	CLAY	STONEWARE CLAY	DAMP	40	NO	CL	4-5
9	TOP SOIL	WHITE SANDS MISSILE RANGE	DRY		YES	SW	280
10	SAND	CAPE HATTERAS, N.C.	DRY		NO	SP	180
11	TOP SOIL	MCLEAN, VA. (SAI)	(VEGETATION) DRY		YES	ML	40
12	TOP SOIL	AF #1	DRY	35	YES	SM	4
13	TOP SOIL	AF #2	DRY	32	YES	SM	5
14 (14')	TOP SOIL	NTS FRENCHMAN FLATS	HUMID		NO		70-280
15	SAND	WHITE SANDS MISSILE RANGE	DRY		NO		
16	CLAY	KAOLINITE	DRY		NO		
17	CLAY	PYROPHYLLITE	DRY		NO		
18	CLAY	MONTHMORILLENITE	DRY		NO		
19	TOP SOIL	NTS YUCCA FLATS	6%		NO		
20	TOP SOIL	PEARLITE	DRY		NO		
21	TOP SOIL	NTS YUCCA FLATS	2.8%		NO		
22	TOP SOIL	NTS FRENCHMAN FLATS	3.0%		NO		
23	TOP SOIL	MINUTEMAN VR11	DRY		NO		
24	TOP SOIL	MINUTEMAN VP4	HUMID		NO		
25	CLAY	MINUTEMAN VQ10	DRY		NO		

adequately describes the size distribution for the drag sensitive dust. The lower end of the size spectrum exhibits a steeper slope best described by a log-normal distribution. No correlation of size distribution with soil moisture content has been noted for dust. The size distribution previously derived for NTS soils ($dn/da=a^{-4.0}$) is reserved for that soil type. SAI has measured the mean grain size for a number of soil samples and this information is included where appropriate.

SOIL OPTICAL PROPERTIES

Backscattered thermal radiation, characterized by a soil reflectivity or albedo is an important optical property of soils that needs to be recorded. Earth satellite data have recently been summarized, and are presented in Table 7. Reference 3 contains considerable background information on this area.

SUMMARY

The soil samples used in the solar furnace test are listed in Table 8 along with measured properties. Typical chemical compositions of NTS soils are given in Table 9.

Table 9. NTS Soil Chemical Composition

	Atomic Percentages	
Element	Dry	Wet
	6% moisture	16% moisture
H	18	28
O	55	52
Al	4	4
Si	17	15
Ca	0-3	0-1
Misc.	3-6	0-1

Source - Reference 7

Section 4

TEST DATA ANALYSIS

INTRODUCTION

The goal of this phase of work in soil blow-off was a series of parametric experiments under carefully controlled conditions designed to yield quantitative results. This is in contrast with the first phase which focussed on exploratory work on the qualitative features of blow-off. It was determined in the initial work that fluence (or fluence after blow-off) was the appropriate scaling variable and that soil moisture and grain size influenced the air temperature.[1] In this work these trends were studied in some detail. The key question involves the role of flux dependency of blow-off. Simulation techniques cannot match the peak flux experienced in the nuclear case, although fluences can be matched. How important is the time factor of the radiation? Clearly for low fluxes there will be no blow-off no matter what fluence. Also if fluence is sufficiently low there will be no blow-off no matter how high the flux. One important time scale for the development of blow-off is the Fourier modulus related to the heat conduction, which is defined as

$$F_o = t\partial/d^2 \quad .$$

F_o <0.02 implies a semi-infinite solid behavior for time t, depth d, and diffusivity ∂. The optical depth of most soils is of the order of 1 to 2 mm. This is a minimum distance for d. In practice it may be larger because of soil conduction and the irregularity of surface conditions. Using the formula we calculate t_{min}<0.1 to 0.2 sec. In other words, below this value of time the soil response is flux independent. Since blow-off fluence thresholds average around 5 cal/cm^2 it is anticipated that at flux levels of 25 to 50 cal/cm^{2}sec no further dependency on flux levels will be found, at least for soils that satisfy the requirements of this simplified heat conduction argument analysis.

In the following sections detailed parametric studies of blow-off phenomena are reported for the major categories of available data.

FLUX AND FLUENCE THRESHOLDS FOR DUST GENERATION AND PARTICLE BLOW-OFF

Raw data taken during the two phases of the experimental program include 63 high speed films taken in August and September 1974, 42 high speed films taken in March 1975, and low speed movies taken both prior to and after the high speed photography runs. A total of about 150 films were available for study. The results of the first phase are summarized as follows. Fluence threshold varies between 4 to 6 cal/cm^2 for smoke or fine dust for all soils and fluxes tested. Flux dependencies of a factor of 2 between 5-80 cal/cm^{2}sec were noted under the same conditions. The flux region from 10 to 40 showed no noticeable variation. Large particle blow-off occurred at from 5 to 45 cal/cm^2 for certain soil type especially those with clays. Flux variations were not striking for particle blow-off - along the lines as that seen for smoke or fine dust.

Based on these qualitative observations a second phase effect was expended to investigate possible flux variations in the fluence threshold. Figures 10 and 11 represent the results from a careful set of experiments for Sample No. 14. As can be seen, the fluence threshold is a function of flux, within the range 5 to 25 cal/cm^{2}sec. Factor of 2 variations are observed for both smoke and particle ejection. The expected statistical spread in fluence thresholds is larger near flux threshold, but becomes considerably smaller at higher flux. These data are consistent with that observed in the first phase.

The role of moisture in the fluence threshold value is represented by data for Sample 14 (see Figure 12). Moisture may suppress blow-off of particles altogether but otherwise there is no moisture dependency of smoke or particle thresholds for this sample. Table 10 summarized the fluence threshold data for each soil sample tested.

DUST AND BLOW-OFF GENERATED WEIGHT LOSS

Differential weighing of the soil samples prior to and after irradiation is the measure of soil weight loss. This weight loss consists of:

- Blow-off particles that do not return to the soil sample
- Dust generation
- Moisture loss.

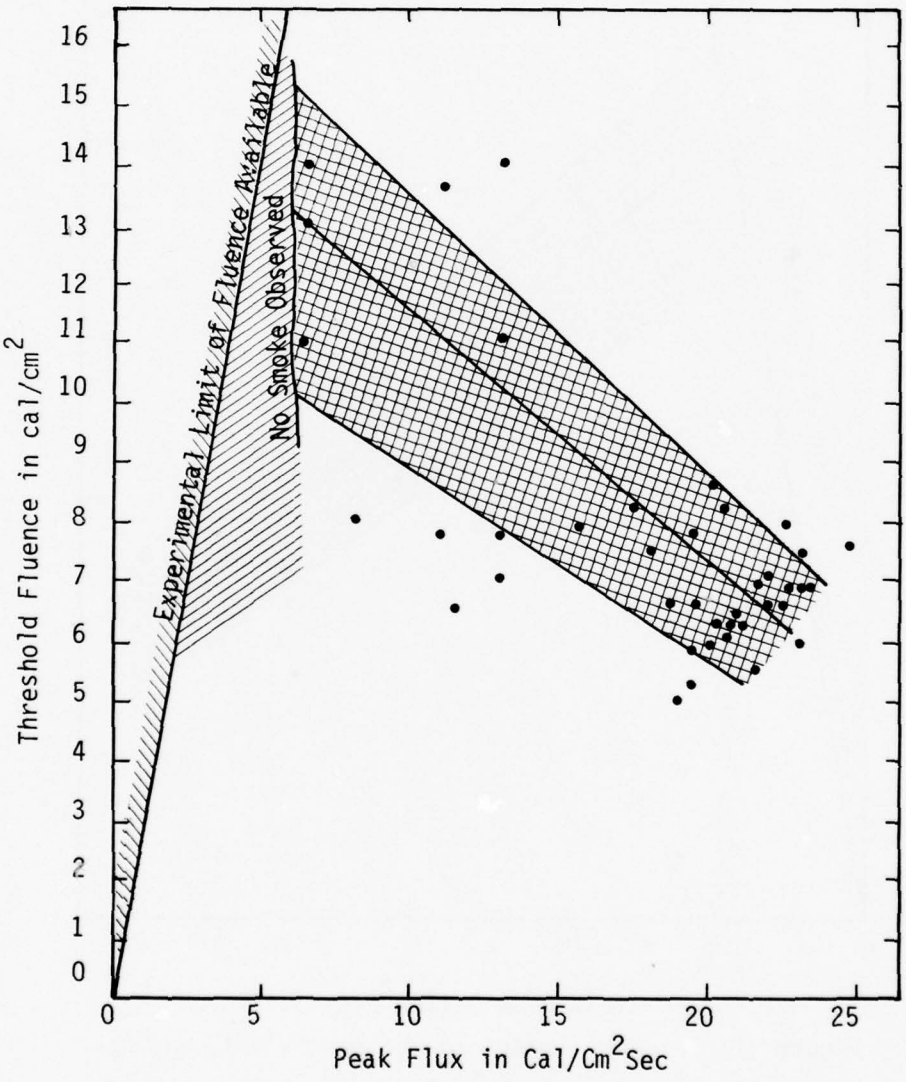

Figure 10. Fluence Threshold for Smoke Generation vs. Peak Flux (Sample 14)

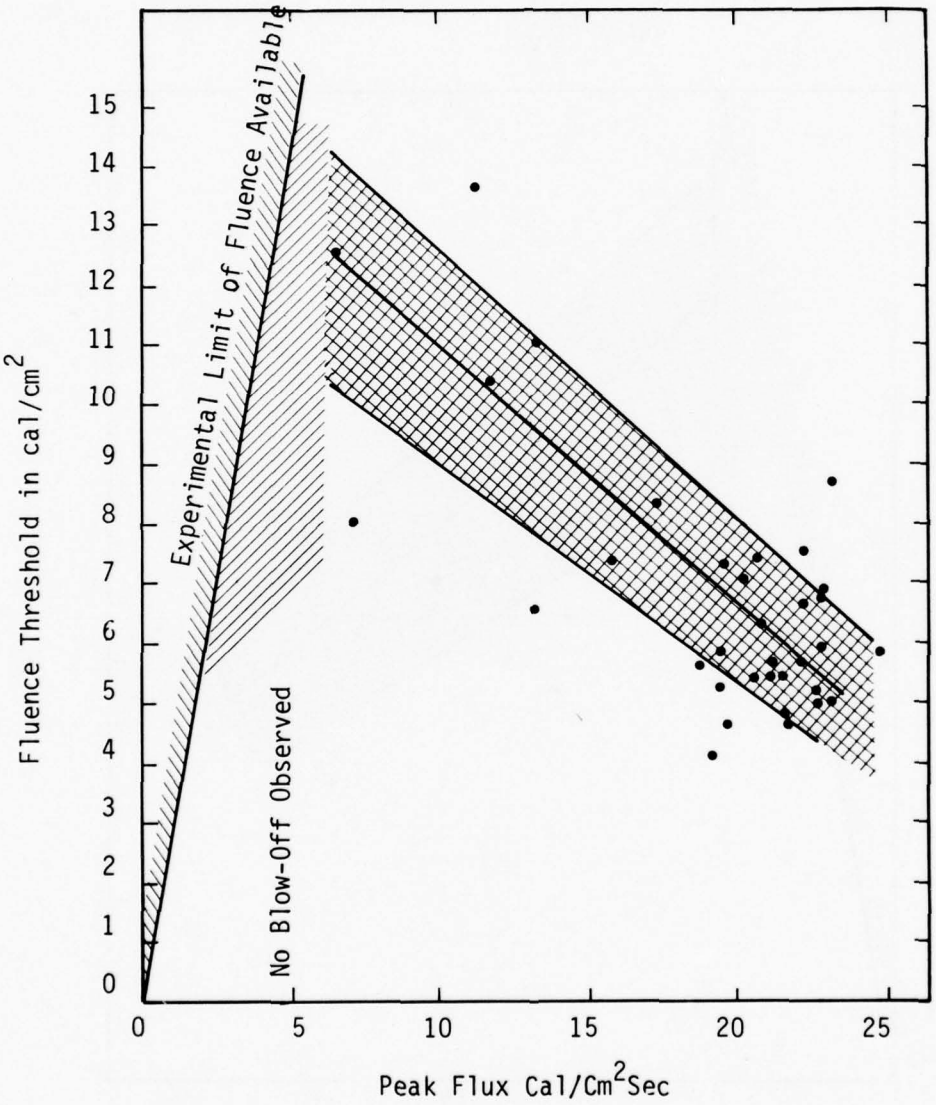

Figure 11. Fluence Threshold for Particle Ejection vs. Peak Flux (Sample 14)

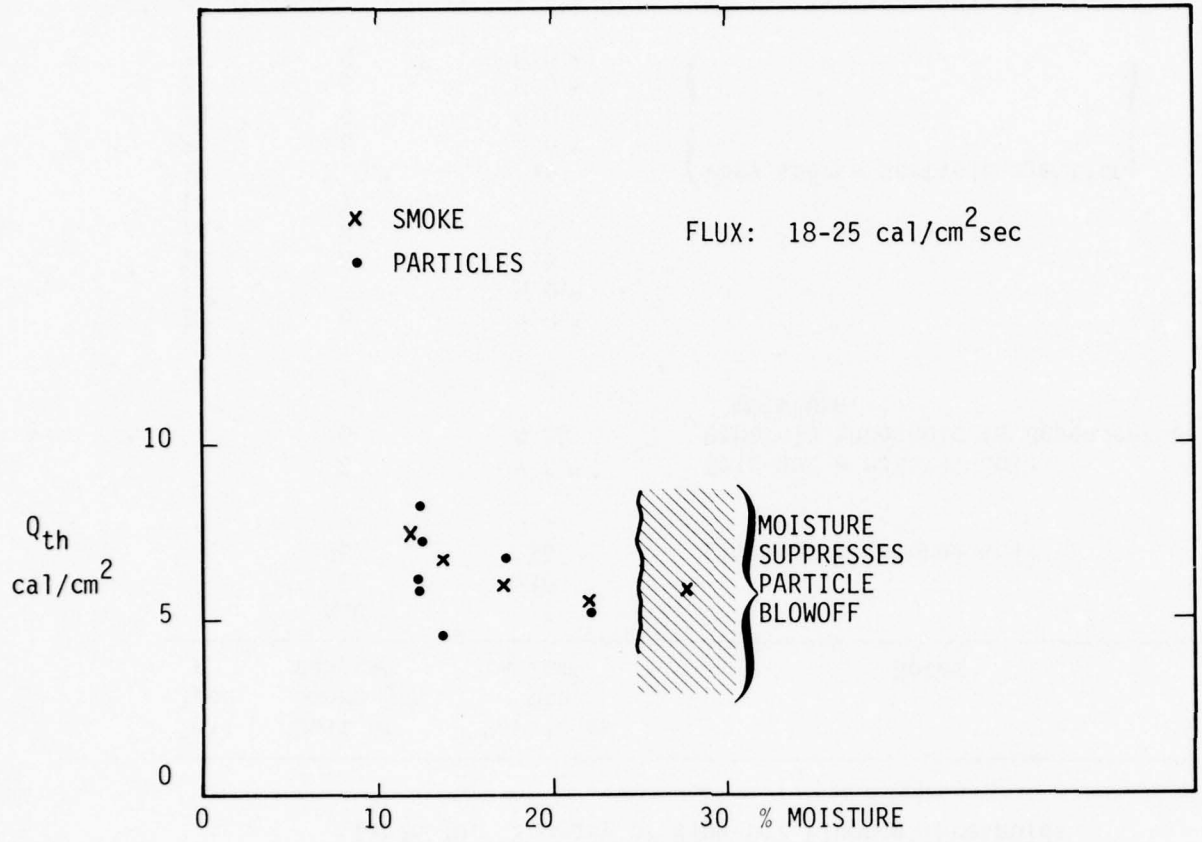

Figure 12. Fluence Threshold vs. Moisture (Sample 14)

Table 10. Summary of Blow-Off Fluence Thresholds

Soil Type #	Dust or Smoke Qth cal/cm^2	Particles Qth cal/cm^2	Notes
1	N.O.*	5	
2	6	10	
3	25	55	Lime-not a natural soil
4	4	7	
5			
6	8	N.O.*	Talc-not a natural soil
7	6	4-20	Particle threshold is dependent on moisture
8	4	4	
9			
10	6	N.O.*	
11	5	N.O.*	
12	6	15	
13	4	25	
14	7	6	
19	N.O.*	15	Very sparse particle ejection
21	6	N.O.*	
23	5	N.O.*	
24	6	N.O.*	
25	5	N.O.*	

Conclusion: For all natural soils the fluence threshold for smoke or dust ejection is between 4 and 8 cal/cm^2, and for those soils that exhibit particle ejection, between 4 and 25 cal/cm^2. Particle blow-off can be highly dependent on moisture.

*N.O. indicates none observed in tests even well past expected thresholds.

Studies of weight loss in the first phase indicated a strong fluence dependency. In order to avoid large changes in values, a scaled or normalized value $\Delta W/\Delta Q$, (where ΔQ and ΔW are total values for the particular test) should be used in comparison with other works. The final tables present these data in this form. In the first phase some data were presented in $\Delta W/\Delta Q$ peak which is approximately equal to $\Delta W/\Delta Q \times 100$ for these tests.[1]

Careful analysis of weight loss trends for NTS Samples 14 and 19 will be presented first. Based on the studies of the previous section normalized weight loss as a function of soil moisture for two samples was investigated first. The findings of this work led to a selected sample of these data for further study. In Figures 13 through 22 data are presented on $\Delta W/\Delta Q$ versus a variety of conditions and variables as summarized below:

Figure	Variable	Sample	Condition
13	% moisture	14	All tests
14	% moisture	19	All tests
15	irrad. time, Δt	14	All tests
16	irrad. time, Δt	19	Natural moisture (5.2%) only, all flux levels
17	Flux, $\dot{Q}$	14	All tests except Δt=2sec
18	$\dot{Q}$	19	Natural moisture only
19	Fluence, Q	14	All tests
20	Fluence, Q	19	Natural moisture
21	$\dot{Q}$	14	All tests, $\Delta W/\Delta Q'$ plotted
22	Δt	14	Natural moisture, $\Delta W/\Delta Q'$ ($Q' = Q-Qth$)

These figures show that Sample 14 (Frenchmans Flats NTS) has a weight loss largely independent of moisture content. This supplements the data of Figure 12 on the fluence threshold independence of moisture effect for the same sample. Within the data clustering of certain $\dot{Q}$ and Δt, values are seen that will be referred to later. Since there are no trends vs. moisture, all data on Sample 14 will be lumped independent of original moisture content.

Sample 19 (Yucca Flats NTS) shows distinctly different behavior and has large variations in normalized weight loss vs. moisture. Comparing the behavior of the two samples (14 vs. 19) emphasizes the necessity of a careful test program since the basic soil type is Alluvial Playas. Due to the rapid variation in moisture, only one moisture content (natural 5.2%), was used in subsequent work.

Another finding concerns irradiation times. Data for both samples show a factor of 2 peak in normalized weight loss in the region

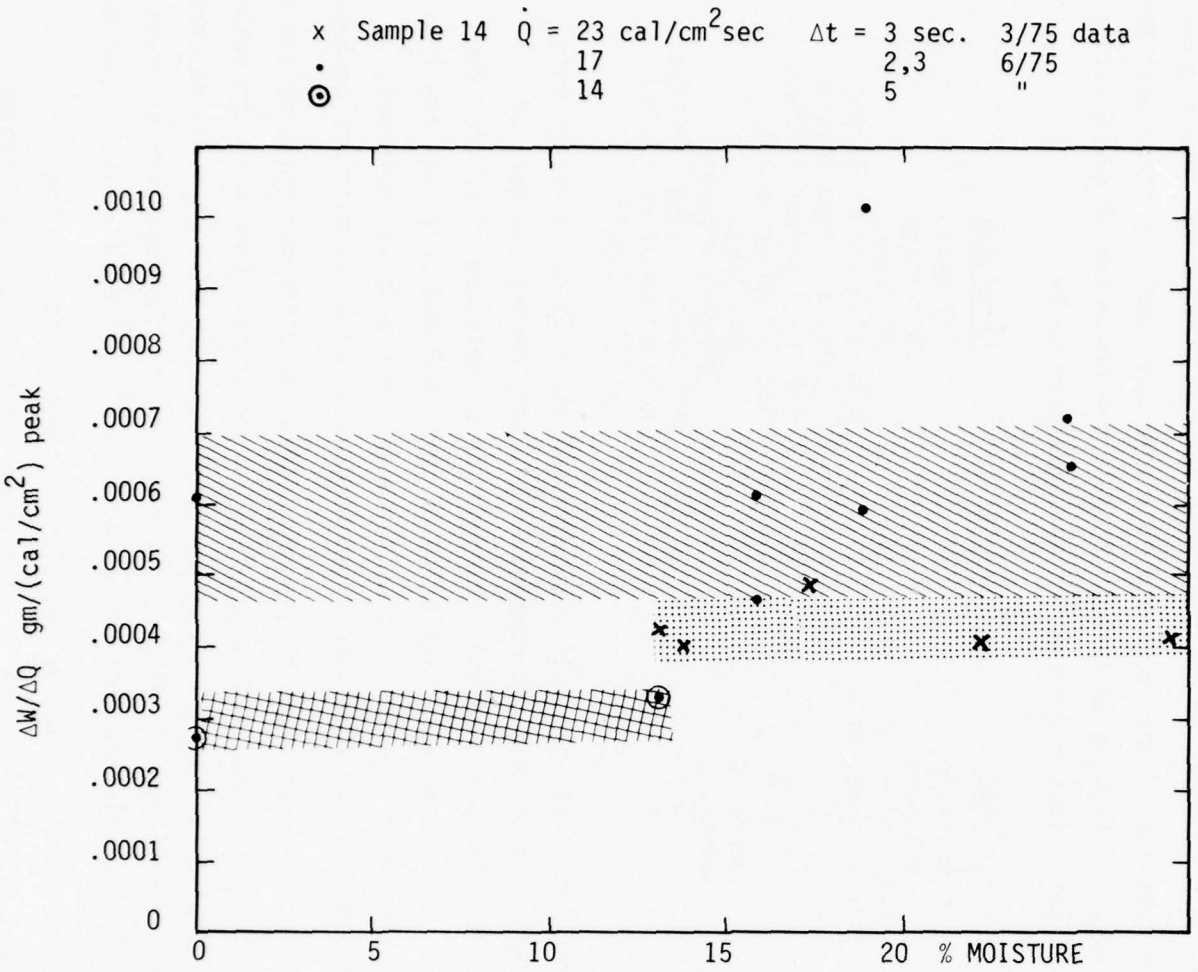

Figure 13. ΔW/ΔQvs. Moisture (Sample 14)

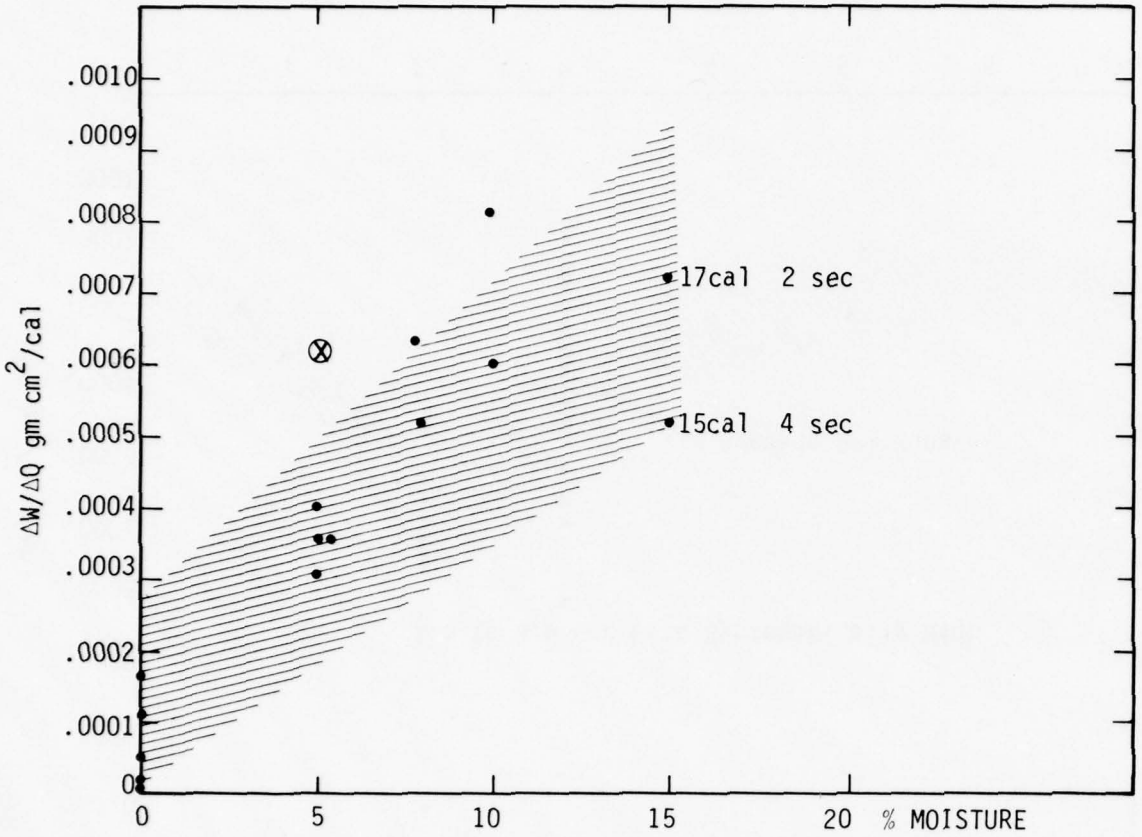

Figure 14. $\Delta W/\Delta Q$ vs. Moisture (Sample 19)

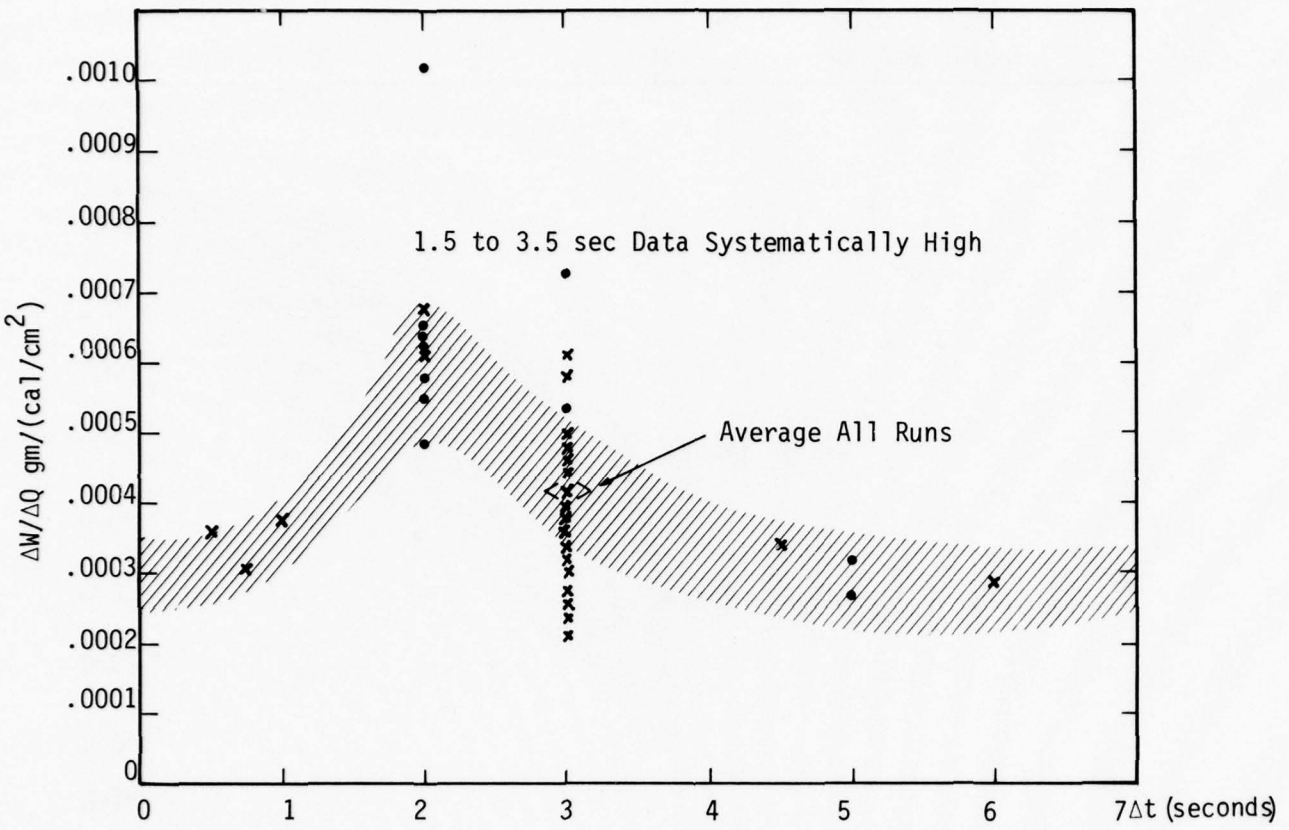

Figure 15. ΔW/ΔQ vs. Irradiation Time, Sample 14, All Moisture Conditions

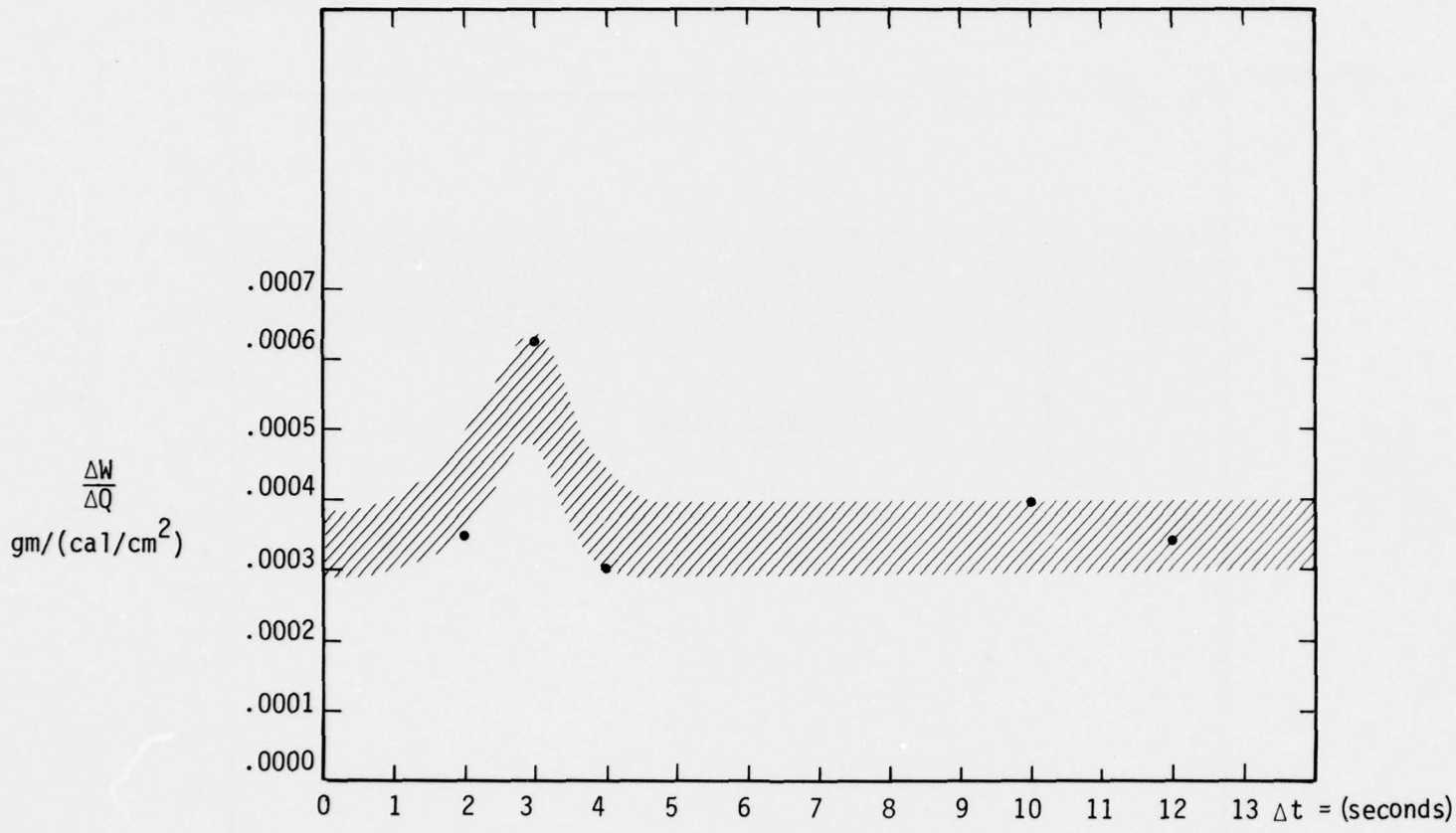

Figure 16. $\Delta W/\Delta Q$ vs. Irradiation Time Sample 19, 5.2% Moisture, $\dot{Q}$, 5 to 18 cal/cm^{2}sec.

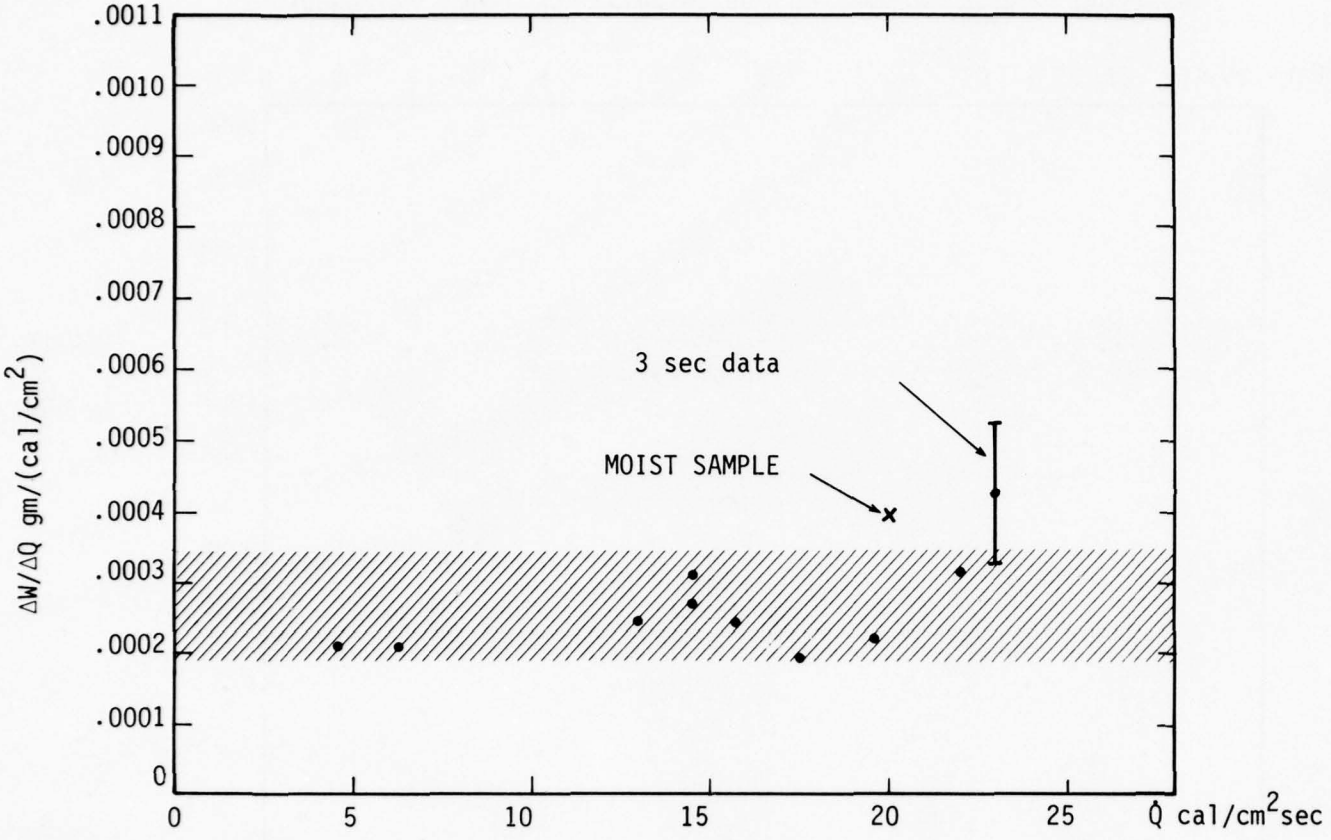

Figure 17. ΔW/ΔQ vs. Flux for Sample 14 All Tests Except Δt = 2 seconds

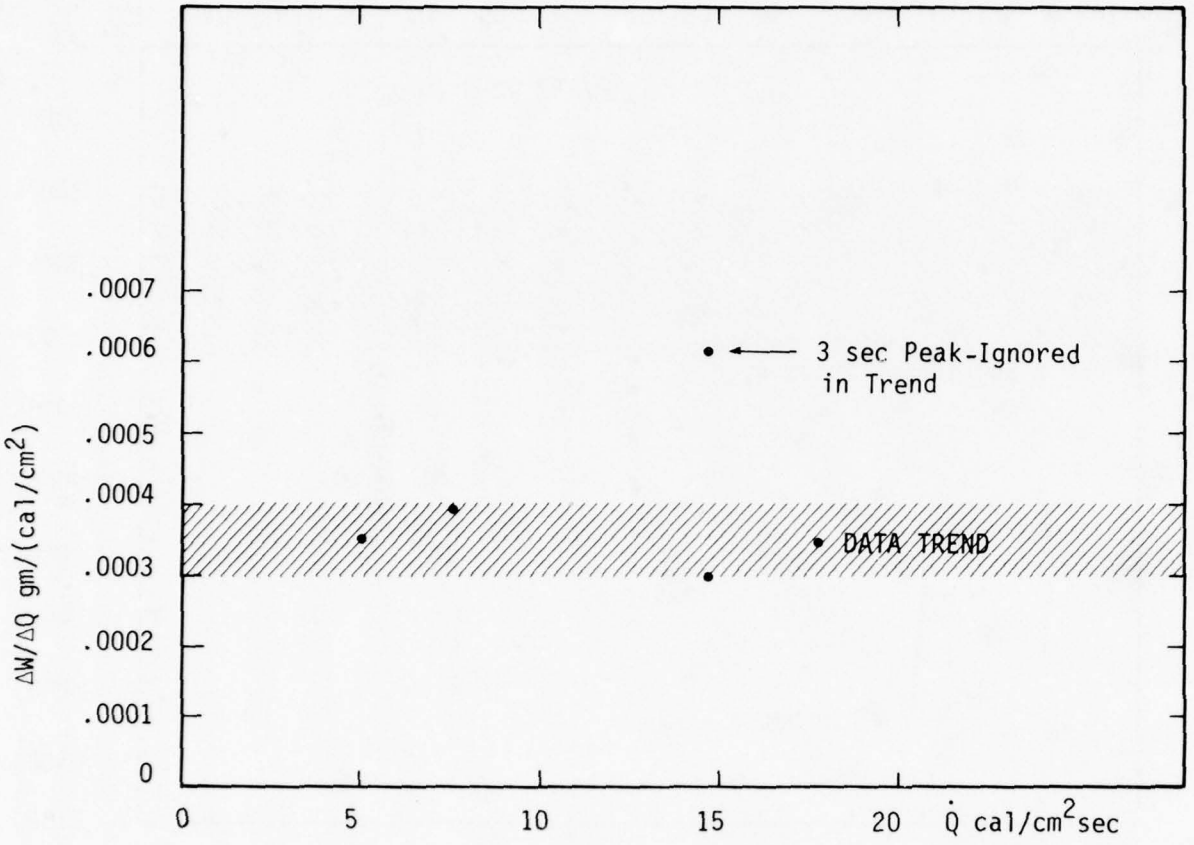

Figure 18. ΔW/ΔQ vs. Flux for Sample 19, 5.2% Moisture

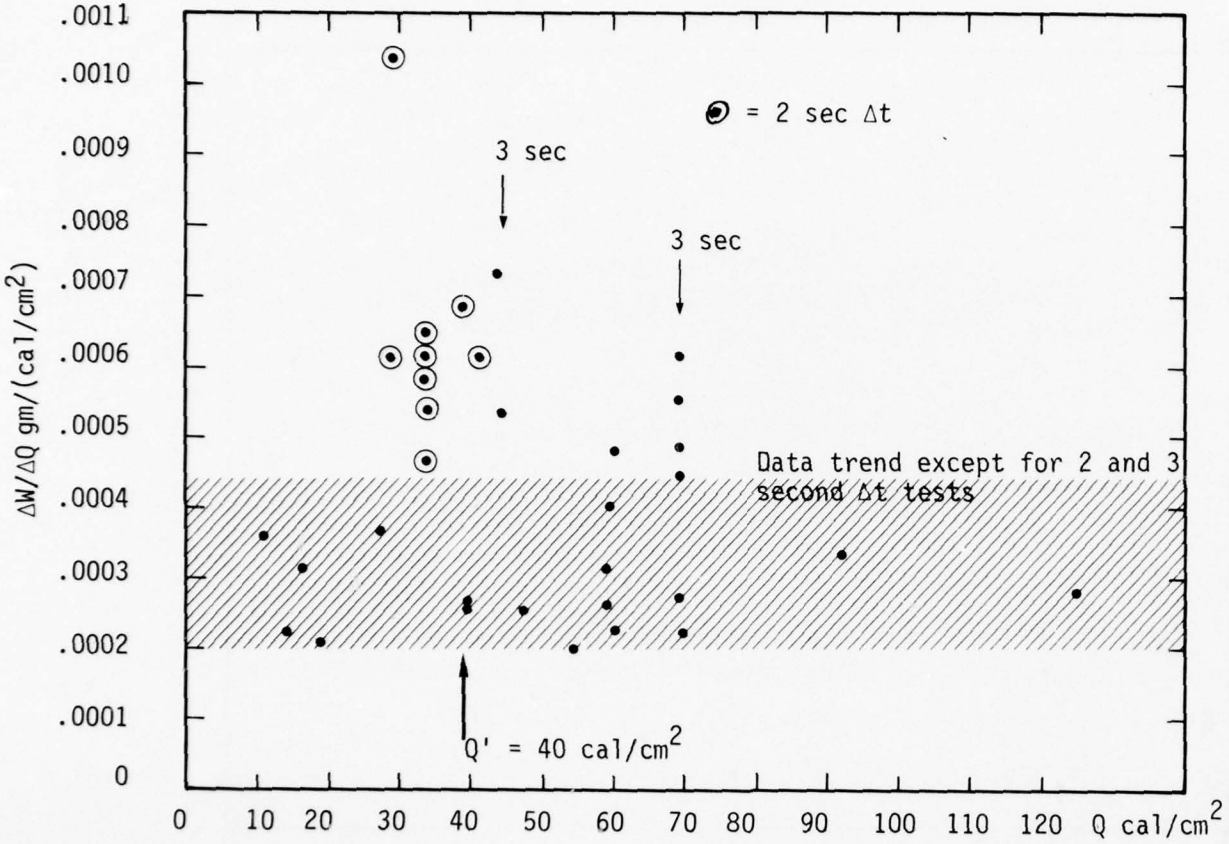

Figure 19. ΔW/ΔQ vs. Fluence, Sample 14, All Runs

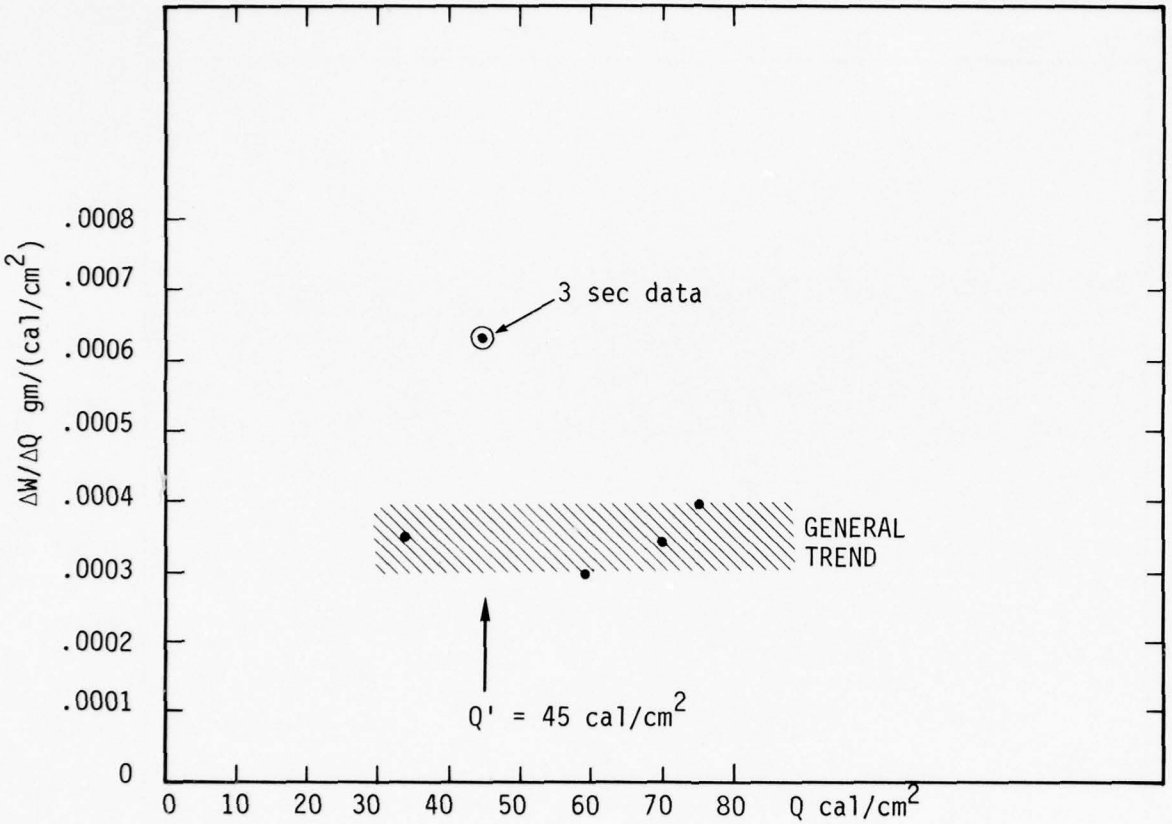

Figure 20. ΔW/ΔQ vs. Fluence, Sample 19, 5% Moisture Only

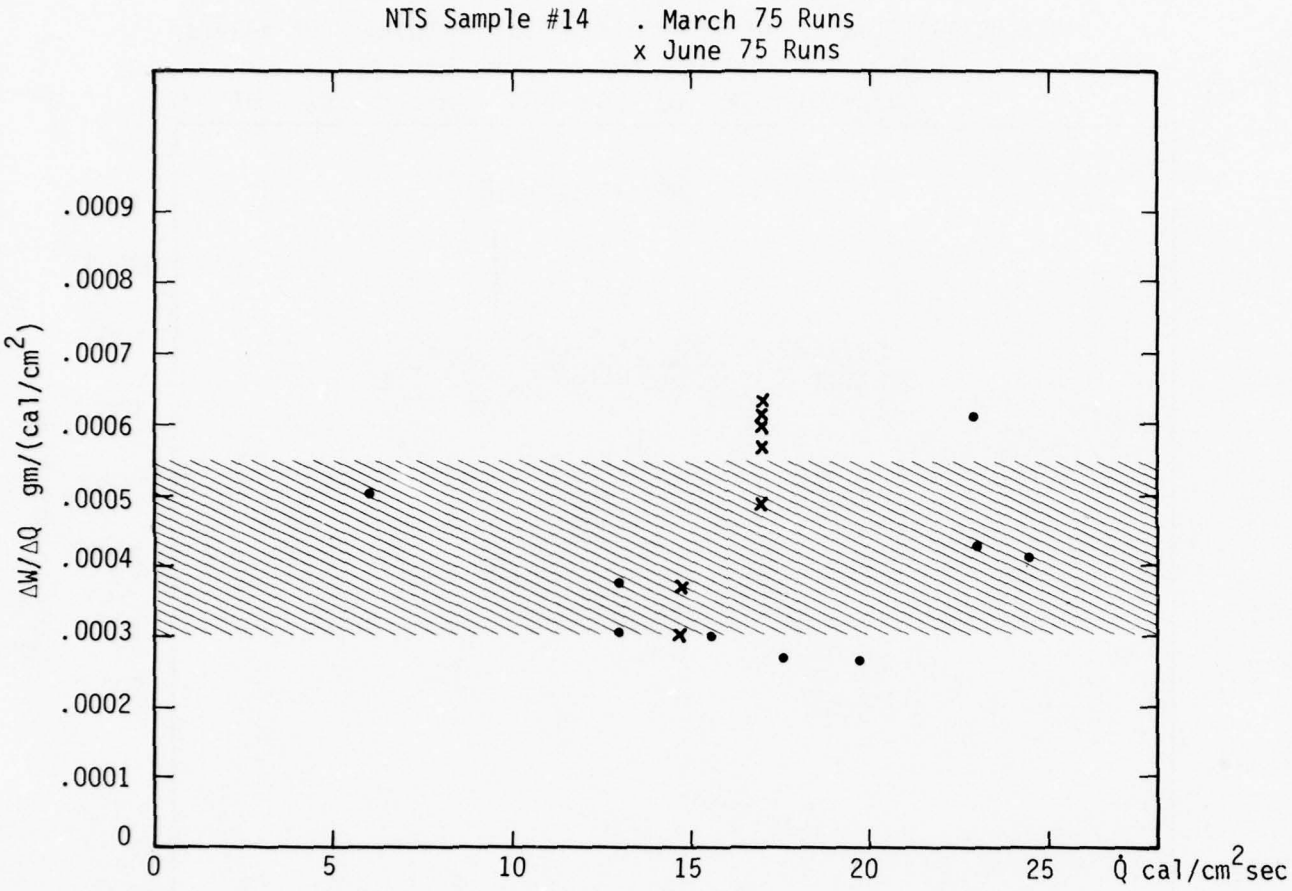

Figure 21. $\Delta W/\Delta Q'$ vs. Flux, Sample 14, All Tests

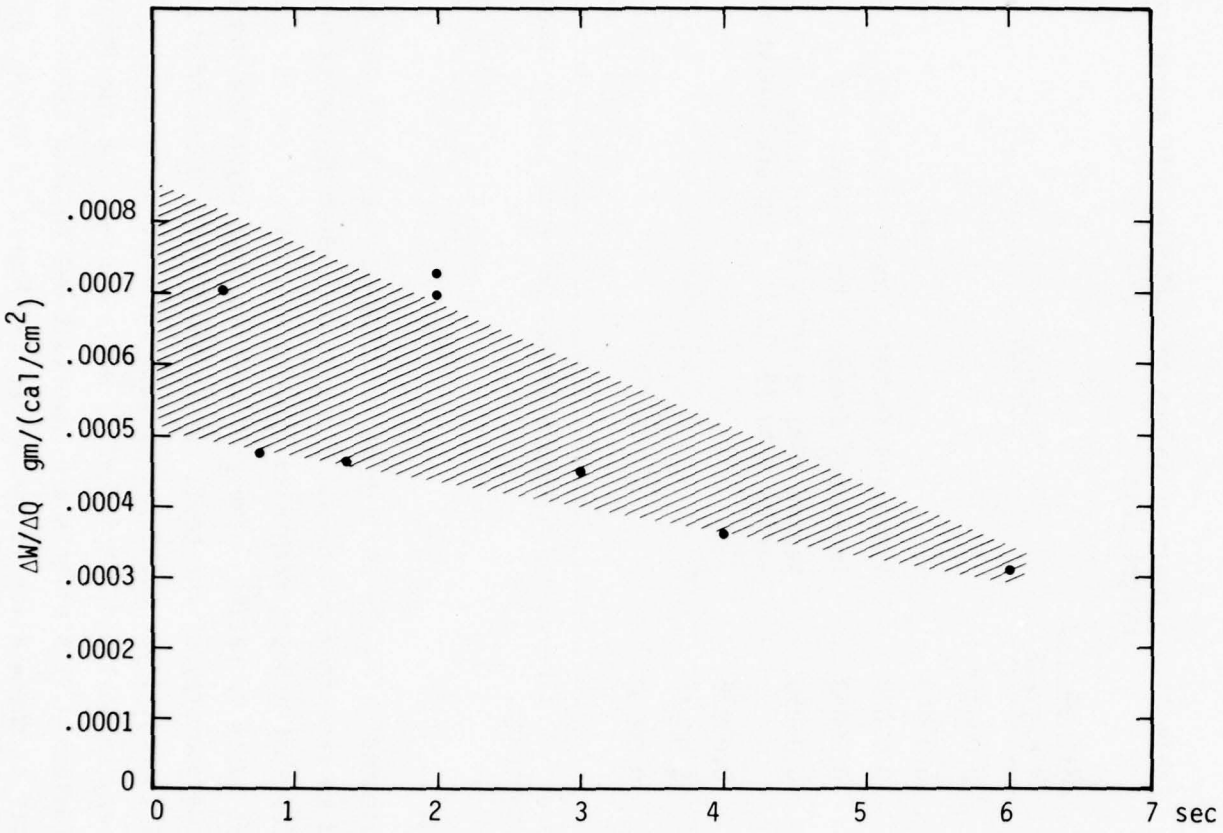

Figure 22. ΔW/ΔQ' vs. Irradiation Time Sample 14, All Data

Δt = 2 to 3 sec. When the Δt = 2 to 3 data are removed there are no trends in either sample displayed versus flux or fluence. When the quantity $\Delta W/\Delta(Q\text{-}Q_{threshold}) = \Delta W/\Delta Q'$ is formed no variation versus flux, and a more understandable variation versus Δt is indicated. Evidently there is a saturation effect in the ability for fluence to cause weight loss. Table 11 is a summary table of weight loss values.

Table 11. Summary of Values of Soil Blow-Off Normalized Weight Loss

Sample #	$\frac{\Delta W(\text{gm})}{\Delta Q\ \text{cal/cm}^2}$	Notes
7	0.00040*	
8	0.00060	
14	0.00030	Increases factor 2 for Q' 40cal/cm^2
19	0.00050	Increases factor 2 for Q' 45cal/cm^2
21	0.00050	Varies -50% to +100% if moisture varies 0 to 15% (5% = natural moisture)
23	0.00035	
24	0.00065	
25	0.00030	

*Average over fluence and moisture levels for each sample unless noted to contrary.

OBSCURATION

Obscuration is the ability of the blow-off particles and dust to shield the ground surface from additional irradiation. When obscuration is observed it signifies that a basic mechanism thought responsible for the thermal layer development is in operation, namely volumetric dust layer heating and expansion. Although the geometry of the tests during the first and second phase did not allow full thermal layer development, some information concerning the physical processes may be analyzed. Moisture is again singled out for initial study, and, as previously, its effects are important but to some extent unpredictable. The analysis of obscuration is summarized in Figures 23 through 31 as listed below.

Figure	Title
23	% Obscuration vs. moisture, Various Samples
24	% Obscuration vs. weight loss, Sample 14
25	% Obscuration vs. irradiation time, Sample 14
26	Schematic of variables in obscuration calculation
27	Obscuration - calculated vs. measured
28	% Obscuration vs. flux, Sample 14, Δt = 3 sec data
29	% Obscuration vs. fluence,Sample 14, natural moisture
30	Obscuration vs. $\Delta W/\Delta Q'$
31	Δ(Obscuration)/ΔQ vs. $\Delta W/\Delta Q'$

Some facts emerge from the analysis concerning obscuration. In sands, where free water (moisture) is necessary to produce blow-off, obscuration and moisture are positively correlated. In clays where water may inhibit blow-off, or serve as an alternate heat sink, a negative correlation is observed. Obscuration is correlated with weight loss; some of the spread in Figure 24 is reduced when accounting for the irradiation time effect. Obscuration saturated with irradiation time is due to the finite size of the test (only 1/2 meter height above soil sample). A straightforward calculation of the consistency of blow-off weight loss and obscuration is illustrative. Good agreement is found. Obscuration is fluence dependent but not flux dependent at constant fluence. Finally the scaled obscuration Δ(Obscuration)/ΔQ vs. scaled weight loss $\Delta W/\Delta Q'$ is tightly correlated. Average values are Δ(Obscuration)/ΔQ = 0.0045 at $\Delta W/\Delta Q'$ = 0.0035.

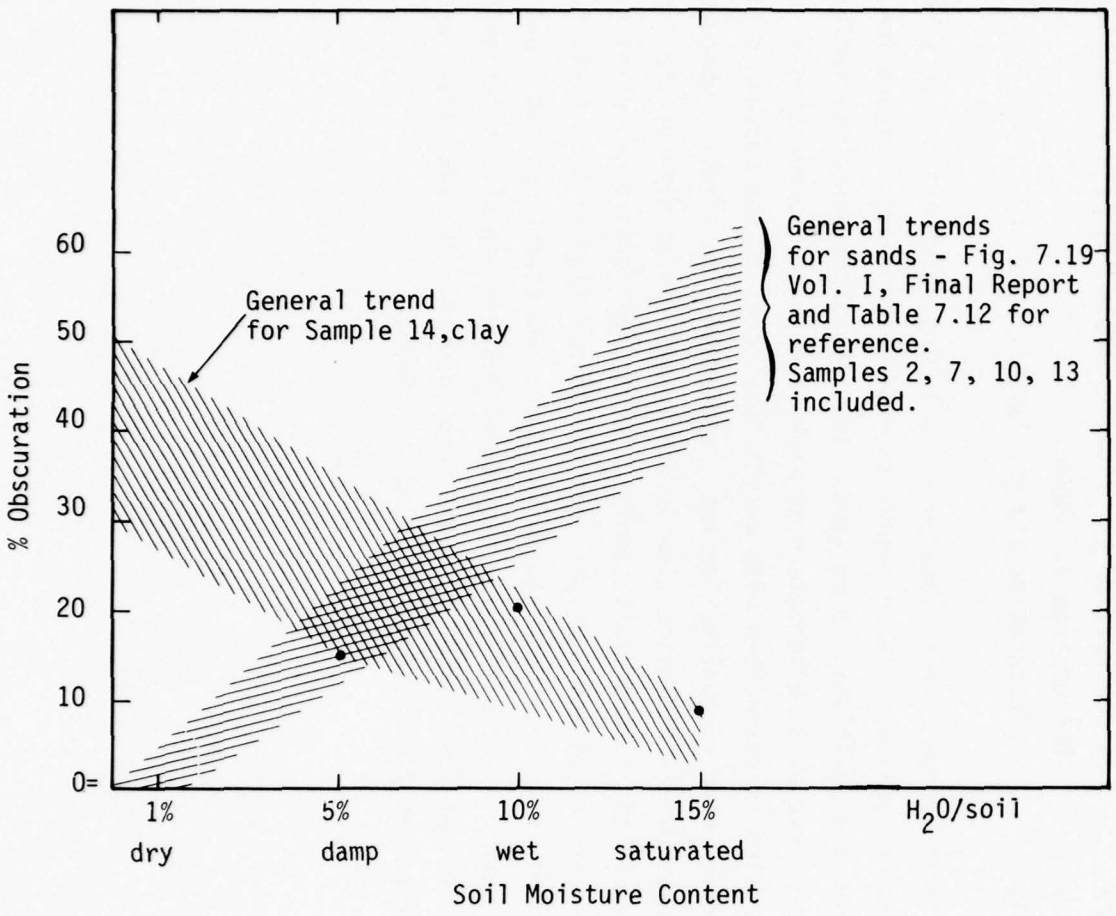

Figure 23. Percent Obscuration vs. Soil Moisture Content for Various Samples

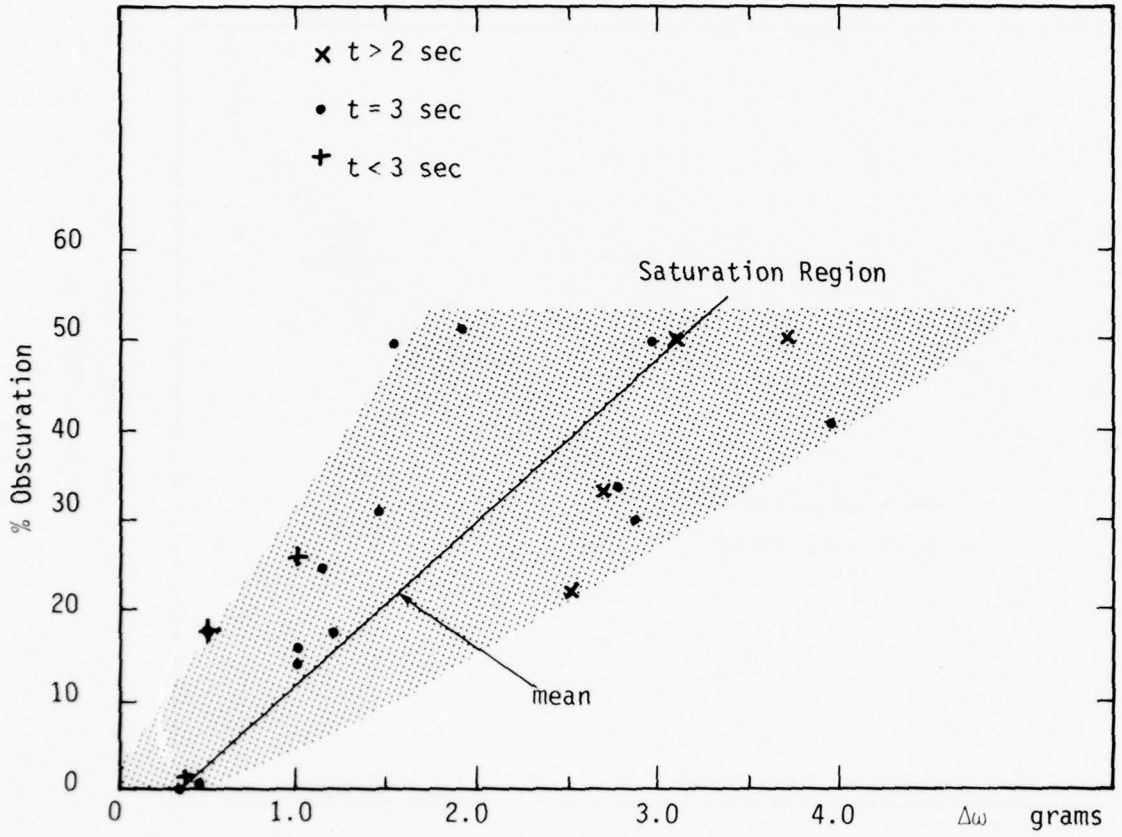

Figure 24. Percent Obscuration vs. Weight Loss for Sample 14, Natural Moisture

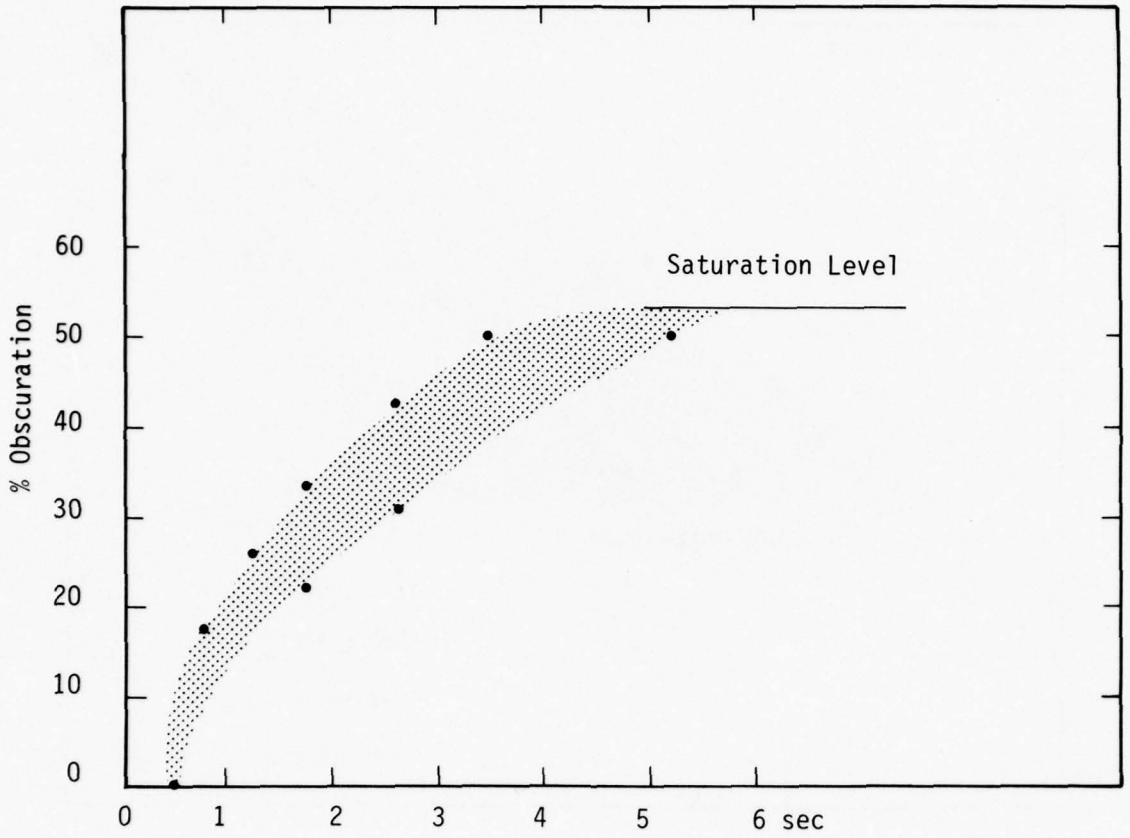

Figure 25. Percent Obscuration vs. Irradiation Time for Sample 14, Natural Moisture, Flux of 22 cal/cm^{2}sec

OBSCURATION: $T=e^{-a}$, $a = N\sigma\ell$

$$A=1 - T = 1 - e^{-N\sigma\ell}$$

$$A = 1 - \exp - \left[\frac{\Delta W}{\Delta Q} \quad \frac{\dot{Q}h}{123\langle r\rangle\rho_s v}\right]$$

Units: h (cm), v(cm/sec), $\dot{Q}$ (cal/cm^2 sec), $\langle r\rangle$ cm
ρ_s (gm/cm^3), $\Delta W/\Delta Q$ (gm/cm^2)/(cal/cm^2)
Reference 1, page 7-53

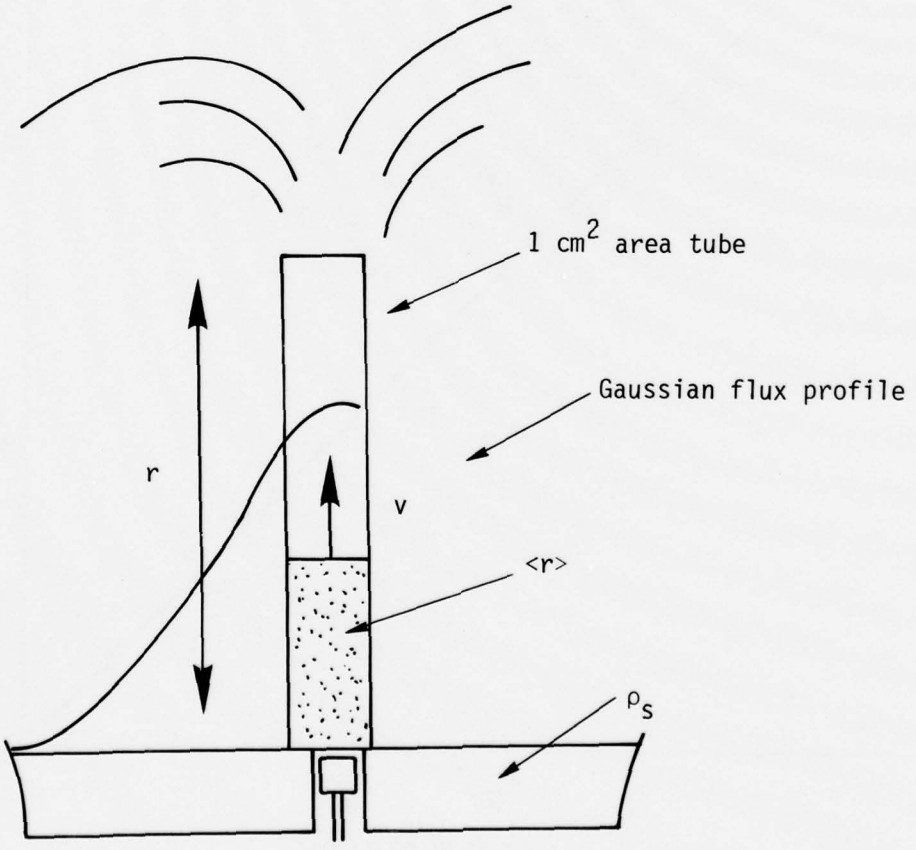

Figure 26. Schematic Diagram of Variables Used in Obscuration Calculation

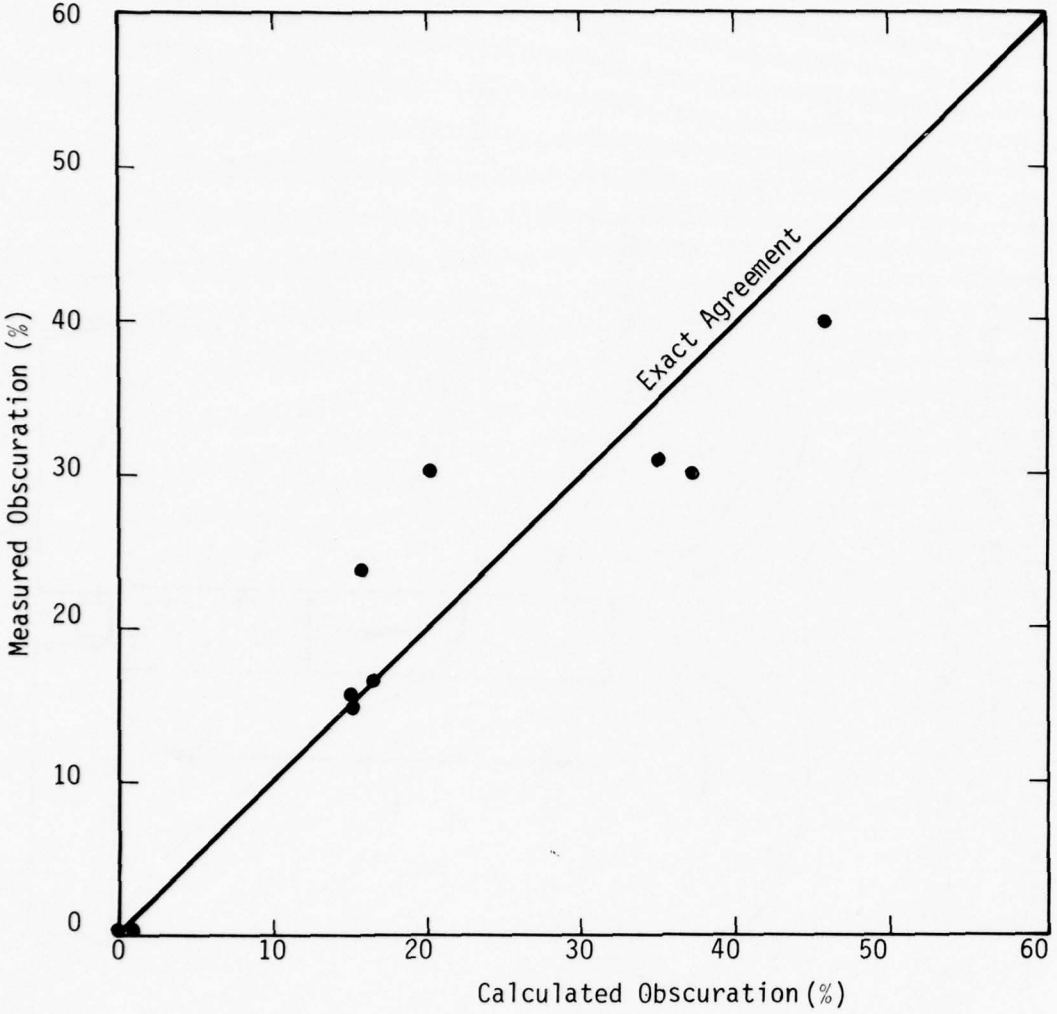

Figure 27. Comparison of Calculated vs. Measured Obscuration Data From 4.5 to 25 cal/cm^{2}sec exposures of sample 14 (dry NTS soil). Theory assumes <r> = 5μ, v = 1m/sec.

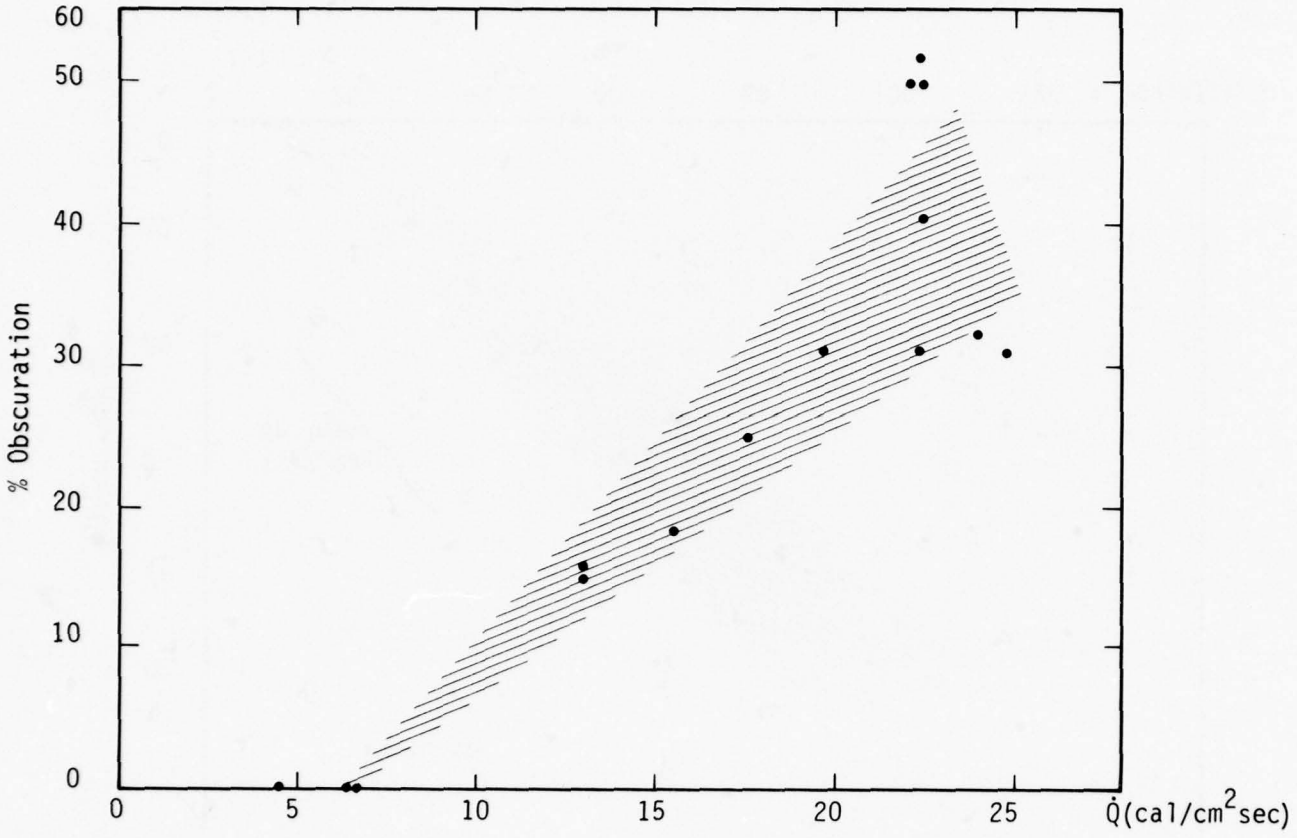

Figure 28. Percent Obscuration vs. Flux for Sample 14, Natural Moisture, Δt=3 sec Data

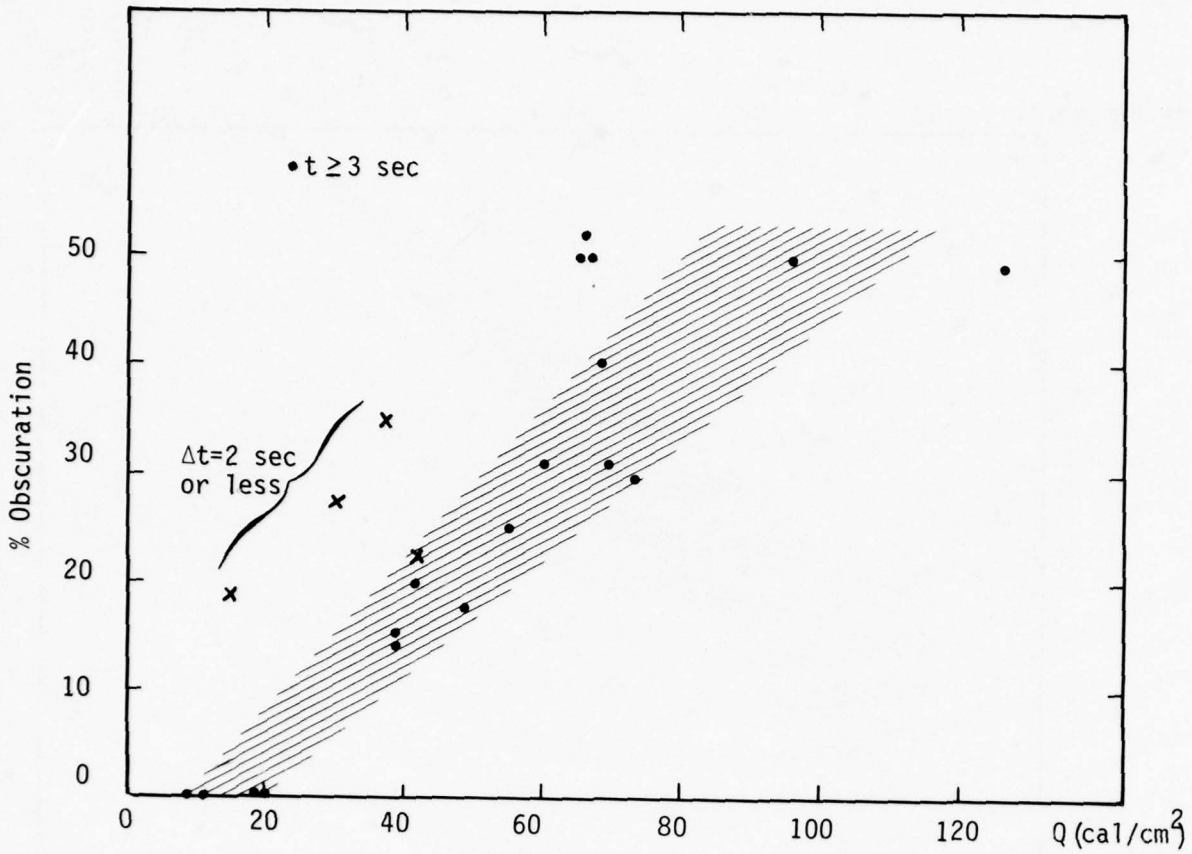

Figure 29. Percent Obscuration vs. Fluence for Sample 14, Natural Moisture

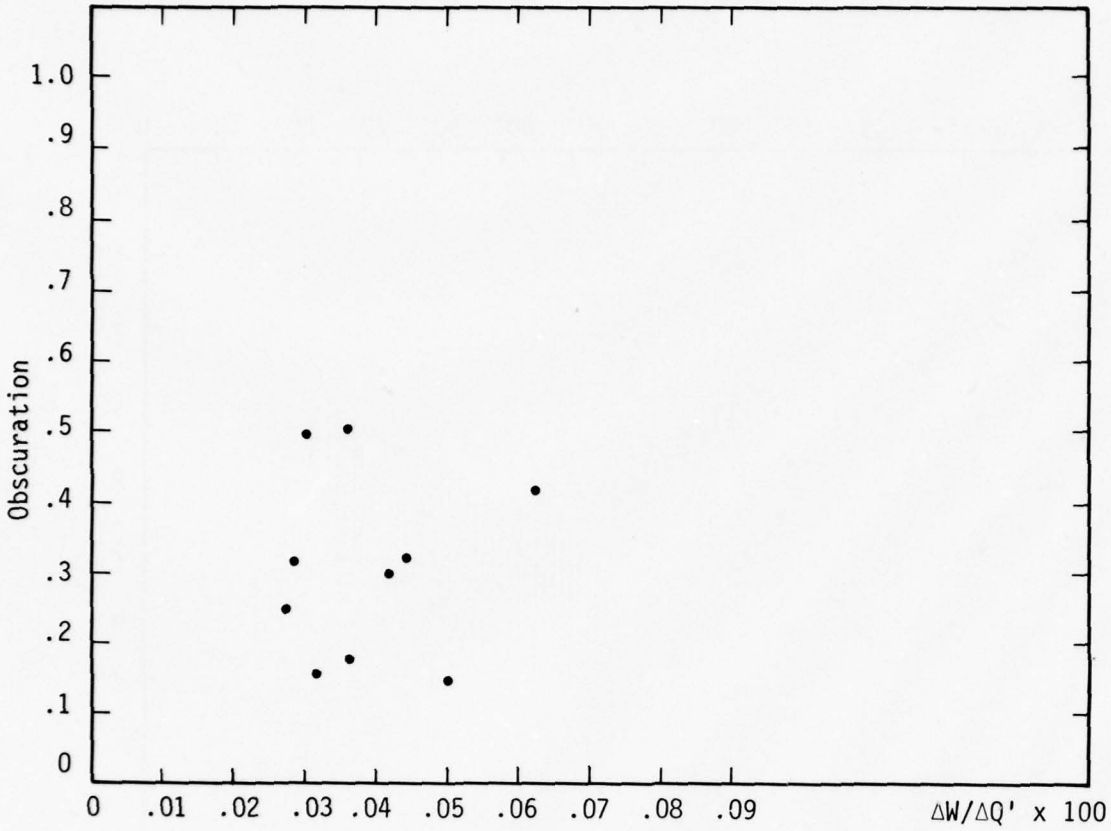

Figure 30. Obscuration vs. Normalized Weight Loss for Sample 14, Natural Moisture and $\Delta t \geq 3$ sec

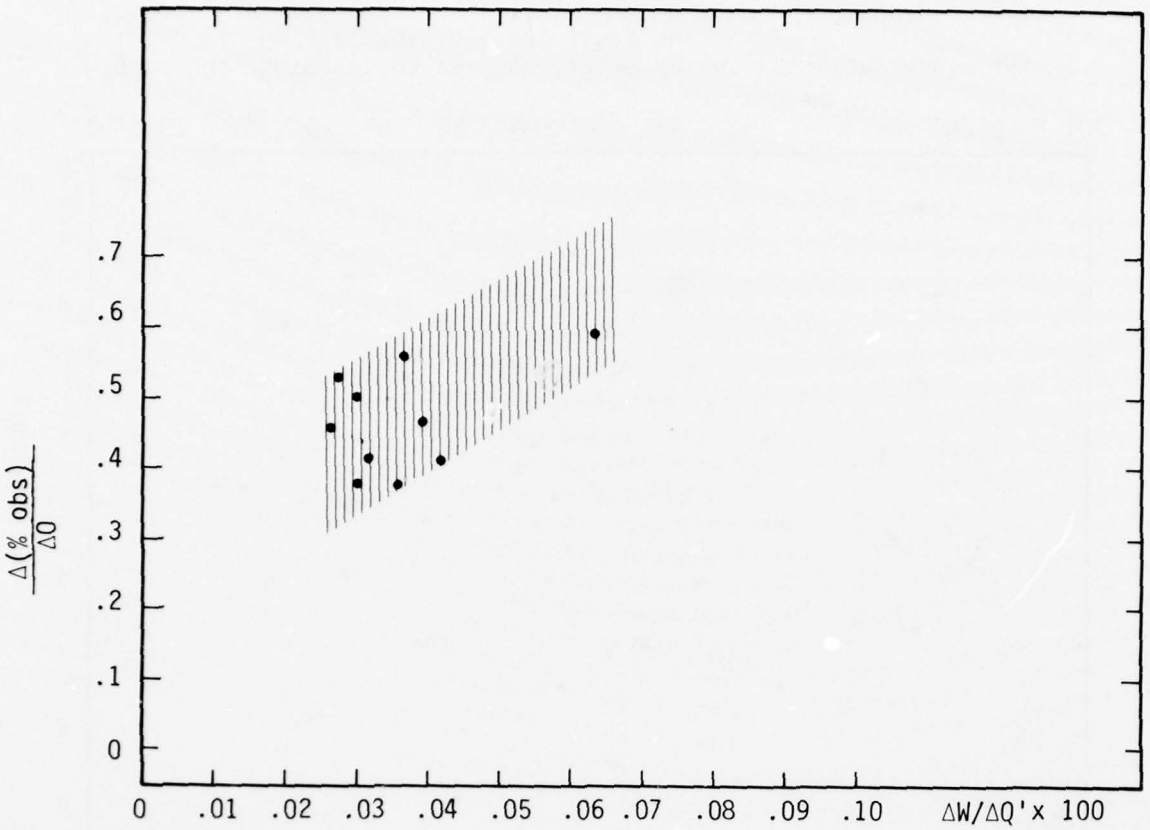

Figure 31. Normalized Percent Obscuration vs. Normalized Weight Loss for Sample 14, Natural Moisture Conditions $\Delta t = 3 \geq$ sec Data Used

AIR TEMPERATURE

One of the most important single indications of thermal layer development is air temperature. In phase 1 indications of air temperature ranges were given by a series of tests involving temperature sensitive paints on graphite rods above the soil sample. Air heating was recorded over all samples tested. Surprisingly hot air was produced even where little blow-off was observed. This was attributed to conductive air heating by the hot soil. In phase 2 aspirated thermocouples were mounted over the soil surface to record air temperatures accurately. Because of the finite test sample size and three-dimensional effects, less volumetric air heating was observed than that expected for a true 1-D simulation. Volumetric heating will, in the case of a one-dimensional, geometric configuration drive the dusty air layer and cause higher temperature gradients than seen in these tests.

Figure 32 is a schematic view of the test set-up showing the aspirated thermocouple probe location. Figure 33 gives details of the air temperature probe design which allows double wall flux shielding. The thermocouple junction is at the flow stagnation point and is made of 1 mill thermocouple wire. The probes were calibrated using a standard heat source. The probe output was recorded by oscillographs located in an instrument trailer adjacent to the solar furnace. About 100 tests were performed using these probes (4 each test). An outstanding endurance record was achieved; out of a total of 410 probe exposures to hot dusty air (up to 1100^{0}F) 2 failures were recorded: one open circuit at the hot junction, one short at the cold junction. Probes shields were repolished, and the probes were ultrasonically cleaned between runs. Table 12 highlights the accomplishments of the SAI thermoprobe.

Analysis of the air temperature data revealed trends depending upon moisture. Figures 34 and 35 show the general temperature versus fluence trends. Fluence again proved to be a good scaling variable and was used extensively with analysis. Justification of this approach is given by solution of the one-dimensional heat conduction - expansion problem in air by the Crank-Nicholson method. Figure 36 gives typical results. In the data

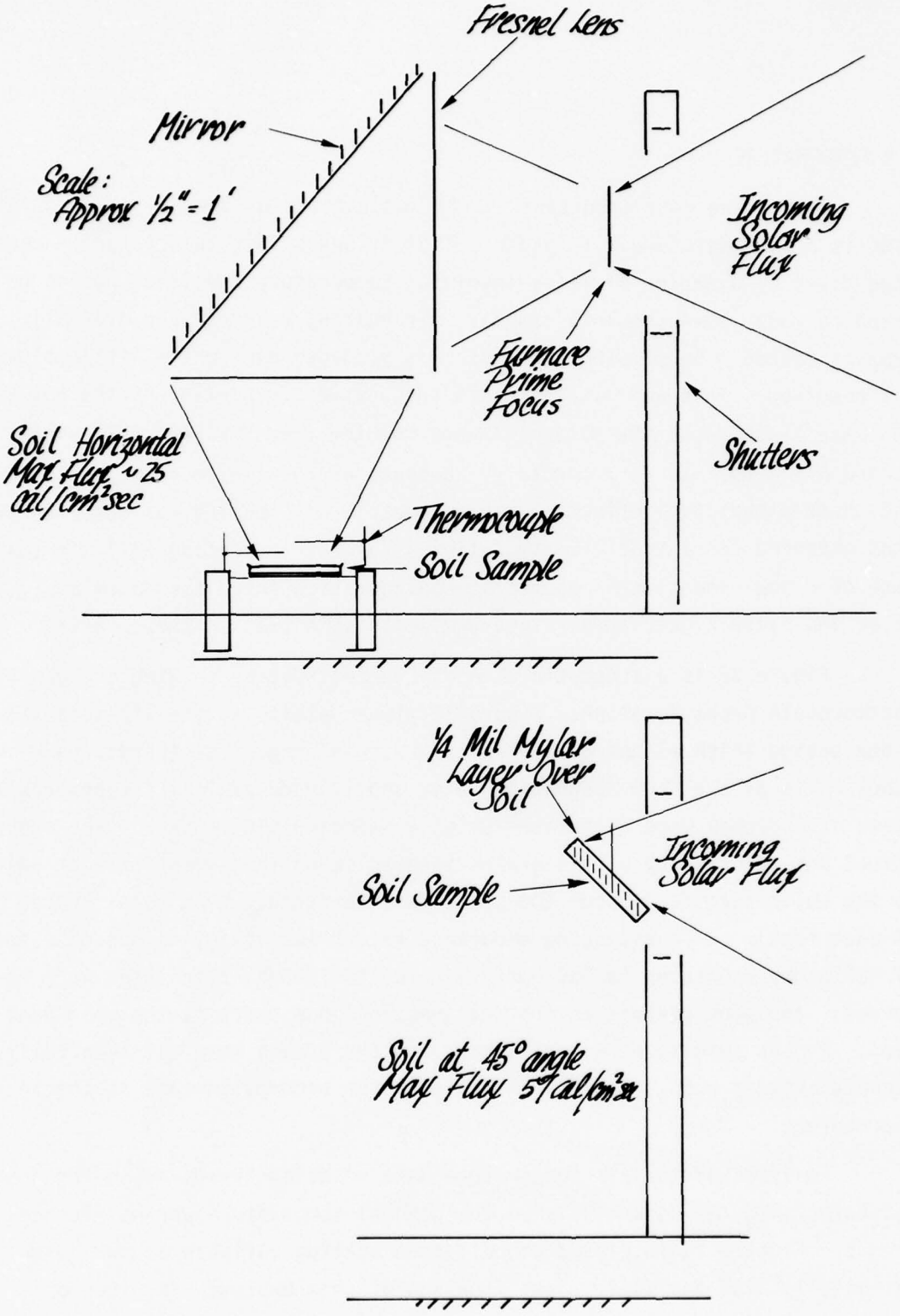

Figure 32. Schematic of Test Configuration at WSMR

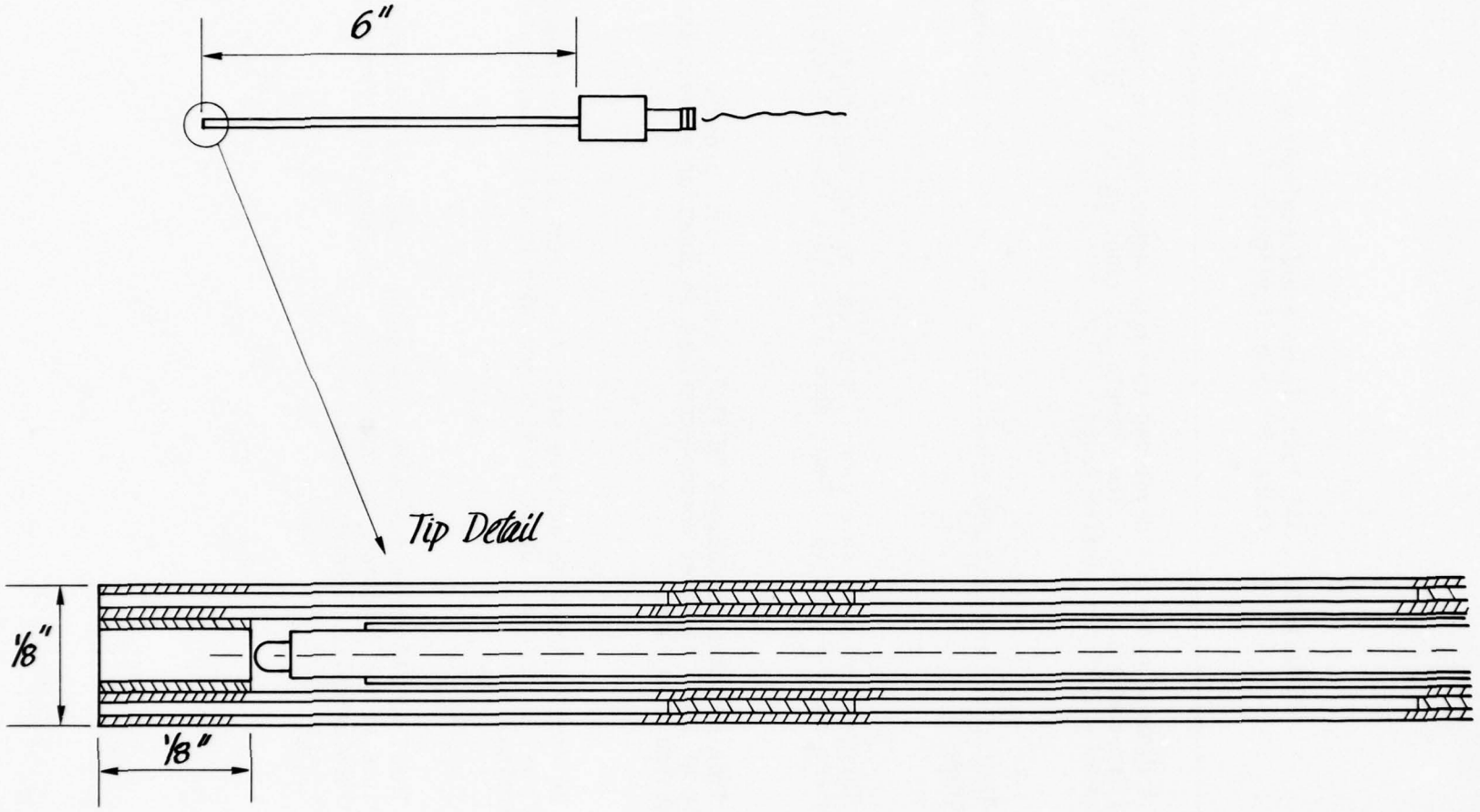

Figure 33. Aspirated Thermocouple Probe

Table 12. SAI Total Temperature Aspirating Probe, Program Highlights

---

- A dynamic probe was developed to sense temperature in compressible fluid two-component flow. The temperature range was 0 to 1200°F, calibrated to ± 20°F over entire range.

- Heated air and dust are drawn through an orifice to a thermocouple junction.

- Thermal radiation shielding is provided by two concentric shields which are totally passive. Tests show $\Delta T/\Delta Q$ less than 0.3 $^{o}C/(cal/cm^2 sec.)$

- Time response to changes in fluid energy is of order of milliseconds by use of 1-mil diameter chromel-constant in junction at manufacturer's designated flow rate.

- Orifice designed to achieve stagnation point at active element. Flow 75 ft/sec, 1 ltr/min. Outer shields grounded to avoid electrostatic flow separation.

- Total of 410 probe exposures were made; 2 failures recorded, one open circuited at hot junction, one shorted at cold junction. Probes polished and ultrasonically cleaned between runs.

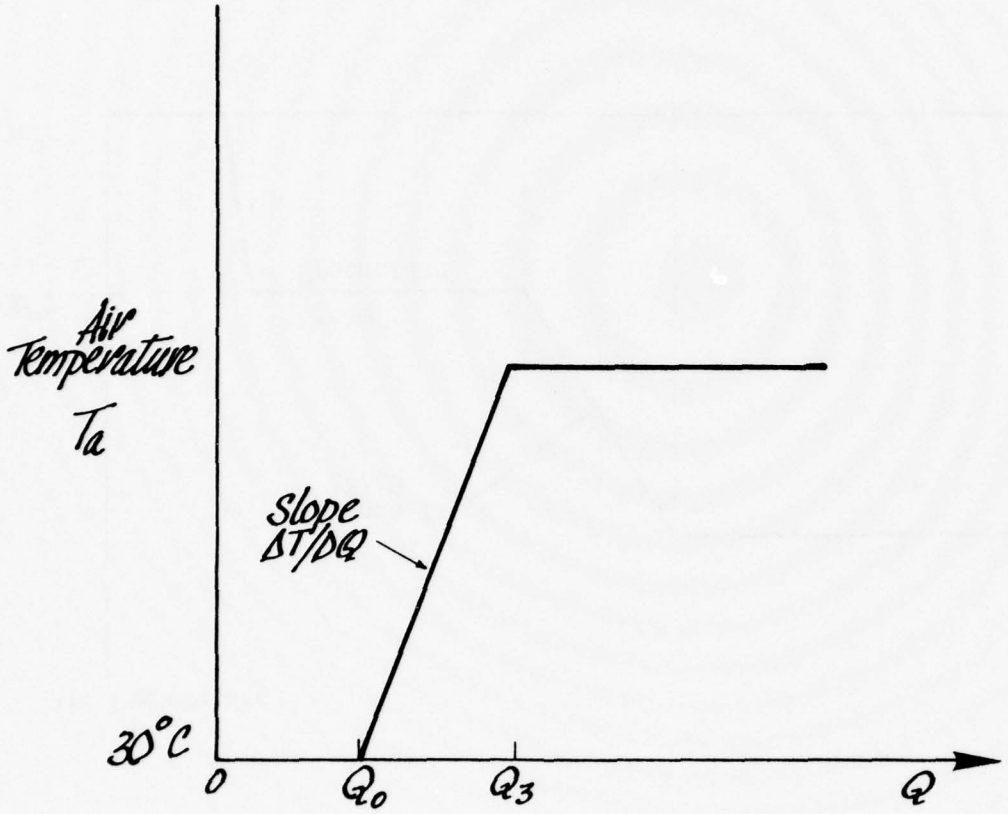

Figure 34. Air Temperature vs. Fluence (Dry Soils)

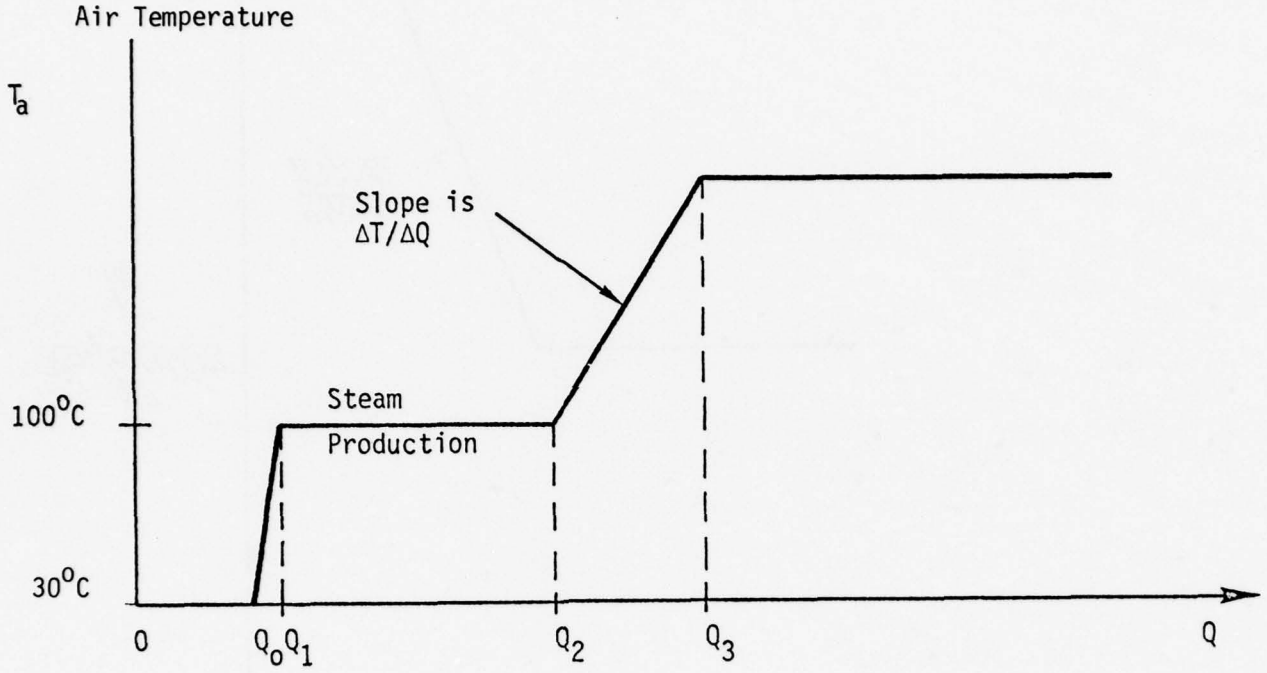

Figure 35. Air Temperature vs. Fluence (Wet Soils)

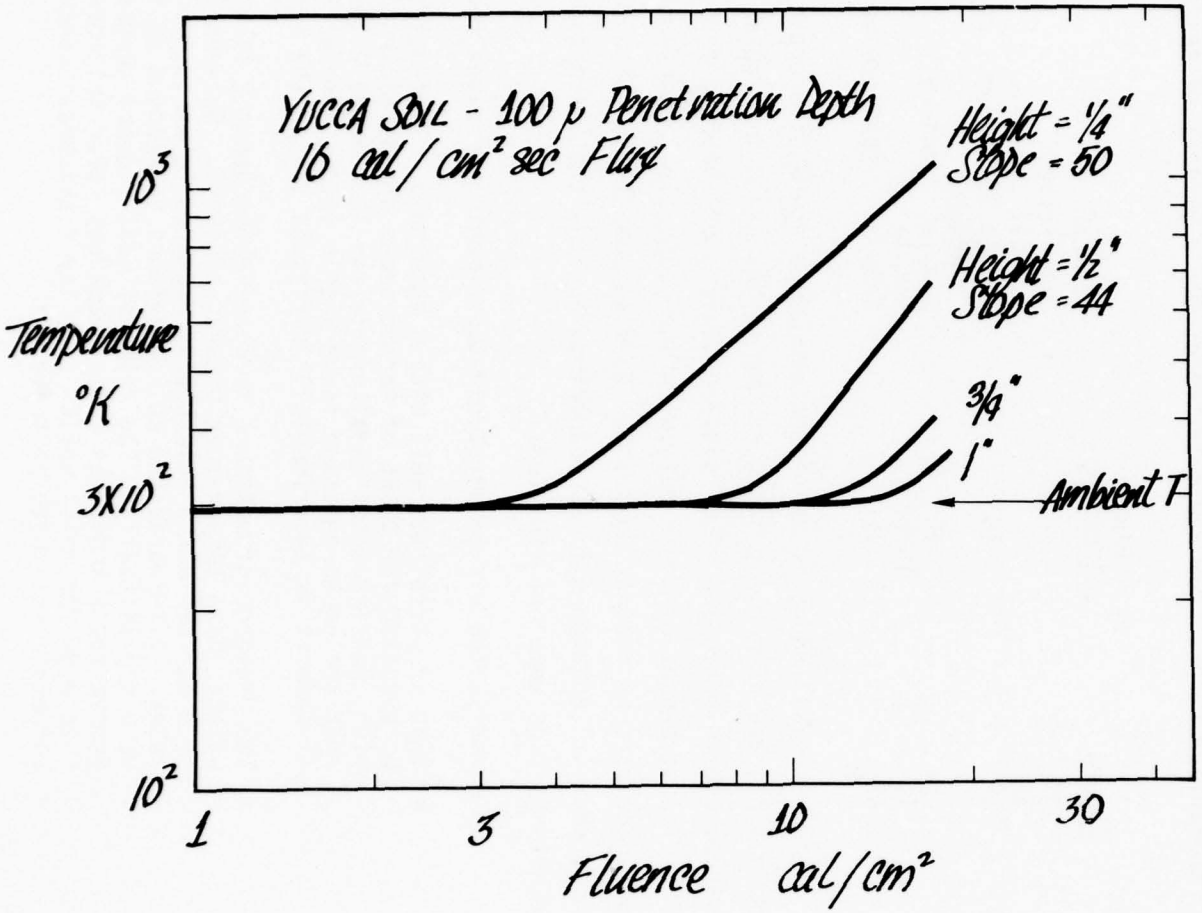

Figure 36. Solutions to the Crank-Nicholson Heat Conduction - Expansion Problem in Air

saturation of the temperature rise takes place due to the two-dimensional flow and due to blow-off. On the temperature traces, blow-off can be observed as a rapid rise and fall of the air temperature due the passage of a hot particle. In some tests temperature inversion is evident which indicates that volumetric heating is dominating the situation. Figures 37 through 42, summarized below, show raw data traces for a variety of tests:

Figure	Flux cal/cm^{2}sec	Sample
37		Data Format
38		Typical Trace
39	16	Sample 19, 3 runs, moisture varied
40	18	Samples 8 and 25
41	16,57	Sample 19
42	16	Sample 7, moisture varied

An analysis and summary of the air temperature data organized by sample type, and summarized based on the format given in Figures 34 and 35 is presented in Table 13. The relative scaling of the data versus Q is evident. The agreement of these data with the conduction expansion model was studied as part of another contract. Good agreement was found at early times, when (a) no blow-off was occurring, and (b) the assumptions of one-dimensional flow were not violated.

In summary, the air temperature measurements indicated that

- $Q_o$at ¼" correlates well with Q threshold. This was to be expected for cases of marked smoke and particle ejection, and indicates an alternate way to measure Q threshold when the smoke emission is very thin (e.g., Sample 19) or when it is experimentally difficult to see the surface.

- The presence of moisture is noted above about 2.5% by weight, by a temperature plateau at 100^{o}C. Between 10 to 4 cal/cm^2 per % moisture is required to exhaust the water. Afterwards the soil continues to respond as if it were dry initially. The value of heat fluence needed to remove water indicates a diathermanous layer thickness of 2 to 6 mm for moist soils. The layer thickness seems to correlate well with particle size.

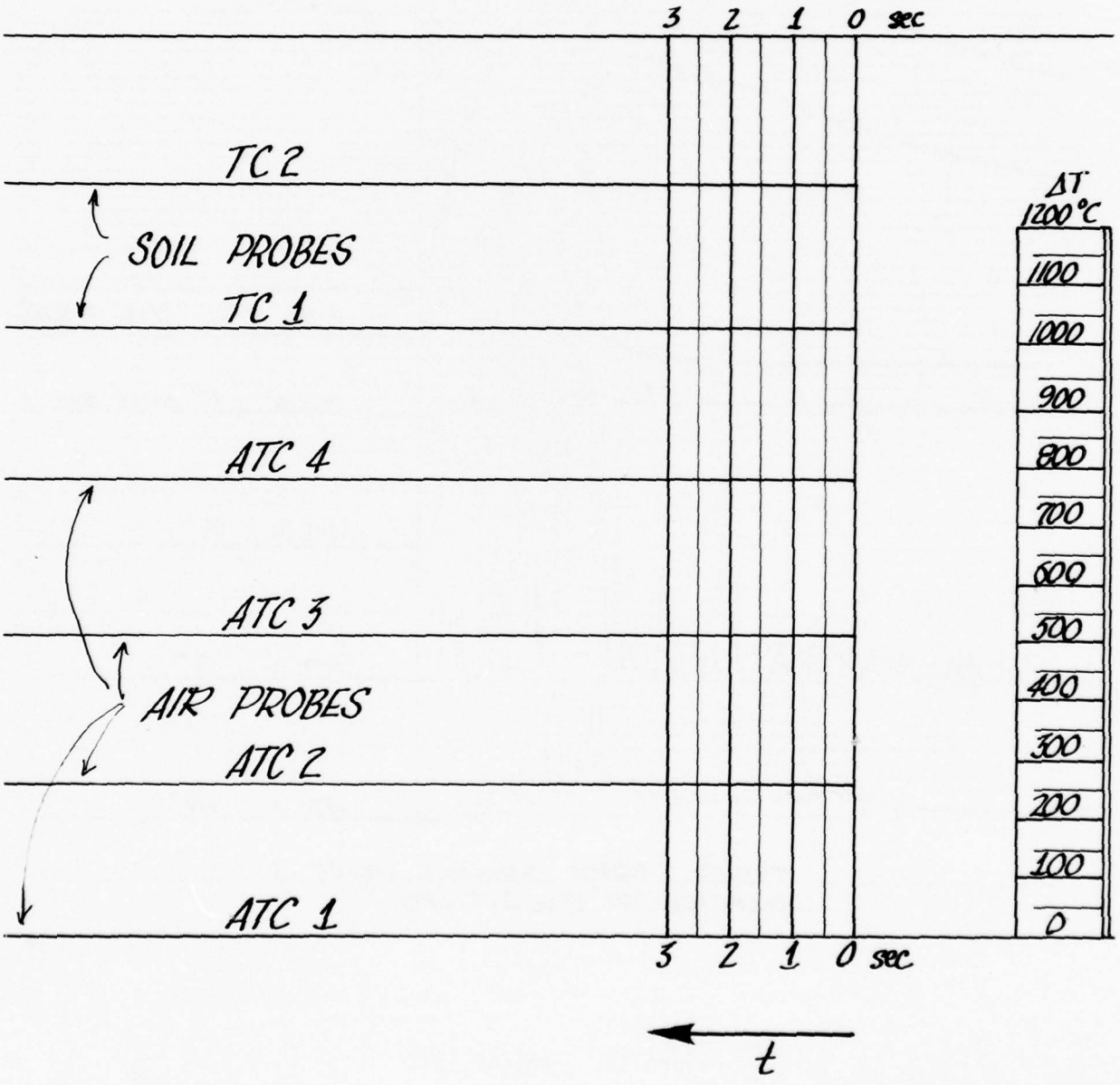

Figure 37. Data Format

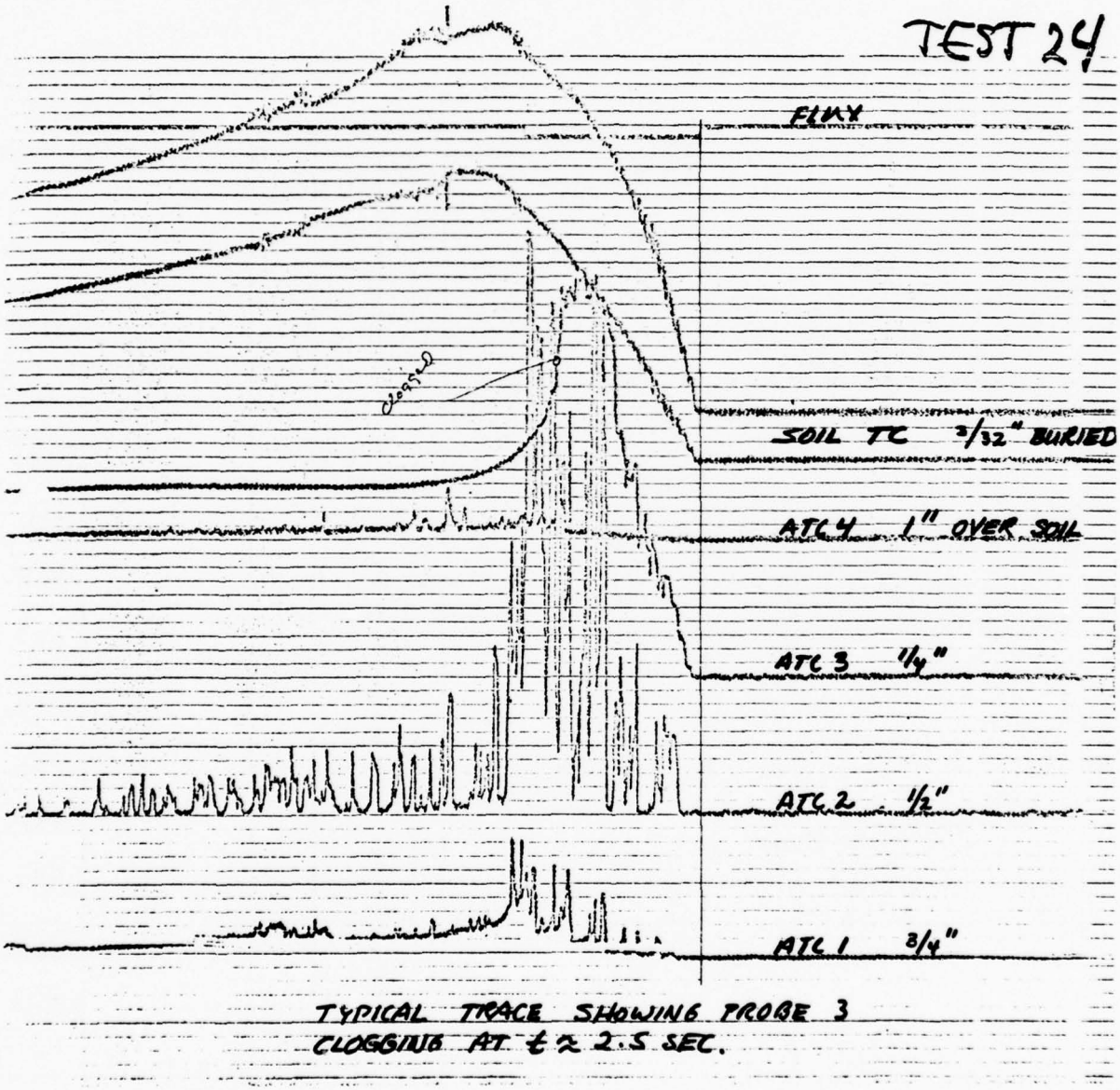

Figure 38. Typical Test

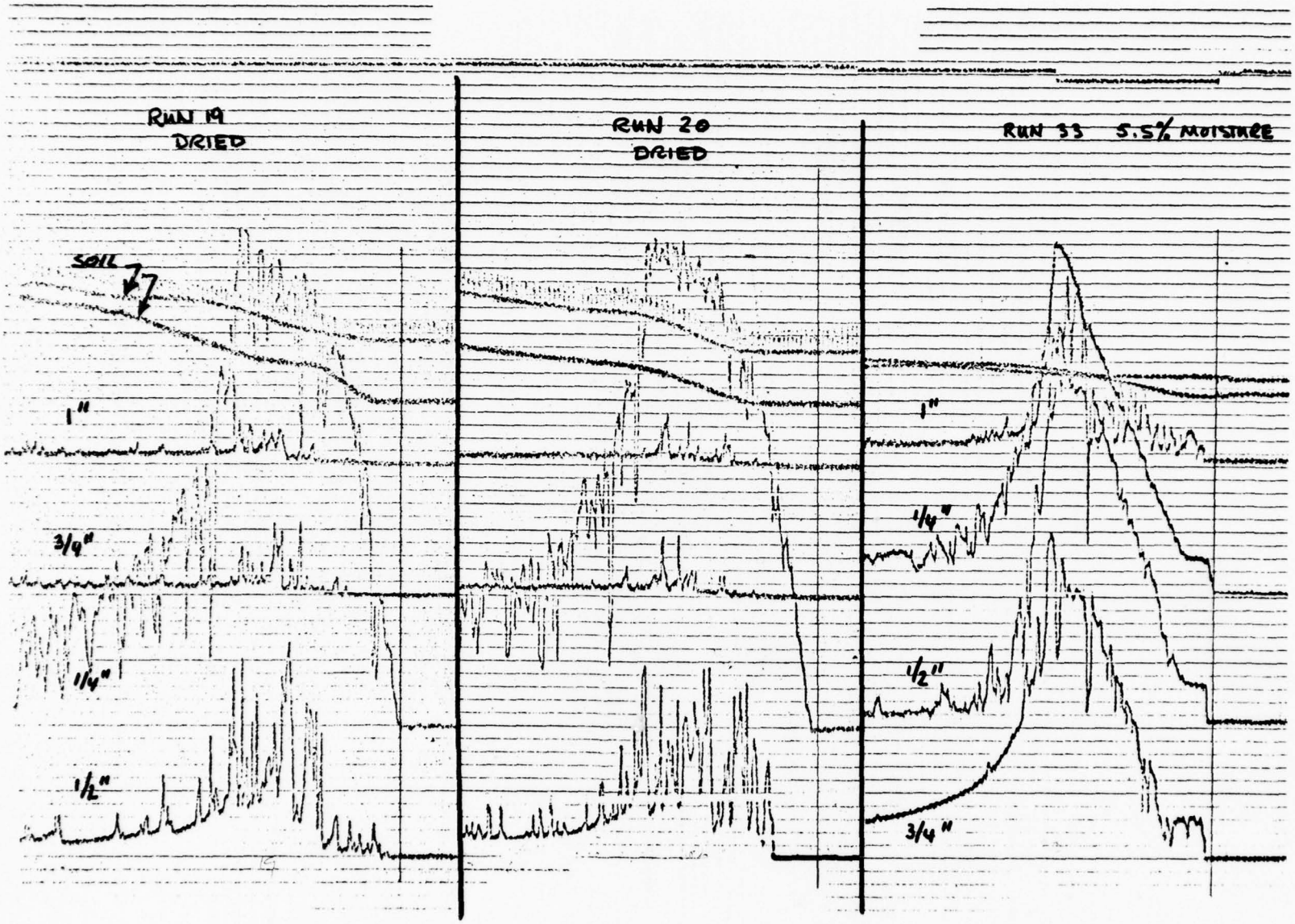

Figure 39. Comparison of Yucca Soils

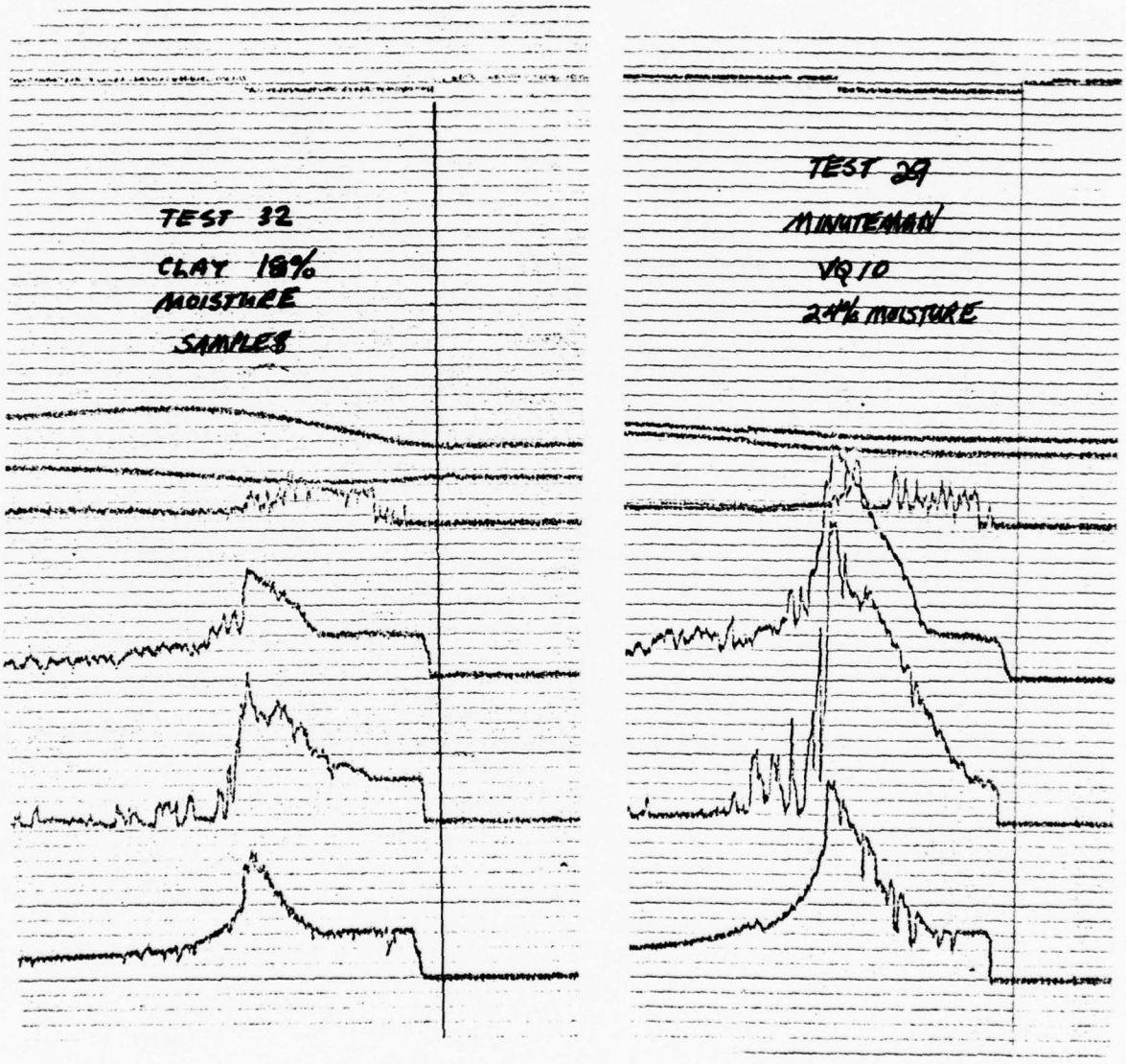

Figure 40. Additional Tests with High Moisture Content

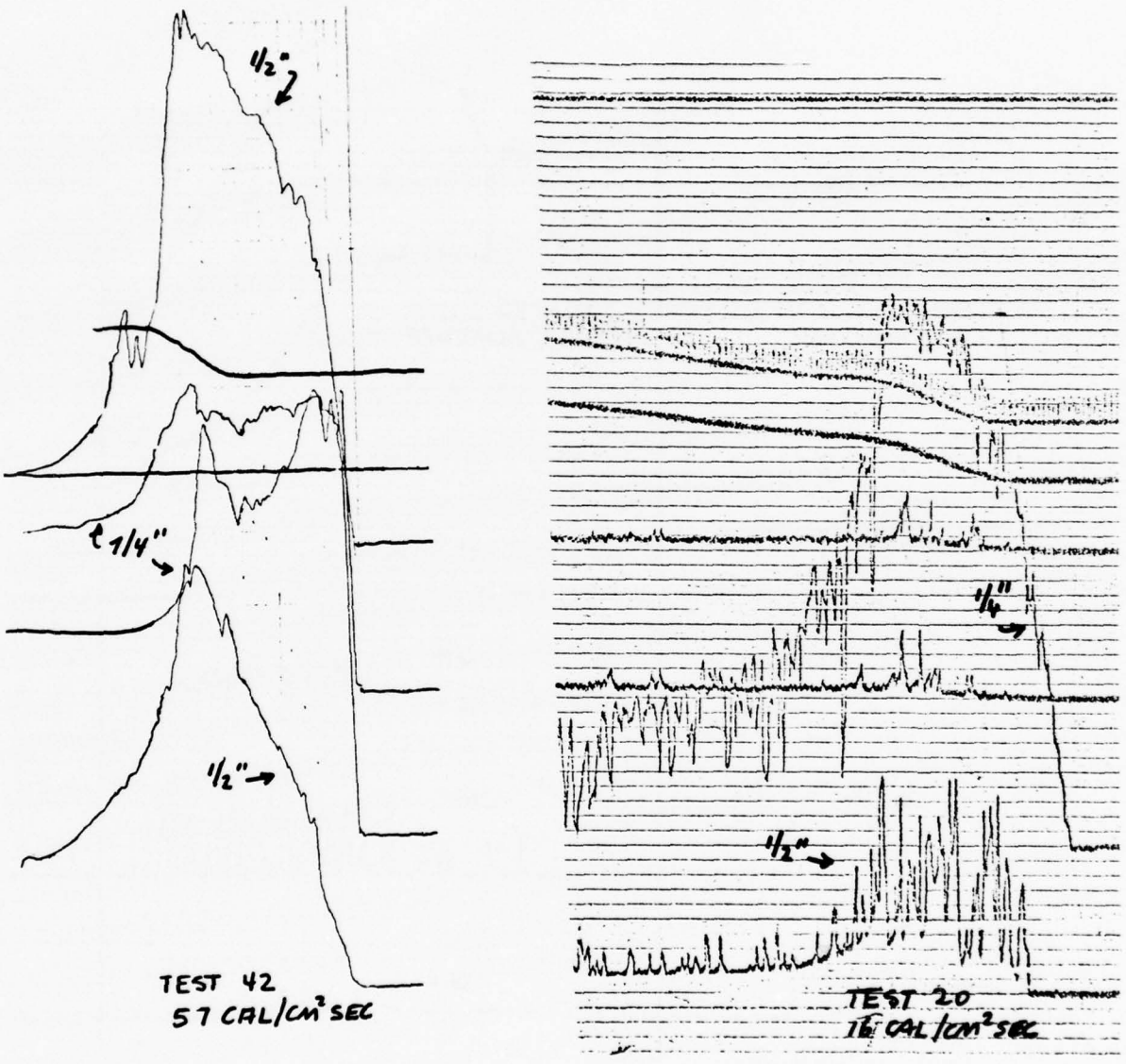

Figure 41. Comparison of Yucca Soils at Two Flux Levels

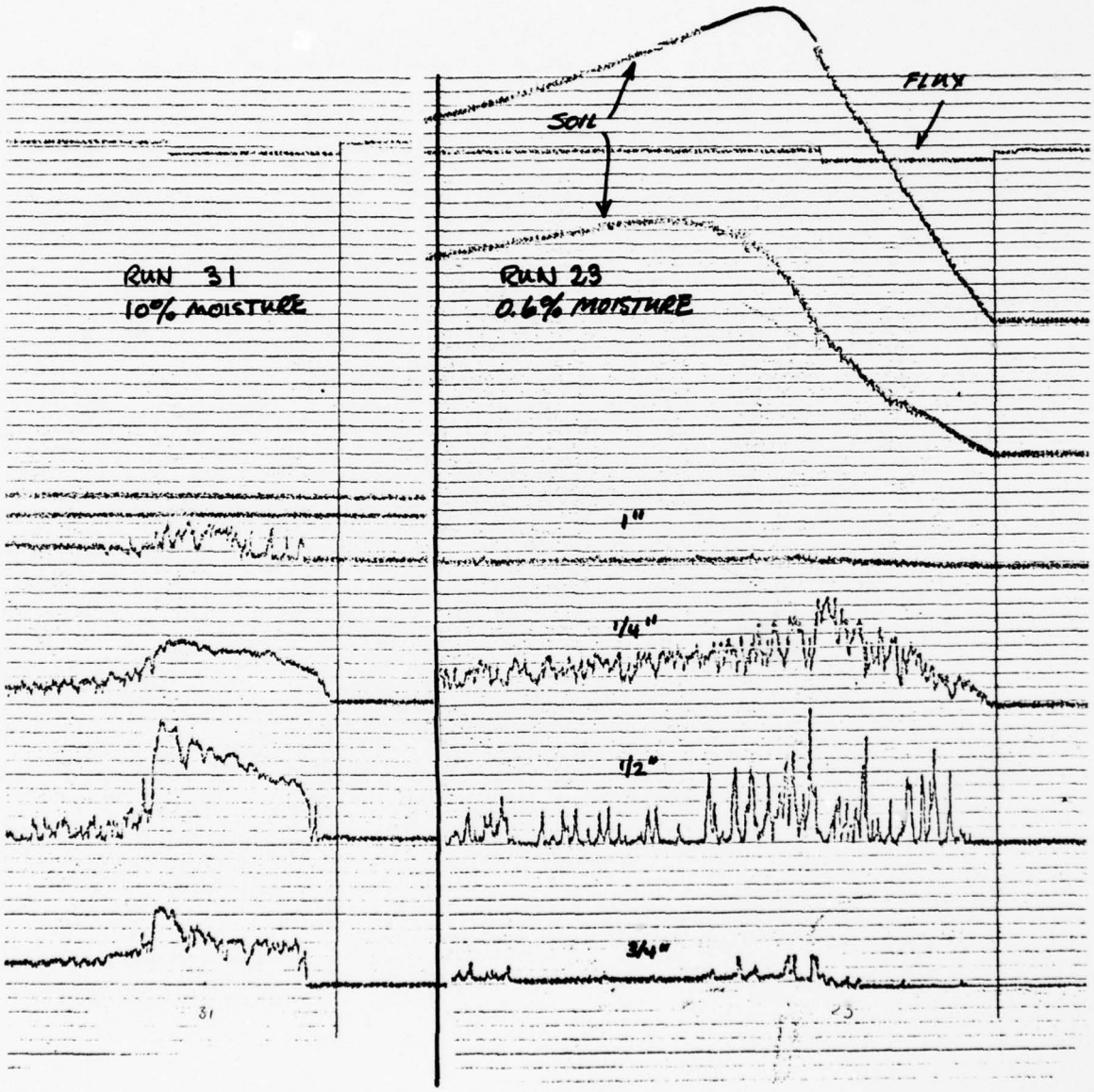

Figure 42. Comparison of Sand Samples at 16 cal/cm^{2}sec

Table 13. Summary Analysis of Air Temperature Measurements
Units Q, cal/cm^2; $\dot{Q}$, cal/cm^{2}sec $\Delta T/\Delta Q$ $^{o}C/(cal/cm^2)$

SAMPLE	SOIL % MOISTURE	RUN #	h = .25 in						h = .50 in					h = .75 in					h = 1.0 in				
			$\dot{Q}$	Q_o	Q_1	Q_2	$\Delta T/\Delta Q$	Q_3	Q_o	Q_1	Q_2	$\Delta T/\Delta Q$	Q_3	Q_o	Q_1	Q_2	$\Delta T/\Delta Q$	Q_3	Q_o	Q_1	Q_2	$\Delta T/\Delta Q$	Q_3
7	0	23	15.5	3	x	x	3	50	8	x	x	2	50	15	x	x	1	50	20	x	x	1/2	50
	10	31	18.0	4	8	50	—	—	9	10	25	3	40	9	12	45	—	—	20	30	40	—	—
8	0	21	15.5	3	x	x	20	20	5	x	x	10	30	8	x	x	6	30	10	x	x	2	40
	0	22	15.5	3	x	x	13	30	4	x	x	8	30	8	x	x	3	30	10	x	x	1	30
	9	32	18.0	3	5	36	3	50	4	5	25	5	50	6	8	36	5	50	18	19	36	—	40
	9	34	18.0	3	5	18	14	50	4	5	7	14	50	6	8	20	10	50	6	8	25	—	—
	0	56	57.5	5	x	x	—	—	5	x	x	—	—										
	0	57	57.5	5	x	x	—	—	8	x	x	—	—										

Table 13. Summary Analysis of Air Temperature Measurements
Units Q, cal/cm^2; $\dot{Q}$, cal/cm^{2}sec;$\Delta T/\Delta Q$,^{o}C/(cal/cm^2)

- continued -

SAMPLE	SOIL % MOISTURE	RUN #	$\dot{Q}$	Q_o	Q_1	Q_2	$\Delta T/\Delta Q$	Q_3	Q_o	Q_1	Q_2	$\Delta T/\Delta Q$	Q_3	Q_o	Q_1	Q_2	$\Delta T/\Delta Q$	Q_3	Q_o	Q_1	Q_2	$\Delta T/\Delta Q$	Q_3
19	0	16	16	N/A	x	x	50	16	8	x	x	6	40	8			3	48	16			2	48
	0	19	16	N/A	x	x	50	20	8	x	x	10	32	16			3	48	20			2	48
	0	20	16	N/A	x	x	50	16	10	x	x	15	32	20			3	48	20			2	48
	6	45	57.5	6	x	x	30-40	16	(12)	x	x	10	(30)										
	0	48	57.5	N/A	x	x	30-50	16	5	x	x	12	40										
	20	59	57.5	6	7	40	—	80	10	12	40	10	x										
21	0	17	16	N/A	x	x	50	16	4	x	x	6	48	12	x	x	3	48	16	x	x	2	48
	5.5	33	18	1	3	8	14	48	3	4	8	14	48	4	4	16	16	48	4	8	20	10	48
	0	42	57.5	N/A	x	x	60	10	6	x	x	10	20										
	0	43	57.5	N/A	x	x	60	10	6	x	x	10	20										
	5.5	47	57.5	6	x	x	30-50	12	10	x	x	10	20										
22	0	44	57.5	6	x	x	50	12	12	x	x	50	20										
	12.6	46	57.5	10	x	x	50	20	12	x	x	20	40										
	0	49	57.5	12	x	x	50	18	12	x	x	50	20										

Units Q: (cal/cm^2)
$\dot{Q}$: (cal/cm^{2}sec)
$\Delta T/\Delta Q$: ^{o}K/(cal/cm^2)

Table 13. Summary Analysis of Air Temperature Measurements
Units Q, cal/cm^2; $\dot{Q}$, cal/cm^{2}sec; $\Delta T/\Delta Q$, $^oC/(cal/cm^2)$

- continued -

SAMPLE	SOIL % MOISTURE	RUN #	$\dot{Q}$	Q_o	Q_1	Q_2	$\Delta T/\Delta Q$	Q_3	Q_o	Q_1	Q_2	$\Delta T/\Delta Q$	Q_3	Q_o	Q_1	Q_2	$\Delta T/\Delta Q$	Q_3	Q_o	Q_1	Q_2	$\Delta T/\Delta Q$	Q_3
23	0	24	15.5	3	x	x	20	30	6	x	x	10	50	9	x	x	3	50	12	x	x	1	50
	10	27	19.0	4	5	6	13	40	5	7	15	4	60	6	8	23	10	60	12	20	60	—	—
	NAT.	51	57.5	7	x	x	80	15	8	x	x	15	—										
	0	53	57.5	6	x	x	80	15	9	x	x	15	—										
24	0	25	17.5	3	x	x	20	45	5	x	x	25	30	8	x	x	10	50	10	x	x	3	50
	8	28	19.0	4	6	18	2.5	60	8	9	20	5	60	8	12	30	2.5	60	12	14	60	—	—
	NAT.	52	57.5	18	x	x	43	30	N/A														
	0	54	57.5	6	x	x	30	40	8	x	x												
25	0	26	17.5	2	x	x	13	40	4	x	x	19	40	8	x	x	6	50	12	x	x	1	60
	13	29	19.0	4	6	27	10	60	6	7	15	10	60	8	9	27	5	60	12	14	—	—	—
	NAT	50	57.5	6	x	x	12	—	8	x	x	—	—										
	0	55	57.5	6	x	x	—	—	6	x	x	—	—										

- Air heating rates of from 5 to 80 $^{o}K/(cal/cm^2)$ were observed in the tests. For air the value $C_p \sim 7$ cal/mole ^{o}K yields a theoretical value of $\Delta T/\Delta Q_1 = 3000\ ^{o}K$ (cal/cm^3) where Q_1 is the net heating to a 1 cm^3 cell of air. This argument indicates that the air heating observed is due to an approximately 1% efficient conversion of incoming radiant energy, per cm^3. Volumetric air heating over a 50 to 100 cm path would have similar efficiencies.

SCANNING ELECTRON MICROSCOPE EVALUATION OF POST SHOT MATERIAL

Samples 23, 24 and 25 (Minuteman Sites) exhibited a glassy layer post shot due to the action of the thermal radiation. Figures 43 through 46 show scanning electron microscope pictures of this material for Sample 23. The variation in magnification allows one to appreciate the complexity of the structure which appears to be hollow glassy spheres - sometimes shattered - contained within smaller sections of spheres or planes. Apparently a bubbling action of evolved gasses in a melted glass matrix was taking place during irradiation.

DIFFERENTIAL THERMAL ANALYSIS

A differential thermal analysis was made of Samples 12, 13, and 14 in an attempt to understand some aspects of the reactions which may take place in heated soil. The technique involves recording the difference in temperature between the soil sample and an inert sample (Al_2O_3) both heated in an oven at $10^{o}C$/minute for the Aluminum oxide. When the soil temperature lags that of Al_2O_3, endothermic reactions such absorbed water released as steam are taking place. Alternatively when the soil sample temperature leads that of the inert sample, exothermic reactions are taking place. Examples of the later are CO_2 evolution from organics or recrystalization after release of bound water. The tests indicate temperature points of relative importance to blow-off of steam, dust, and particulate material. Further testing of a wider range of soils may allow a correlation of blow-off phenomenon with soil type. This is an issue to be investigated in future work.

Figures 47, 48 and 49 show the test records for the three soil types that were tested.

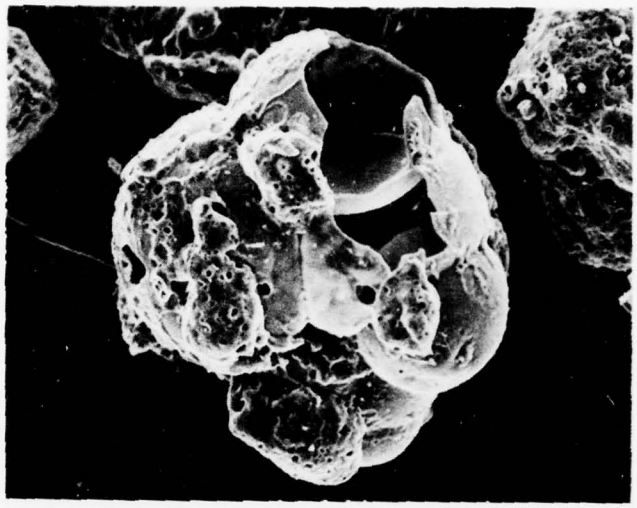

Figure 43. VR11 Post Shot, 500X

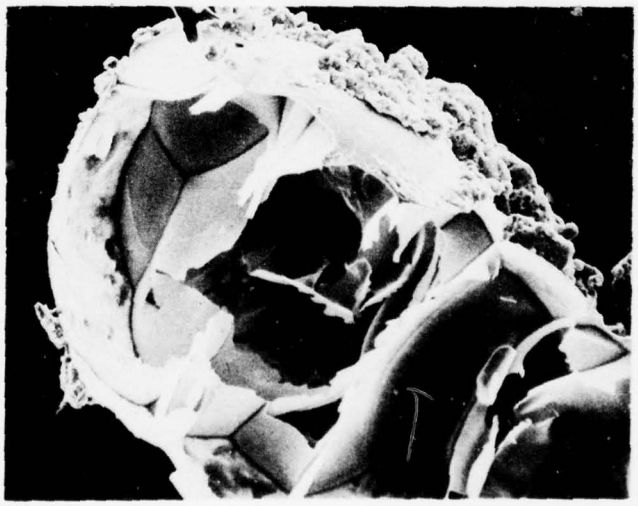

Figure 44. VR11 Post Shot, 375X

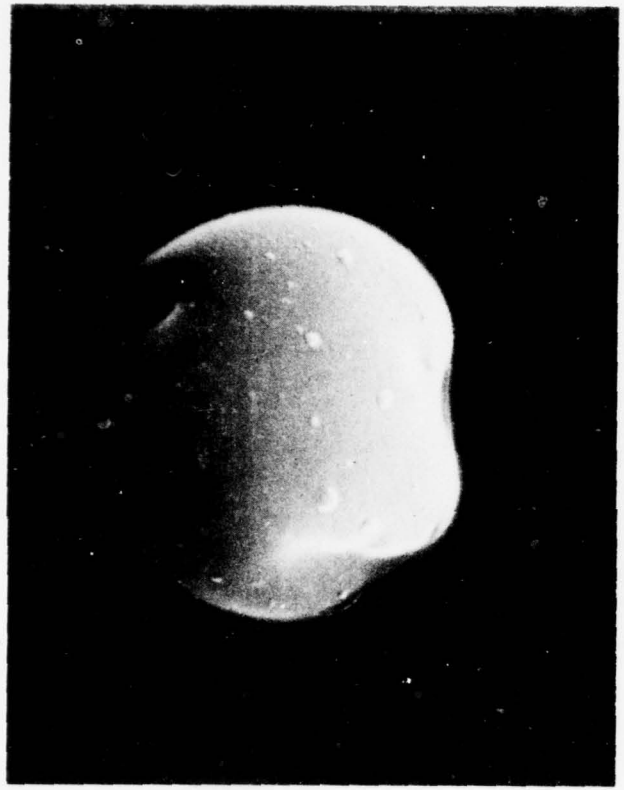

Figure 45. YR11 Post Shot, 10,000X

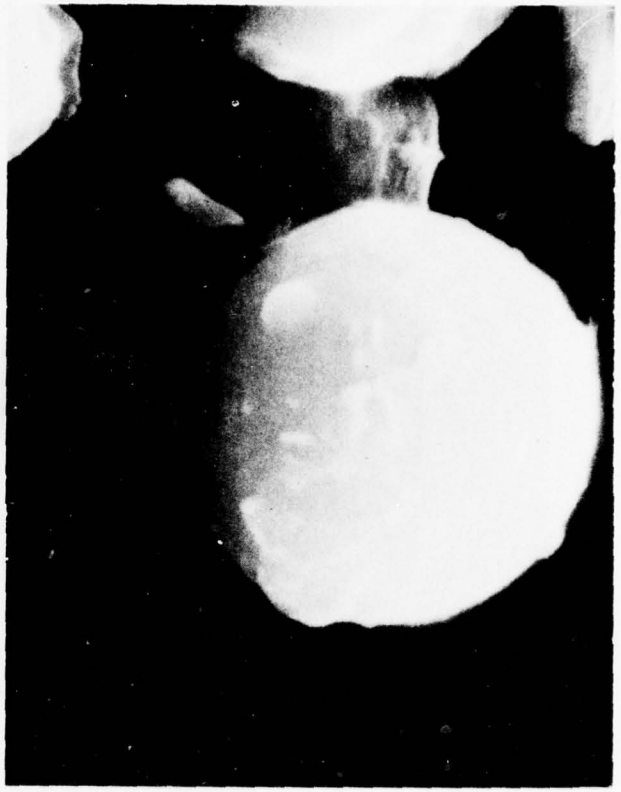

Figure 46. YR11 Post Shot, 20,000X

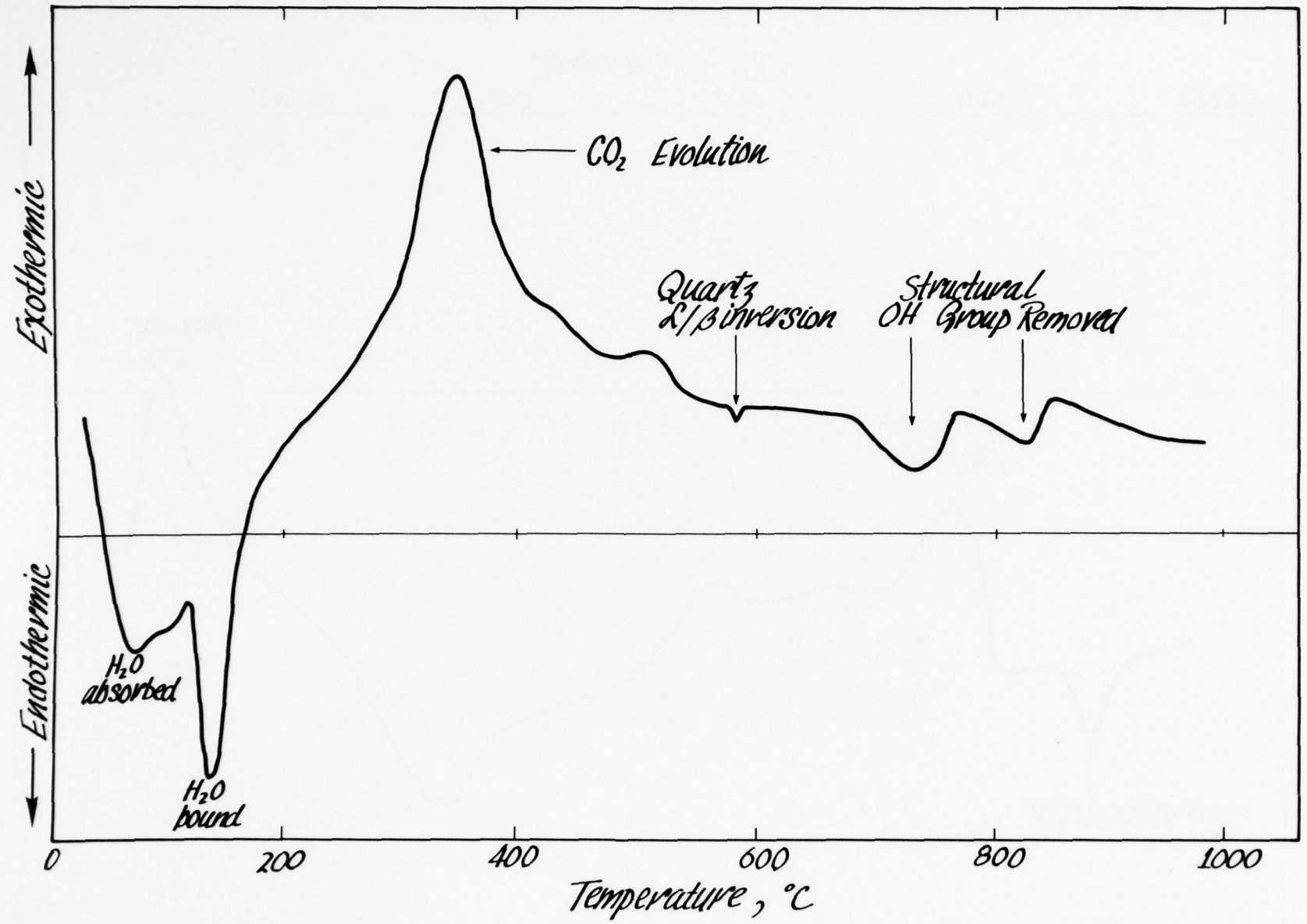

Figure 47. Differential Thermal Analysis Record for Sample 12 (Regions of Marked Thermal Reaction are Noted)

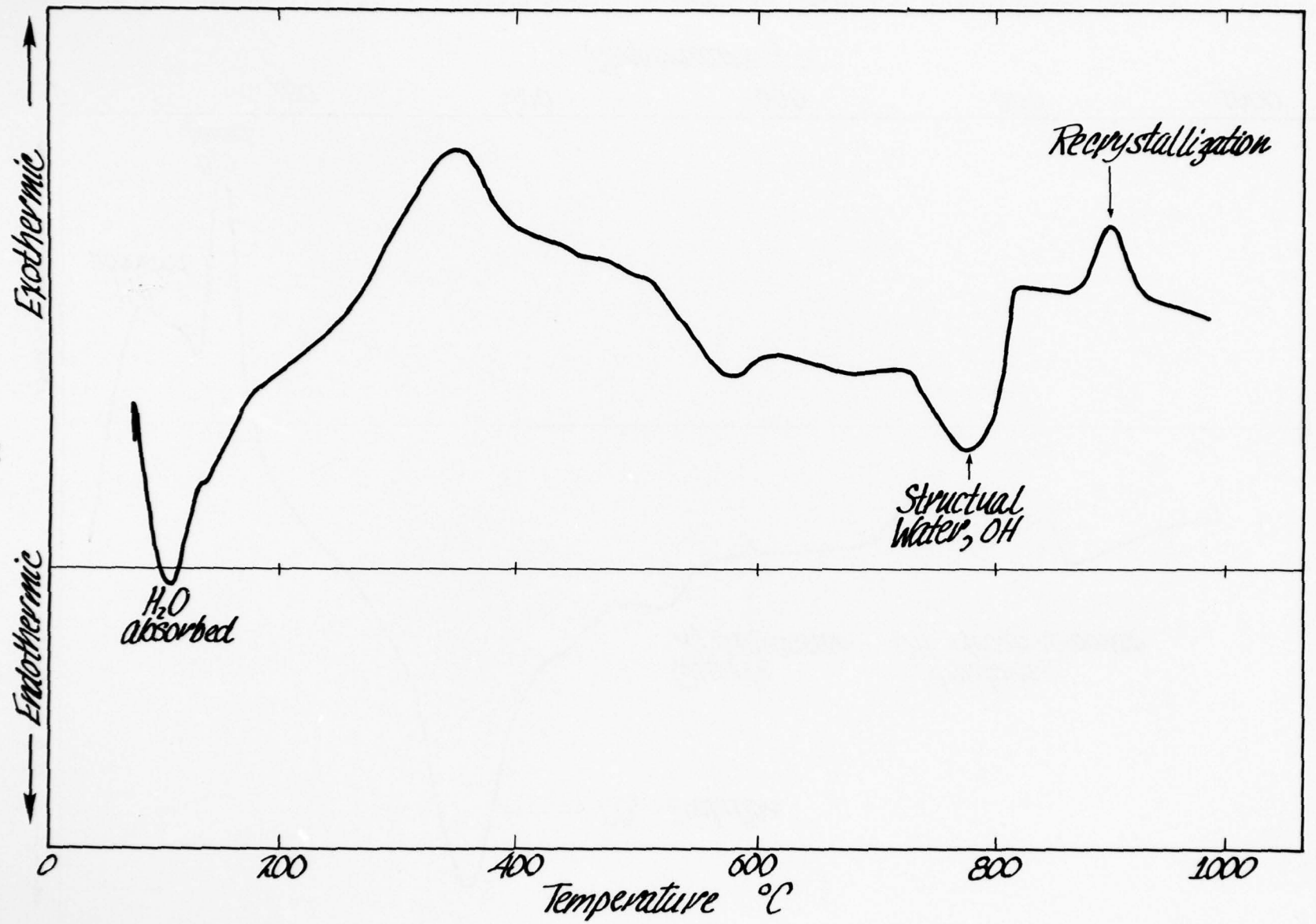

Figure 48. Differential Thermal Analysis Record for Sample 13 (Regions of Marked Thermal Reaction are Noted)

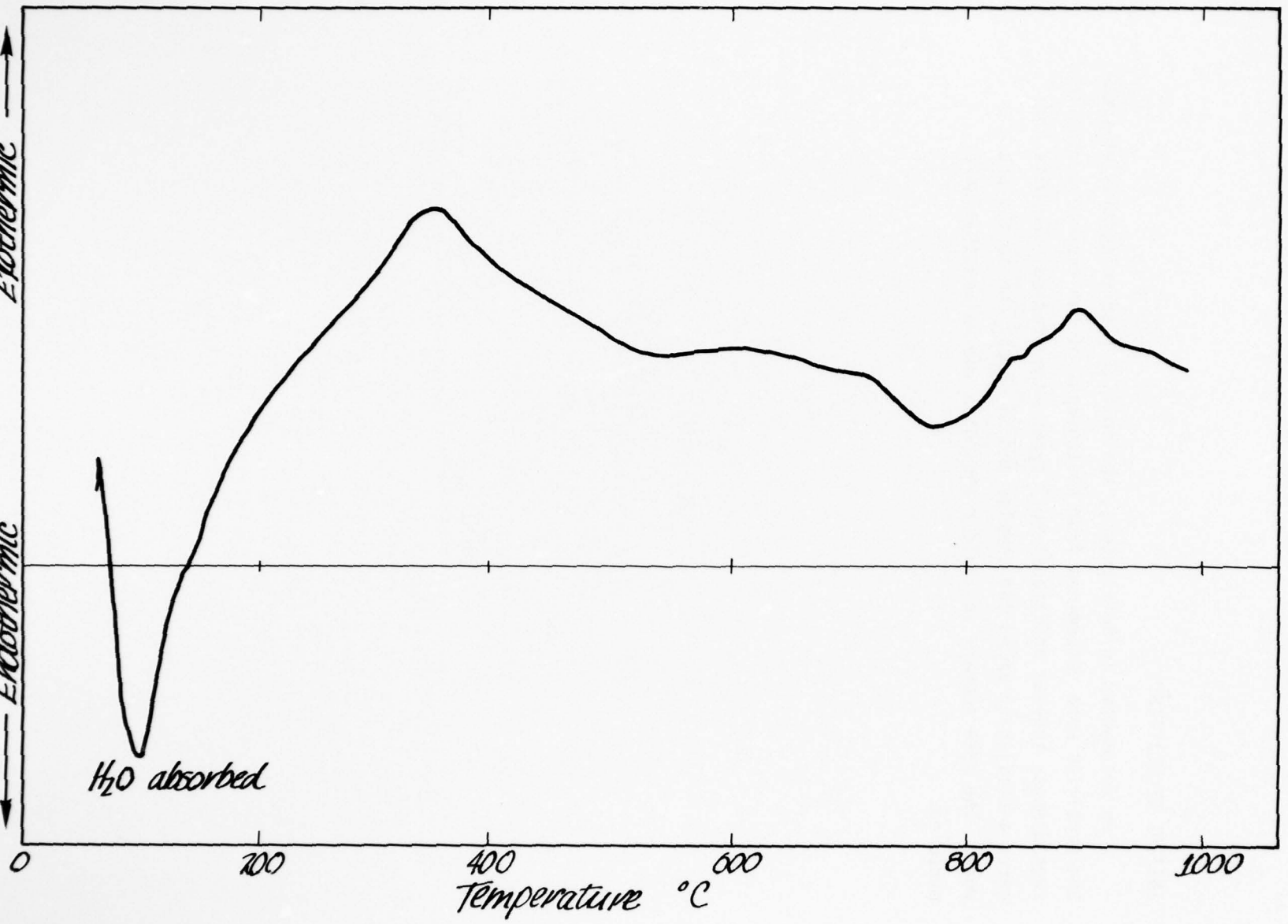

Figure 49. Differential Thermal Analysis Record for Sample 14 (Regions of Marked Thermal Reaction are Noted)

INITIAL VELOCITIES

As documented in Reference 1, the initial rise velocities of smoke and particles were determined from photographs of the tests. During the second phase several additional soil types were studied. Results indicated a similarity among the samples and in comparison to the phase 1 work. The data summary in Table 2 indicates the values that were measured.

REFERENCES

1) T. M. Knasel, "Thermal Induced Blow-Off - A report on Experimental Studies," Vol. I and II, DNA 3723F-1 and 2, 15 April 1975.

2) J. T. Powers, R. T. Liner, and John E. Mansfield, "Precursor Sweep-Up Dust Cloud Model and Thermal Layer Model Development," DNA 3876F, 1 December 1975.

3) T. M. Knasel, P. L. Versteegen, and J. A. Powers, "Thermal Layer Development Modeling," SAI-78-541-WA, May 1977.

4) R. T. Liner, Jr., R. Ryan and W. R. Seebaugh, "Effects of Geology on the Crater Ejecta Environment," SAI-76-561-WA.

5) D. Gicking, F. Hains, E. Kownacki, B. Lieu, J. Mansfield, J. McGahan, M. Tobriner, "Technology Support for Environmental Defense," SAI-74-217-WA, Final Report, DNA001-74-C-0074, October 1974.

6) See for further explanation:

F. L. Bartman, "The Reflectance and Scattering of Solar Radiation by the Earth," NASA-CR-83954, February 1967.

S. Mills, "Earth Albedo and Emitted Radiation," NASA-SP-8067, July 1971.

K. Y. Kondratyere, "Radiation in the Atmosphere," Academic Press, New York 1969.

7) NCRL Report 12339, Volume I.

DISTRIBUTION LIST

DEPARTMENT OF DEFENSE

Assistant to the Secretary of Defense
Atomic Energy
ATTN: Honorable Donald R. Cotter

Director
Defense Advanced Rsch. Proj. Agency
ATTN: Technical Library
ATTN: NMRO
ATTN: PMO
ATTN: STO

Director
Defense Civil Preparedness Agency
Assistant Director for Research
ATTN: Admin. Officer

Defense Documentation Center
Cameron Station
12 cy ATTN: TC

Director
Defense Intelligence Agency
ATTN: DB-4C, Edward O'Farrell
ATTN: DT-1C
ATTN: DT-2, Wpns. & Sys. Div.

Director
Defense Nuclear Agency
ATTN: TISI, Archives
ATTN: DDST
2 cy ATTN: SPSS
3 cy ATTN: TITL, Tech. Library

Chairman
Dept. of Defense Explo. Safety Board
ATTN: DD/S&SS
ATTN: Thomas Zaker

Commander
Field Command, DNA
ATTN: FCPR
ATTN: FCT
ATTN: FCTMOF

Chief
Livermore Division, Fld. Command, DNA
Lawrence Livermore Laboratory
ATTN: FCPRL

Commandant
NATO School (SHAPE)
ATTN: U.S. Documents Officer

Chief
Test Construction Division
Field Command Test Directorate
ATTN: FCTC

Under Secretary of Def. for Rsch. & Engrg.
Department of Defense
ATTN: AE
ATTN: S&SS (OS)

DEPARTMENT OF THE ARMY

Dep. Chief of Staff for Rsch. Dev. & Acq.
ATTN: Technical Library

Chief of Engineers
ATTN: DAEN-MCE-D
ATTN: DAEN-RDM

Deputy Chief of Staff for Ops. & Plans
ATTN: Technical Library

Commander
Harry Diamond Laboratories
ATTN: DELHD-NP
ATTN: DELHD-TI, Tech. Lib.

Commander
Redstone Scientific Information Ctr.
U.S. Army Missile Command
ATTN: Chief, Documents

Director
U.S. Army Ballistic Research Labs.
ATTN: J. H. Keefer, DRDAR-BLE
ATTN: Julius J. Meszaros, DRXBR-X
ATTN: Tech. Lib. Edward Baicy
ATTN: W. Taylor, DRDAR-BLE

Director U.S. Army Engr. Waterways Exper. Sta.
ATTN: Guy Jackson
ATTN: John N. Strange
ATTN: Technical Library
ATTN: William Flathau

Commander
U.S. Army Mat. & Mechanics Rsch. Ctr.
ATTN: Technical Library

Commander
U.S. Army Materiel Dev. & Readiness Cmd.
ATTN: Technical Library

Commander
U.S. Army Mobility Equip. R&D Ctr.
ATTN: Technical Library

Commander
U.S. Army Nuclear & Chemical Agency
ATTN: Library

DEPARTMENT OF THE NAVY

Chief of Naval Material
ATTN: MAT 0323

Chief of Naval Operations
ATTN: OP 981
ATTN: OP 03EG

Commander
David W. Taylor Naval Ship R&D Ctr.
ATTN: Code L42-3, Library

DEPARTMENT OF THE NAVY (Continued)

Chief of Naval Research
ATTN: Code 461, Jacob L. Warner
ATTN: Code 464, Thomas P. Quinn
ATTN: Nicholas Perrone
ATTN: Technical Library

Officer-in-Charge
Civil Engineering Laboratory
Naval Construction Battalion Center
ATTN: R. J. Odello
ATTN: Technical Library

Commander
Naval Electronic Systems Command
Naval Electronic Systems Cmd. Hqs.
ATTN: PME 117-21A

Commander Naval Facilities Engineering Command
Headquarters
ATTN: Code 03A
ATTN: Technical Library
ATTN: Code 04B

Director
Naval Research Laboratory
ATTN: Code 2600, Tech. Lib.

Commander
Naval Sea Systems Command
ATTN: ORD-91313, Library
ATTN: Code 03511

Commander
Naval Ship Engineering Center
ATTN: NSEC 6105G
ATTN: Technical Library

Officer-in-Charge
Naval Surface Weapons Center
ATTN: Code WA501, Navy Nuc. Prgms. Off.

Commander
Naval Surface Weapons Center
Dahlgren Laboratory
ATTN: Technical Library

Director Strategic Systems Project Office
ATTN: NSP-272
ATTN: NSP-43, Tech. Lib.

DEPARTMENT OF THE AIR FORCE

AF Geophysics Laboratory, AFSC
ATTN: LWW, Ker C. Thompson

AF Institute of Technology, AU
ATTN: Library, AFIT Bldg. 640, Area B

AF Weapons Laboratory, AFSC
ATTN: DES-S, Maj Ganong
ATTN: DES-C, Charles Needham
ATTN: SUL
ATTN: DEX

Headquarters, Air Force Systems Command
ATTN: DLCAW

Hq. USAF/IN
ATTN: INATA

DEPARTMENT OF THE AIR FORCE (Continued)

Hq. USAF/RD
ATTN: RDQSM

Commander in Chief
Strategic Air Command
ATTN: NRI-STINFO, Library

DEPARTMENT OF ENERGY

Albuquerque Operations Office
ATTN: Doc. Con. for Tech. Library

Division of Headquarters Services
Library Branch G-043
ATTN: Doc. Con. for Class. Tech. Lib.

Nevada Operations Office
ATTN: Doc. Con. for Tech. Lib.

Division of Military Application
ATTN: Doc. Con. for Test Office

University of California
Lawrence Livermore Laboratory
ATTN: Larry W. Woodruff, L-96
ATTN: Tech. Info. Dept. L-3

Los Alamos Scientific Laboratory
ATTN: Doc. Con. for Reports Lib.

Sandia Laboratories
Livermore Laboratory
ATTN: Doc. Con. for Tech. Lib.

Sandia Laboratories
ATTN: Doc. Con. for Org. 3422-1,
Sandia Rpt. Coll.

DEPARTMENT OF DEFENSE CONTRACTORS

Aerospace Corporation
ATTN: Tech. Info. Services

The Boeing Company
ATTN: Aerospace Library

Civil/Nuclear Systems Corp.
ATTN: Robert Crawford

EG&G Washington Analytical Services Center, Inc.
ATTN: Technical Library

General Electric Company
TEMPO-Center for Advanced Studies
ATTN: DASIAC

IIT Research Institute
ATTN: Technical Library

Institute for Defense Analyses
ATTN: IDA Librarian, Ruth S. Smith

Kaman Sciences Corporation
ATTN: Library

Lockheed Missiles & Space Co., Inc.
ATTN: Technical Library

DEPARTMENT OF DEFENSE CONTRACTORS (Continued)

Physics International Company
ATTN: Doc. Con. for Coye Vincent
ATTN: Doc. Con. for E. T. Moore
ATTN: Doc. Con. for Tech. Lib.

R&D Associates
ATTN: J. G. Lewis
ATTN: Technical Library
ATTN: Robert Port

Science Applications, Inc.
ATTN: Technical Library

Science Applications, Inc.
ATTN: R. D. Shunk

Science Applications, Inc.
ATTN: J. Dishon

Science Applications, Inc.
ATTN: T. M. Knasel
ATTN: J. Cockayne
ATTN: A. Houghton

Southwest Research Institute
ATTN: A. B. Wenzel
ATTN: Wilfred E. Baker

SRI International
ATTN: George R. Abrahamson
ATTN: Burt R. Gasten

DEPARTMENT OF DEFENSE CONTRACTORS (Continued)

Systems, Scinece and Software, Inc.
ATTN: Donald R. Grine
ATTN: Technical Library

TRW Defense & Space Sys. Group
2 cy ATTN: Peter K. Dai, R1-2170
ATTN: Tech. Info. Center, S-1930
ATTN: D. H. Baer, R1-2136

TRW Defense & Space Sys. Group
San Bernardino Operations
ATTN: E. Y. Wong, 527-712

The Eric H. Wang
Civil Engineering Rsch. Fac.
The University of New Mexico
ATTN: Larry Bickle
ATTN: Neal Baum

Weidlinger Assoc. Consulting Engineers
ATTN: Melvin L. Baron

Weidlinger Assoc. Consulting Engineers
ATTN: J. Isenberg

END